

DETERMINATION OF GEOIDAL HEIGHT DIFFERENCE USING RING INTEGRATION METHOD

A. TSEN

August 1992



**TECHNICAL REPORT
NO. 158**

PREFACE

In order to make our extensive series of technical reports more readily available, we have scanned the old master copies and produced electronic versions in Portable Document Format. The quality of the images varies depending on the quality of the originals. The images have not been converted to searchable text.

DETERMINATION OF GEOIDAL HEIGHT DIFFERENCE USING RING INTEGRATION METHOD

Arthur Tsen

Department of Surveying Engineering
University of New Brunswick
P.O. Box 4400
Fredericton, N.B.
Canada
E3B 5A3

August 1992

© Arthur Tsen, 1991

PREFACE

This technical report is a reproduction of a thesis submitted in partial fulfillment of the requirements for the degree of Master of Science in Engineering in the Department of Surveying Engineering, September 1991. The research was supervised by Dr. Petr Vaníček, and funding was provided partially by the Natural Sciences and Engineering Research Council of Canada.

As with any copyrighted material, permission to reprint or quote extensively from this report must be received from the author. The citation to this work should appear as follows:

Tsen, A. (1992). *Determination of Geoidal Height Difference using Ring Integration Method*. M.Sc.E. thesis, Department of Surveying Engineering Technical Report No. 158, University of New Brunswick, Fredericton, New Brunswick, Canada, 164 pp.

ABSTRACT

With the advent of artificial satellites, it is possible to determine relative positions of points to an accuracy of a few parts per million (ppm). The coordinate differences can, in turn, be transformed into differences in latitude, in longitude and in height on a ellipsoid, provided that their positions relative to the geocentric cartesian coordinate system are known. For some applications, such as mappings and vertical crustal movements, orthometric heights or height differences are needed. In order to convert these ellipsoidal heights to orthometric heights, geoidal heights are required.

A software has been developed to determine geoidal height differences utilizing terrestrial gravity anomalies. The approach used here is the ring integration which consists of compartments formed by the intersection of rings and lines radiating out from the point of interest. In this approach, the integration is regarded as the summation of all the predicted gravity anomalies at the midpoints of the compartments. The difference of summation of all the predicted gravity anomalies between endpoints of the line is then multiplied by a constant (0.0003 m/mGal) to obtain the geoidal height difference for the inner zone contribution. The remote zone contribution is obtained using the high order geopotential model - RAPP180. The contributions from these two zones are then summed up to obtain a full geoidal height difference.

The results generated from this software are compared to the results obtained from other independent methods, such as GPS/Levelling method and the UNB Dec.'86. A mean-relative-accuracy (MRA) of 1.7 ppm was obtained between the ring integration method and the GPS/Levelling method using a cap size of radius, $\psi_0 = 0.6^\circ$ radius. The comparisons showed that an improvement of the geoidal height difference was possible when the inner zone contribution was added to the remote zone contribution - improve from MRA of 4.0 ppm to MRA of 1.7 ppm. The mean-relative-accuracy between the ring integration method and the UNB Dec.'86 approach is 0.92 ppm using a cap radius of 0.4° .

TABLE OF CONTENTS

ABSTRACT.	ii
LIST OF FIGURES.	vi
LIST OF TABLES.	viii
ACKNOWLEDGEMENTS.	ix

<u>Chapter</u>	<u>Page</u>
1. INTRODUCTION.	1
2. DEFINITIONS.	7
2.1 The Gravity Potential of the Earth	7
2.2 The Gravity Potential of the Ellipsoid	8
2.3 Disturbing Potential.	9
2.4 Reference Ellipsoid.	9
2.5 Geoid.	10
2.6 Gravity Anomaly	11
3. THE UNB APPROACH	13
3.1 The Stokes Formula	14
3.2 The Spheroidal Kernel.	20
3.3 The Modified Spheroidal Stokes Function	23
3.4 The Topographic Effect.	26
3.5 The Indirect Effect	29
3.6 The Atmospheric Effect.	30
4. NUMERICAL INTEGRATION FOR THE UNB APPROACH	32
4.1 Input Data.	32
4.1.1 Point Gravity Anomaly.	32

Table of Contents cont'd.

4.1.2	5' X 5' Mean Gravity Anomaly.	34
4.1.3	1° X 1° Mean Gravity Anomaly.	35
4.2	Numerical Integration.	35
4.2.1	The Innermost Zone	36
4.2.2	The Inner Zone.	37
4.2.3	The Outer Zone.	38
5.	RING INTEGRATION METHOD FOR GEOID HEIGHT DIFFERENCE . .	40
5.1	Ring Integration Technique for Geoid Computation	40
5.2	An Algorithm for Generating the Rings.	44
5.2.1	The Inner Sub-Zone.	50
5.2.2	The Middle Sub-Zone	54
5.2.3	The Outer Sub-Zone	56
5.2.4	Computation of Geoidal Height Difference.	58
5.3	Determination of Mean Gravity Anomaly	59
5.3.1	Arithmetic Mean	60
5.3.1.1	Method 1: Arithmetic Mean from Free-Air Anomalies.	60
5.3.1.2	Method 2: Arithmetic Mean from Bouguer Anomalies	61
6.	RESULTS OF THE TESTS.	62
6.1	The Manitoba GPS Network	62
6.2	Comparison of Results	65
6.2.1	Recovery on ΔN from Geopotential Model	66
6.2.2	Comparison on ΔN Between UNB Dec.'86 Solution and GPS/Levelling Solution.	67
6.2.3	Comparison on ΔN Between Ring Integration Solution and GPS/Levelling Solution.	70
6.2.3.1	Comparison Between ΔN using the "reduced" and the "unreduced" gravity anomalies	70

Table of Contents cont'd.

6.2.4	Comparison on ΔN Between Ring Integration Solution and UNB Dec.'86 Solution.	74
6.2.5	Analysis of ΔN with respect to Baseline Lengths and Azimuths.	75
6.3	Error Analysis	78
6.3.1	Random Errors	78
6.3.2	Systematic Errors	82
6.3.2.1	Error Caused by Gravity Datum Inconsistency . .	83
6.3.2.2	Error Caused by Vertical Datum Inconsistency . .	83
6.3.2.3	Error Caused by Horizontal Datum Inconsistency	84
6.3.3	Errors From the Remote Zone Contribution	86
7.	SUMMARY, CONCLUSIONS AND RECOMMENDATIONS	87
	REFERENCES	92
	APPENDICES.	97
I.1	Description of Programs.	98
I.2	Program RININT.RED	104
I.3	Program RININT.UNRED.	122
I.4	Program POT.RED	140
I.5	Program POT.UNRED	143
I.6	Test on $\Delta\Phi$	159
I.7	Test on $\Delta\psi$	160
I.8	Comparisons of Geoidal Height Differences	161
I.9	Transformation from gravity disturbance to gravity anomaly.	162
I.10	An Example for Computing the scale N_c to match the spacing of the point gravity anomalies	163

LIST OF FIGURES

<u>Figure</u>	<u>Page</u>
3.1 The Disturbing Potential [$W(Q) - U(Q)$]	15
3.2 Comparison Between $S(\psi)$, $S_{20}(\psi)$ and $S_{20}^m(\psi)$	22
3.3 The Relationships Between the Geoid, the Cogeoid and the Ellipsoid.	26
3.4 The Topographic Effect on the Computation Point	27
3.5 The Indirect Effect on the Computation Point.	29
3.6 The Atmospheric Effect Vs. Height.	31
4.1 Structure of Point Gravity Anomalies Files	33
4.2 The Innermost, the Inner and the Outer Zones	39
5.1 The Ring Approach	41
5.2 The $F(\psi)$'s Function	44
5.3 Division of Rings and Compartments	45
5.4 The Inner Sub-Zone	50
5.5 Determination of Coordinates for the center of the Compartment	52
5.6 Cell (Shaded Area) Used for Predicting Δg	53
5.7 The Boundary Limits of the cell	53
5.8 The Middle Sub-Zone	55
5.9 The Outer Sub-Zone	57
6.1 Distribution of GPS Stations	63
6.2 Deterioration of Accuracy with respect to Distance	64
6.3 The Recovery of ΔN From Rapp180 Geopotential Model Taken to Various n_{max}	67

List of Figures cont'd.

6.4	Comparisons Between ΔN Using Reduced Δg and Unreduced Δg in Manitoba ($n_{\max} = 180$)	71
6.5	Comparison of ΔN Using Combination of Various n_{\max} as the Reference Model with Various Spherical Cap Radii (GPS Vs. Ring)	73
6.6	Comparison of ΔN Using Combination of Various n_{\max} as the Reference Model with Various Spherical Cap Radii (Ring Vs. UNB Dec.'86).	74
6.7	The Recovery of ΔN with Various n_{\max} (Ring is computed with $\psi_o = 0.6^\circ$) . .	75
6.8	Plots of Misclosures Against Distances	76
6.9	Plots of Misclosures Against Azimuths	77
6.10	The Shaded Region Shows the Area Which are not Common to the Inner Zones of Points "A" and "B" Where ΔN is Being Computed.	79

LIST OF TABLES

<u>Table</u>	<u>Page</u>
4.1	Structure of the 5' by 5' Mean Gravity Anomaly Files 34
5.1	The Stability of Thickness $\Delta\Phi_{12}$ of Successive Rings Computed to give a 0.0002 m/mgal Contribution to N for 1 mGal per Compartment with a 10° apex angle 50
6.1	Results From Manitoba GPS Campaign 64
6.2	Results of $\Delta N_{GPS/LEV}$ and $\Delta N_{UNB Dec.'86}$ 69
6.3	The Relationships Between the Proportion Q , the Distance s and the Spherical Cap Radius c 80
6.4	Number of Compartments (n) Used to Calculate N_A which Are Not Used to Compute N_B 81
6.5	Error in ΔN over Various s Due to Random Error in Δg 82
6.6	Error in ΔN Due to Systematic Error in Δg . Assuming $\epsilon_{\Delta g}$ of 1.0 mGal Presents Between Gravity Data Used Exclusively For N_A and that used Exclusively For N_B 86

ACKNOWLEDGEMENTS

My sincerely thanks to my Supervisor, Dr. Petr Vanicek, for his guidance, encouragement and suggestions on this thesis.

I would also like to express my appreciation to Dr. Nick Christou and Mr. Changyou Zhang for their helps during my stay at UNB, and to Dr. Andre Mainville from Canadian Geodetic Survey who provided me with the GPS/Levelling solutions.

Special thanks are due to Mrs. Rosa Hong, for printing of this excellent manuscript, and to Mrs. Maureen Osinchuk for proofreading the first draft of this manuscript for correct English usage.

Above all, I owe a debt of thanks to my parents and Irene for their love, support and believe that this thesis is possible.

CHAPTER ONE

INTRODUCTION

The determination of heights has been dated back to its origin in ancient Egypt when the Great Pyramid of Khufu (480 feet high) at Giza was built in 2700 BC [Encyclopaedia Britannica, vol.17, pp 828, 1978]. In the 2nd century BC, the Greeks introduced an instrument called "the astrolabe" for measuring the altitudes of stars, or their angle of elevation above the horizon. Surveyors of ancient times in the 15th century BC determined level lines by primitive instruments, which consisted of a tube turned upward at both ends and filled with water, used for establishing the grades of canals. In other words, heights or height differences were being determined with reference to equilibrium water levels.

With the advance of science, mankind has realized that heights determined from the form of an equilibrium liquid surface (which we now call the 'geoid') is dependent on the earth's gravity field, and hence the concept of height roused instinctively in the ancient days could be exactly defined in a physico-mathematical form as the vertical distance between the equipotential surfaces of the earth's gravity field [Biro, 1983].

The determination of height has always had a major impact on the economy of human society. With human's ability to determine height , the shape of the earth is no more a mere imaginary concept, such as the belief man once held that the earth was a flat disc floating on an infinite ocean. Height determination is important because it forms the

foundation of many scientific theories, and it is a factor in the management of economic life, and in the scheme and performance of all sorts of technical designs.

With the launching of artificial satellites in space, the determination of the geoid has been one of the prime goals of geodesy. For example, the Global Positioning System (GPS) provides coordinate differences in a geocentric cartesian coordinate system. These coordinate differences can, in turn, be converted to differences in latitude, in longitude and in height on an ellipsoid, provided that their positions relative to the geocentric cartesian coordinate system are known. However, these ellipsoidal heights are not those heights (known as orthometric heights) which are obtained from spirit levelling.

Height has been defined in many ways depending on the reference surface that is chosen. For example, normal height uses a quasigeoid as the reference surface, while orthometric and dynamic heights use the geoid [Vanicek and Krakiwsky, 1982]. However, it is not the intention here to give anything more than a brief review of heights. Nassar [1977] and Carrera [1984] discussed many different types of height systems and their reference surfaces, and interested readers can refer to them.

For mapping and other purposes, orthometric heights are used exclusively in practice rather than geometrical ellipsoidal heights [Schwarz et al., 1987]. Since heights obtained from artificial satellites are ellipsoidal heights (h), it is required to transform these heights into orthometric heights (H) using the well known relationship:

$$H = h - N \quad 1.1$$

where N is the separation between the geoid and the ellipsoid, known as the geoidal height. Likewise for points, whose heights obtained from spirit levelling, require geoidal heights to transfer to ellipsoidal heights for the reduction of distances on the ellipsoid. When

orthometric heights, rather than the ellipsoidal heights, are used for the reduction of distance, approximately one part per million of relative error could be introduced for every 6.4 metres of height [Vanicek and Krakiwsky, 1982]. Therefore, determining geoidal height with respect to some reference surface is necessary for the accurate reduction of ellipsoidal height to orthometric height or reduction of surface distance to reference surface.

Other than the above reductions, geoidal heights have been used in many other applications, such as in studies related to sea surface topography, vertical crustal movements, postglacial deformations, etc. Scientists have often turned their attention to explore paths which could extend our knowledge of geoidal heights in surveyed areas to that in unsurveyed areas based on the fundamental assumption that the geoid in the unsurveyed areas bears specific predictable relationships to that in the surveyed areas.

The arrival at such a solution has been achieved utilizing various data such as (1) deflection of the vertical, (2) surface gravimetry data, (3) satellite-derived information related to the gravitational field of the earth, (4) or the combination of using data (1), (2) and (3). Data (2) are used to determine the short wavelength of the geoidal height using the classical Stokes's formula and data (3) is obtained by employing different techniques of satellite tracking which represent the long wavelength components of the geoidal height. Tools, such as Global Positioning Systems(GPS), transits and geodetic measurement instruments, can be used to obtain geoidal height, either directly or indirectly. The GPS satellite positioning and the Doppler satellite positioning determine the ellipsoidal height. Together with orthometric height known from spirit levelling, the geoidal height can be derived as mentioned above.

The method of mixing the lower degree components of geopotential from satellite technique with the terrestrial gravity data has led to a new breed of geoid determination

called the "combination solution". This method has been tested very extensively throughout the United States and Canada and has shown a substantial improvement in the accuracy of the geoidal height where gravimetric data were available in sufficient coverage along with satellite data [Engelis, et al.(1984, 1985), Schwarz, et al.(1987), Mainville (1987), Vanicek and Kleusberg (1987), Rapp and Kadir (1988)]. The fundamental idea of this theoretical relation is to construct a means to unite the gravity anomalies derived from surface gravity measurements with the geopotential coefficients derived from observations of the satellite orbit.

Geoidal height computation had been carried out by various researchers, such as Schwarz and Sideris [1985], Kearsley [1985, 1986a, 1986b] and Vanicek and Kleusberg [1986]. The results of the various authors differ with respect to the gravity data available and the methods employed for handling the non-uniform distribution of the data. Vanicek and Kleusberg produced geoidal heights by combining GEM9 solutions with terrestrial gravity anomaly derived results, while Schwarz and Sideris computed geoidal heights using a combination of a 36 by 36 geopotential model (GEM10b), terrestrial gravity anomalies and terrain effects. The traditional "Ring" method had been used by Kearsley to obtain geoidal heights. He combined the results obtained from terrestrial gravity anomalies with the results obtained from the 180 by 180 geopotential model (RAPP180). In other words, the geoidal height is obtained by two parts: (a) the inner zone contribution which is derived from terrestrial gravity anomalies, and (b) the remote zone contribution which is derived from geopotential coefficients.

This thesis has two main objectives, namely: to develop a software package for computing geoidal height difference using terrestrial gravity anomalies; and to compare its results (after adding to the remote zone contribution) with the results which are derived from other independent methods. The algorithm used to develop the software is very

similar to that of the investigation conducted by Kearsley [1985, 1986a, 1986b] where geoidal height computation for the inner zone contribution is carried out by ring integration. Theoretically, gravity anomaly data are supposed to be known at every point on the earth's surface. However, these are still missing over large parts of the oceans and lands. This method, at which geoidal height is computed in two parts, can overcome the problem in getting all the data. One such approach for computing the inner zone contribution is simply to divide the surface of the earth into rings and each ring into compartments. The other approach is the division of the earth's surface in terms of "fixed blocks" which are formed by grid lines of geographical coordinates. Since, in practice, not all the compartments would have gravity anomalies, predicted values in the centers of all compartments are therefore being sought to facilitate the process. These predicted values in each of the compartments are then summed up to give geoidal height difference for the inner zone contribution.

In Chapter Two, some terminology which is used in this thesis will be defined and each of the terms will be defined in a separate section.

Chapter Three describes Vanicek et al.'s [1986] method using the classical Stokes approach to compute geoidal heights. The derivation of formulas for the Stokes(UNB) approach will be shown in the first four sections. The purpose of this is to employ their results (called the "UNB Dec.'86" solution) for comparison with the ring integration solutions in the later chapter. This UNB Dec.'86 solution is computed using the University of New Brunswick's program, named "GIN" [Chang et al., 1986]. Effects on geoidal heights, such as the "squashing" of masses onto the geoid, the changes of mass distribution which is called the "indirect effect", and the air masses on the surface of the earth, are reviewed in last three sections.

Chapter Four describes the types of data and the numerical integration techniques which are used in the computation for the UNB Dec.'86 geoid. The numerical integration has been carried out in three different zones: namely, the innermost zone, the inner zone and the outer zone. Each of these zones will be discussed in a separate section.

Chapter Five is devoted to the development of the ring approach. This chapter is divided into four sections. The first section shows the theory and the techniques applied for geoidal height computation. An algorithm for generating the rings is then designed in the second section and this section is further subdivided into three subsections for the inner, middle and outer sub-zones contributions. The third section presents the method of arithmetic mean used for prediction of mean gravity anomalies.

Chapter Six focuses on the results of the computations and compares the derived geoidal height differences obtained from the Ring Integration approach with the results obtained from other independent methods. This chapter is composed of three sections: the first section discusses the Manitoba GPS Network from which its results are used as the control data; in the second section, intercomparisons between the results obtained from the UNB approach, the ring integration approach and the GPS approach will be shown; and finally, the error analysis is discussed briefly in the last section.

Chapter Seven summarizes the contribution of the development of the computer software. The conclusion is based on the results of this investigation. Furthermore, recommendations are discussed for improvements of the softwares and its results.

Finally, the list of references is found toward the end of this thesis.

CHAPTER TWO

DEFINITIONS

Before we proceed any further, let us define some of the terminology in this chapter. Although one might find that the terms are interrelated, they will be discussed separately wherever possible.

2.1 Gravity Potential of the Earth

The earth we live on is a rotating body with its axis of rotation passing through the center of mass. Because of the presence of the earth's mass and the motion of its rotation, a body at rest with respect to the earth's surface would feel two forces acting on it. One of the forces is known as the gravitational force F_g , which is caused by the earth's mass, and the other force, called the centrifugal force F_c , is caused by the earth's rotation. The sum of these two forces is known as the gravity force F_s [Vanicek and Krakiwsky, 1982].

$$F_s = F_g + F_c. \quad 2.1.1$$

In practice, it is customary to deal with accelerations, rather than with forces. Since the gravity force is a product of acceleration a_s and mass m as we know from Newton's

Second Law:

$$F_s = ma_s, \quad 2.1.2$$

we can then treat m as the scale of the gravity force and put more emphasis on the gravity acceleration. This gravity acceleration \mathbf{a}_s , as can be seen from equation (2.1.1), can also be expressed as the sum of the gravitational acceleration \mathbf{a}_g and centrifugal acceleration \mathbf{a}_c :

$$\mathbf{a}_s = \mathbf{a}_g + \mathbf{a}_c. \quad 2.1.3$$

When a mass m , which has a gravity force \mathbf{F}_s acting upon it, is moved through a distance h , the change in kinetic energy which takes place in a straight line in the direction of the force is known as work done. The negative amount of the work done to overcome this force is known as the gravity potential W_t . The gravity potential in here can be expressed as the sum of the gravitational potential W_g and centrifugal potential W_c :

$$W_t = W_g + W_c. \quad 2.1.4$$

2.2 The Gravity Potential of an Ellipsoid

Mathematically, the earth is approximated by a biaxial geocentric ellipsoid with the axis of rotation coinciding with the earth's principal polar axis of inertia [Vanicek and Krakiwsky, 1982]. This ellipsoid is chosen in such a way that the deviation of its "normal field" from the actual gravity field is close to zero. The gravity potential of the ellipsoid is known as normal potential U and its gradient ∇U is known as the normal gravity $\vec{\gamma}$.

$$\vec{\gamma} = \nabla U. \quad 2.2.1$$

The normal gravity at any point $P(\phi, \lambda)$ on the reference ellipsoid can be determined through the International Gravity Formula 1980:

$$\gamma_0 = 978.0327(1 + 0.0053024 \sin^2 \phi - 0.0000058 \sin^2 \phi) \text{ gal} \quad 2.2.2$$

with the maximum error of $1\mu\text{Gal}$ [Moritz, 1980].

2.3 Disturbing Potential

For every point P which lies on and outside the surface of the earth, there exists two potentials: the normal gravity potential U and the actual gravity potential W . The deviation of the normal gravity potential U from the actual gravity potential W is called the disturbing potential or anomalous potential and is denoted as T :

$$T = W - U. \quad 2.3.1$$

2.4 Reference Ellipsoid

A reference ellipsoid is an equipotential surface of the field which generates the normal gravity as in equation (2.2.2). It is also a mathematical representation of the size and the shape of the earth. Its center is assumed to coincide with the center of mass of the earth and its mass is assumed to be equal to the mass of the earth. Its axis of rotation and its angular velocity are identical to those of the earth, too. Commonly, the ellipsoid is defined by its major-semi axis and its flattening.

For the last 100 years, geodesists have been estimating the best fitting ellipsoids to the geoid. The question then is: which reference ellipsoid should we adopt to obtain the best representation of the earth? Heiskanen and Moritz [1985] claim that it is the one whose sum of the squares of the deviations of the geoid from the ellipsoid is the minimum.

With today's modern technologies, the determination of the flattening of the earth can be obtained very accurately from the perturbation of artificial satellite orbits [Vanicek and Krakiwsky, 1982]. Highly precise measurements of the earth's semi-major axis can be acquired from distances measured by instruments based on electromagnetic waves.

Since instruments and techniques are improving every day, the fitting of the ellipsoid on the geoid is improving, too. Today, the adopted reference ellipsoid is the Geodetic Reference System 1980 (GRS 80) with its ellipsoidal parameters defined as follows [Moritz, 1980]:

semi-major axis, $a = 6,378,137$ metres,

reciprocal flattening, $1/f = 298.257\ 222\ 101$,

geocentric gravitational constant, $GM = 3\ 986\ 055\ X\ 10^8\ m^3\ s^{-2}$,

angular velocity, $\omega = 7\ 292\ 115\ X\ 10^{-11}\ rad\ s^{-1}$.

2.5 Geoid

We had spoken of the gravity potential in the previous section. If this potential is constant on a surface, we called this surface an "equipotential surface". There are, of course, countless numbers of equipotential surfaces when one selects different values for the potentials. Out of all these countless number of equipotential surfaces, the one which coincides, more or less, with the surface of the oceans is called the "geoid". This definition was given by J.K.F Gauss as being the mathematical figure of the earth [Vanicek and Krakiwsky, 1982].

The geoid represents a horizontal surface at sea level. It continues beneath the continents so as to encircle the earth. The height of the terrain above this geoid is called the orthometric height or the dynamic height. The distance between the ellipsoid and the geoid is called the geoid undulation or simply "geoidal height". One of the reasons that the ellipsoid is often referred to is because its gravity field is analytically defined, i.e., it is easy to handle mathematically. The deviation of the actual gravity field on the geoid from the

normal gravity field on the ellipsoid, as it has been mentioned in the last section, plays an important role in geodesy, e.g. height determination, orbit's perturbation, etc. Merry [1975] in his Ph.D. thesis had mentioned some of the influences of gravity fields on the instruments in the field of surveying. It is clear by now that the geoid is physically meaningful as opposed to the ellipsoid which is a mathematical representation. It is indeed, the use of the geoid that simplifies geodetic problems and makes them accessible to geometrical intuition [Heiskanen and Moritz, 1985].

2.6 Gravity Anomaly

In the previous sections, the geoid and the ellipsoid were defined. Now let us consider gravity observed on the surface of the earth. When observed gravity is reduced onto the geoid at point P_o , it is called the reduced actual gravity. This point is projected down along the ellipsoid normal onto the ellipsoid surface at point Q whose normal gravity is obtained using equation (2.2.2). The difference between the reduced actual gravity and the normal gravity is known as the gravity anomaly.

A double projection has been performed from one surface (the geoid) to another (the ellipsoid). First of all, the observed gravity at point P on the surface of the earth is projected onto the geoid along the plumb line obtaining a point P_o ; and secondly, the gravity at this projected point P_o is then projected further onto the reference ellipsoid surface by means of the straight ellipsoidal normal getting a point Q . This double projection is known as "Pizzetti's projection" [Heiskanen and Moritz, 1985]. The reason that this double projection is adopted is because there is an exact correspondence between the gravity at point P (on the surface of the earth) and the gravity at an ellipsoidal point Q (on the ellipsoid).

Gravity anomalies are the basic material of gravimetry. According to Pick et al. [1973], gravity anomalies were introduced by geophysicists for the study of the internal structure of the earth, particularly the earth's crust. The advantage of working with gravity anomalies, rather than gravity, is that the gravity anomaly values are small and comfortable to handle and thus easy for computations. Although the internal structure of the earth is not important to geodesists, they do take the advantage of the small values of the gravity anomalies for their works and such gravity anomalies have been used very widely in the classical terrestrial geodesy [Vanicek, 1971].

Since gravity anomalies depend on the reference ellipsoid that is used, many different values for the gravity anomalies can be obtained for a point. Therefore, one has to choose the appropriate reference ellipsoid for his work.

CHAPTER THREE

THE UNB APPROACH

The basic mathematical formula for computing a geoidal height N with respect to a reference ellipsoid using gravity anomalies was derived by an English physicist named George Stokes in 1849. Since the gravity anomaly Δg at one point does not relate directly to the geoidal height at the same point, an integration must be performed using all the gravity anomalies over the whole surface of the earth. Unfortunately, gravity has not been observed all around the earth, especially at the ocean. Stokes's formula, hence, had hardly any practical value at the time of its derivations. It was necessary, then, to develop other techniques which could combine all available information in a world geodetic system. Such available information includes the astrogeodetic deflections of vertical, astronomic and geodetic measurements and gravity measurements. Today, with the launching of earth's artificial satellites, information derived from the satellites can be used to compute geoidal heights.

Since the problem with using the classical Stokes's formula is that all gravity anomalies over the earth must be known, it is necessary to modify this formula in such a way that the integration is carried out only over a spherical cap of a limited radius (*e.g.*, $\psi_0 = 6.0^\circ$) as were done by Vanicek et al.[1986]. However, when this integration is restricted within a spherical cap, the N obtained this way is not the full geoidal height but rather a partial contribution to N . In order to recover the other portion of N , long wavelength contribution has to be added to it to obtain a full geoidal height. In other

words, the combination of surface gravity with satellite derived information to compute a full geoidal height. The GEM9 geopotential coefficients were used to compute the long wavelength of "UNB Dec.'86" Geoid. The first, second and third sections will review the derivation of the Stokes formula, the spheroidal kernel and the modified spheroidal kernel, respectively. The succeeding three sections describe the topographic effect, the indirect effect and the atmospheric effect on the geoidal height.

3.1 The Stokes Formula

As mentioned in the previous chapter, the disturbing potential $T(Q)$ was defined as the difference between the actual gravity potential $W(Q)$ and the normal gravity potential $U(Q)$ at point Q (See Figure 3.1) :

$$T(Q) = W(Q) - U(Q), \quad 3.1.1$$

where point Q is given by geocentric radius r , geocentric latitude ϕ , and geocentric longitude λ . The normal gravity potential $U(Q)$ at point Q can be developed in a Taylor's series with respect to point Q_o on surface S_3 :

$$U(Q) = U(Q_o) + N \left(\frac{\partial U(Q_o)}{\partial v} \right) \cos(\eta, v) + \dots, \quad 3.1.2$$

where η and v are the normals to surfaces S_1 and S_3 , respectively and N (geoidal height) is the distance between Q and Q_o . Substituting for $U(Q)$ in equation (3.1.1) from equation (3.1.2), we get

$$T(Q) = W(Q) - U(Q_o) - N \left(\frac{\partial U(Q_o)}{\partial v} \right) \cos(\eta, v) - \dots \quad 3.1.3$$

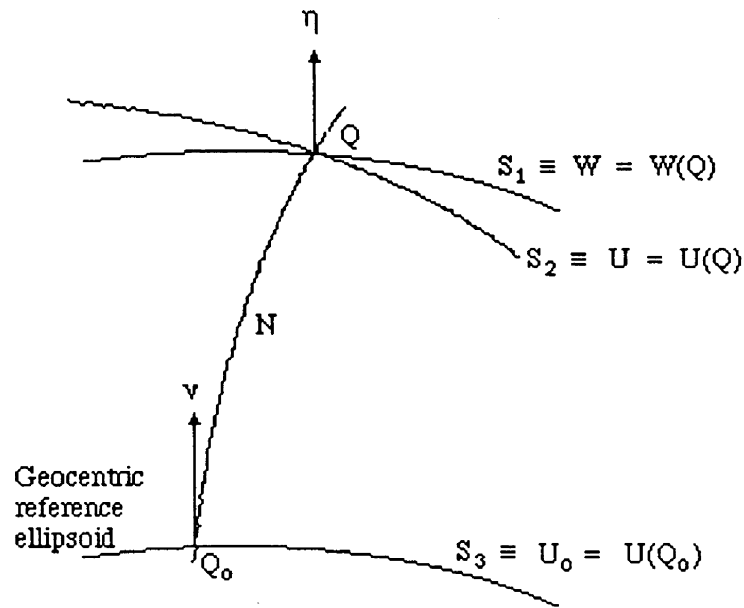


Figure 3.1: The Disturbing Potential [$W(Q) - U(Q)$].

Since [Torge, 1980]

$$\frac{\partial U(Q_o)}{\partial v} = -\chi(Q_o), \quad 3.1.4$$

then

$$T(Q) = W(Q) - U(Q_o) + N \chi(Q_o) \cos(\eta, v) - \dots \quad 3.1.5$$

The angle (η, v) is very small (less than 1 minute); therefore solving equation (3.1.5) for N , we arrive at:

$$N \doteq \frac{T(Q)}{\chi(Q_o)} - \frac{W(Q) - U(Q_o)}{\chi(Q_o)}. \quad 3.1.6$$

When solving the geodetic boundary-value problem, one of the assumptions made is that the potential on the reference ellipsoid $U(Q_o)$ is equal to the potential on the geoid $W(Q)$ [Torge, 1980, p.171]. Then the second term of the right hand side of equation (3.1.6) will become zero. What remains now in equation (3.1.6) is:

$$N \doteq \frac{T(Q)}{\chi(Q_o)}, \quad 3.1.7$$

which is known as the "Bruns's formula".

Since the disturbing potential cannot be measured, the earth's gravity is the main source to be used for computing the geoidal height N . In order to be able to use this, we must differentiate equation (3.1.1) with respect to the direction of the external normal η :

$$\frac{\partial T(Q)}{\partial \eta} = \frac{\partial W(Q)}{\partial \eta} - \frac{\partial U(Q)}{\partial \eta}. \quad 3.1.8$$

Since the derivative of the actual gravity potential with respect to the normal η is the negative earth's gravity, and the derivative of the normal gravity potential with respect to the normal ν is the negative normal gravity:

$$\frac{\partial W(Q)}{\partial \eta} = -g(Q), \quad 3.1.9$$

$$\frac{\partial U(Q)}{\partial \eta} \doteq \frac{\partial U(Q)}{\partial \nu} = -\chi(Q). \quad 3.1.10$$

Then, equation (3.1.8) can be rewritten as follows:

$$\frac{\partial T(Q)}{\partial \eta} \doteq -g(Q) + \chi(Q), \quad 3.1.11$$

where both g and χ are evaluated on surfaces $W = W(Q)$ and $U = U(Q)$, respectively. By expanding $\chi(Q)$ into a Taylor's series with respect to point Q_o , we arrive at:

$$\chi(Q) = \chi(Q_o) + N \left(\frac{\partial \chi(Q_o)}{\partial \nu} \right) \cos(\eta, \nu) + \dots \quad 3.1.12$$

After neglecting the higher order term of equation (3.1.12) and substituting it into equation (3.1.11), we arrive at the following form:

$$\frac{\partial T(Q)}{\partial \eta} = -g(Q) + \chi(Q_0) + N \left(\frac{\partial \chi(Q_0)}{\partial \nu} \right) \cos(\eta, \nu). \quad 3.1.13$$

Since

$$\Delta g(Q) = g(Q) - \chi(Q_0) \quad 3.1.14$$

is the gravity anomaly as defined previously, Δg can be replaced in equation (3.1.13) to yield:

$$\frac{\partial T(Q)}{\partial \eta} = -\Delta g(Q) + N \left(\frac{\partial \chi(Q_0)}{\partial \nu} \right) \cos(\eta, \nu). \quad 3.1.15$$

Therefore

$$\Delta g(Q) = -\frac{\partial T(Q)}{\partial \eta} + N \left(\frac{\partial \chi(Q_0)}{\partial \nu} \right) \cos(\eta, \nu). \quad 3.1.16$$

It should be noted that the direction of the radius vector \mathbf{r} is almost the same as that of the normal to the ellipsoid: i.e.

$$\frac{\partial}{\partial \eta} \doteq \frac{\partial}{\partial \nu} \doteq \frac{\partial}{\partial r}.$$

Since $\cos(\eta, \nu) \doteq 1$ for small η and ν , the second term in equation (3.1.16) can be replaced by

$$N \left[\frac{\partial \chi(Q_0)}{\partial \nu} \right] \doteq \frac{T}{\gamma} \left[\frac{\partial \chi(Q_0)}{\partial r} \right] \doteq -\frac{2}{r} T. \quad 3.1.17$$

Equation(3.1.16), therefore, can be rewritten as follows:

$$\Delta g(Q) = - \frac{\partial T(Q)}{\partial r} - \frac{2}{r} T(Q). \quad 3.1.18$$

It is called the fundamental gravimetric equation of geodesy.

The disturbing potential can be expanded into a series of spherical harmonics, with the omission of the zero and the first degree harmonics:

$$T(Q) = \sum_{n=2}^{\infty} \left\{ \frac{R}{r} \right\}^{n+1} T_n(Q), \quad 3.1.19$$

where R is the geocentric radius of the earth and T_n is the Laplace's surface harmonics of degree n . The reason for omitting the zero and the first degree harmonics is that we assume the mass of the geoid equals to the mass of the equipotential ellipsoid and the center of the ellipsoid coincides with the center of mass of the earth, respectively.

Taking the derivative of $T(Q)$ with respect to r , we get:

$$\frac{\partial T(Q)}{\partial r} = - \frac{1}{r} \sum_{n=2}^{\infty} \left\{ \frac{R}{r} \right\}^{n+1} (n+1) T_n(Q). \quad 3.1.20$$

By substituting equations (3.1.19) and (3.1.20) into equation (3.1.18), we arrive at:

$$\Delta g(Q) \doteq \frac{1}{r} \sum_{n=2}^{\infty} \left\{ \frac{R}{r} \right\}^{n+1} (n-1) T_n(Q). \quad 3.1.21$$

Since we are dealing with the geoid, i.e., the geocentric radius is equal or replaced by the mean radius of the earth R , then equation (3.1.21) becomes:

$$\Delta g(Q) \doteq \frac{1}{R} \sum_{n=2}^{\infty} (n-1) T_n(Q). \quad 3.1.22$$

The gravity anomaly $\Delta g(Q)$ can also be represented by an harmonic expansion [Torge,1980, p.157]:

$$\Delta g(Q) = \sum_{n=2}^{\infty} \Delta g_n(Q). \quad 3.1.23$$

A comparison between equations (3.1.22) and (3.1.23) indicates that

$$\forall n: \Delta g_n(Q) = \frac{n-1}{R} T_n(Q). \quad 3.1.24$$

Solving for $T_n(Q)$, we have

$$\forall n: T_n(Q) = \frac{R}{n-1} \Delta g_n(Q). \quad 3.1.25$$

Then from equation(3.1.19) and setting $r = R$,

$$T(Q) = \sum_{n=2}^{\infty} T_n(Q) = R \sum_{n=2}^{\infty} \frac{\Delta g_n(Q)}{n-1}. \quad 3.1.26$$

The gravity anomalies $\Delta g_n(Q)$ can be computed by integrating Δg over the whole earth's surface [Torge, 1980] :

$$\Delta g_n(Q) = \frac{2n+1}{4\pi} \iint \Delta g P_n(\cos \psi) ds, \quad 3.1.27$$

where $\psi = \cos^{-1}(\sin \phi \sin \phi^* + \cos \phi \cos \phi^* \cos(\lambda^* - \lambda))$ is the spherical distance between the point of interest $Q(\phi, \lambda)$ and the point $Q^*(\phi^*, \lambda^*)$ representing the surface element ds , and $P_n(\cos \psi)$ is the Legendre's polynomial of degree n . Replacing $\Delta g_n(Q)$ in equation (3.1.26) by equation (3.1.27), we obtain:

$$T(Q) = \frac{R}{4\pi} \sum_{n=2}^{\infty} \iint \frac{2n+1}{n-1} \Delta g P_n(\cos \psi) ds. \quad 3.1.28$$

Exchanging the order of the summation and the integration yields:

$$T(Q) = \frac{R}{4\pi} \iint \sum_{n=2}^{\infty} \frac{2n+1}{n-1} P_n(\cos \psi) \Delta g \, ds, \quad 3.1.29$$

or equivalently

$$T(Q) = \frac{R}{4\pi} \iint S(\psi) \Delta g \, ds, \quad 3.1.30$$

where

$$S(\psi) = \sum_{n=2}^{\infty} \frac{2n+1}{n-1} P_n(\cos \psi) \quad 3.1.31$$

is called "Stokes's function". The geoidal height N , can be determined by applying the Bruns's formula:

$$N(Q) = \frac{T(Q)}{\gamma} = \frac{R}{4\pi\gamma} \iint S(\psi) \Delta g \, ds. \quad 3.1.32$$

Equation (3.1.32) is known as "Stokes's formula".

3.2 The Spheroidal Kernel

Today, in most practical cases, the integration in equation(3.1.32) is carried out in two parts: the "low degree" surface N^ℓ and the "high degree" surface δN^ℓ .

$$N(Q) = N^\ell(Q) + \delta N^\ell(Q), \quad 3.2.1$$

where

$$N^\ell(Q) = \frac{R}{4\pi\gamma} \iint \sum_{n=2}^{\ell} \frac{2n+1}{n-1} P_n(\cos \psi) \Delta g(Q^*) \, ds, \quad 3.2.2$$

$$\delta N^{\ell}(Q) = \frac{R}{4\pi\gamma} \iint \sum_{n=\ell+1}^{\infty} \frac{2n+1}{n-1} P_n(\cos \psi) \Delta g(Q^*) ds. \quad 3.2.3$$

The determination of the low degree gravity field constituents from satellite observations is given in terms of an expansion of the gravitational potential in spherical harmonics as follows [Vanicek et al., 1986]:

$$V(r, \phi, \lambda) = \frac{GM}{r} \left[1 + \sum_{n=2}^{\ell} \sum_{m=0}^n \left\{ \frac{a}{r} \right\}^n (J_{nm} Y_{nm}^c + K_{nm} Y_{nm}^s) \right], \quad 3.2.4$$

where GM is the product of the gravitational constant and the mass of the earth; a is the mean earth equatorial radius; Y_{nm}^c and Y_{nm}^s are the normalized spherical harmonic

functions, J_{nm} and K_{nm} are the potential coefficients. The potential field model which is chosen for comparison is the GEM9 and is complete through degree $\ell = 20$. This V is then transformed into T using equation (3.1.1) where W_T is the sum of the gravitational potential and the centrifugal potential 'Z':

$$T = W_T - U = (V + Z) - U. \quad 3.2.5$$

With T known and by applying the Bruns's formula, the geoidal height N can be calculated as follows:

$$N^{\ell} = N_{20}(\phi, \lambda) = R \sum_{n=2}^{20} \sum_{m=0}^n (J'_{nm} Y_{nm}^c + K_{nm} Y_{nm}^s), \quad 3.2.6$$

with R being some mean earth radius and $J'_{nm} = J_{nm}$ for $n \neq 2, 4, 6$ and $m \neq 0$. J'_{nm} for $n = 2, 4, 6$ and $m = 0$ is given in Vanicek et al. [1986]. The accuracy of N_{20} depends on the variances and covariances of the potential coefficients J'_{nm} and K_{nm} . Using the law of error propagation, it is discovered that the geoidal height error induced by GEM9 potential coefficient errors can be up to about 1.75 metres. A well-known computer program (subroutine POT), prepared by Tscherning et al. [1983] can be used to generate N^{ℓ} .

The evaluation of high order surface from terrestrial gravity data is the main issue of this section. This technique was developed by Vanicek et al. [1986] to overcome the incomplete area of integration effect by limiting it to a spherical cap around the point of interest. This high order surface's kernel :

$$S_{\ell}(\psi) = \sum_{n=\ell+1}^{\infty} \frac{2n+1}{n-1} P_n(\cos \psi), \quad 3.2.7$$

which is called "the spheroidal kernel", converges to zero more rapidly than the ordinary Stokes's function, $S(\psi)$ [Vanicek and Kleusberg, 1987] for an increasing spherical distance ψ .

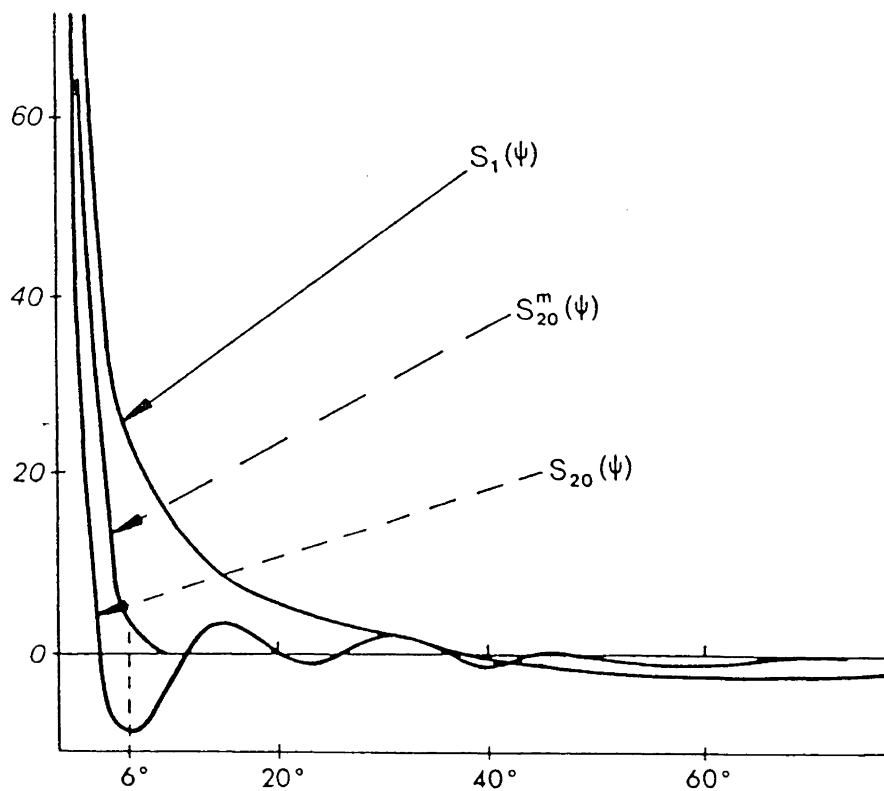


Figure 3.2: Comparison Between $S(\psi)$, $S_{20}(\psi)$ and $S_{20}^m(\psi)$ [after Vanicek and Kleusberg (1986,p.130)].

Figure 3.2 shows the functions $S(\psi)$, $S_{20}(\psi)$ and $S_{20}^m(\psi)$, where $S_{20}^m(\psi)$ is the modified Stokes function which will be described in the next section. It therefore can be concluded that the truncation errors of the spheroidal integration at a certain spherical distance are smaller than those of the ellipsoidal integration. The spheroidal kernel $S_{20}(\psi)$ not only has a smaller truncation error but also has eliminated the effect of the spherical approximation used in the Stokes's formula. The long wavelength's effect would be lessened when this method is used and this leads the spheroidal kernel to attenuate the disadvantage of inhomogeneous coverage of data around the earth. The integration, thus, does not have to be performed globally, but rather within a small spherical cap.

3.3 The Modified Spheroidal Stokes's Function

By limiting the size of the integration area, the accuracy obtained through the spheroidal kernel is degraded. This problem leads to a modification of the spheroidal kernel using the Molodenskij's truncation coefficients. In other words, the spheroidal Stokes's function has to be modified in such a way that its accuracy is not lost. This "modified spheroidal kernel" $S_{20}^m(\psi)$ is obtained through the following expression:

$$S_{\ell}^m(\psi) = S_{\ell}(\psi) - S_{\ell}^*(\psi), \quad 3.3.1$$

where

$$S_{\ell}^*(\psi) = \sum_{i=0}^{\ell} \frac{2i+1}{2} t_i P_i(\cos \psi) \quad 3.3.2$$

and t_i are the coefficients to be determined. The modification of the spheroidal kernel leads to the requirement that the low degree constituents must be subtracted from the terrestrial

gravity anomalies before the integration in equation(3.2.3) is preformed. By expressing the gravity anomalies in terms of spherical harmonics:

$$\Delta g^{\ell}(\psi, \alpha) = \sum_{i=\ell+1}^{\infty} \Delta g_i(\psi, \alpha), \quad 3.3.3$$

equation(3.2.3) can be rewritten as follows:

$$\delta N^{\ell}(Q) = \frac{R}{4\pi\gamma} \iint \sum_{n=\ell+1}^{\infty} \frac{2n+1}{n-1} P_n(\cos \psi) \Delta g^{\ell}(Q^*) ds. \quad 3.3.4$$

By minimizing the truncation error of the high order surface and applying the Schwartz inequality, we come up with a condition:

$$\int_{\psi=\psi_0}^{\pi} S_{\rho}^m(\psi) P_i(\cos \psi) \sin \psi d\psi = 0; \quad i = 0, 1, \dots, \ell. \quad 3.3.5$$

Making use of equations(3.3.1), (3.3.2) and (3.3.5), the following relationship is obtained:

$$\begin{aligned} & \int_{\psi=\psi_0}^{\pi} S_{\rho}(\psi) P_i(\cos \psi) \sin \psi d\psi \\ = & \int_{\psi=\psi_0}^{\pi} \left[\sum_{k=0}^{\ell} \frac{2k+1}{2} t_k P_k(\cos \psi) \right] P_i(\cos \psi) \sin \psi d\psi. \end{aligned} \quad 3.3.6$$

Letting

$$\int_{\psi=\psi_0}^{\pi} S_{\rho}(\psi) P_i(\cos \psi) \sin \psi d\psi = Q_i^{\ell}(\psi_0) \quad 3.3.7$$

and

$$\int_{\psi=\psi_0}^{\pi} P_i(\cos \psi) P_k(\cos \psi) \sin \psi d\psi = e_{ik}(\psi_0), \quad 3.3.8$$

we have,

$$Q_i^\ell(\psi_0) = \sum_{k=0}^{\ell} \frac{2k+1}{2} t_k e_{ik}(\psi_0). \quad 3.3.9$$

Since

$$S_\ell(\psi) = S(\psi) - \sum_{k=2}^{\ell} \frac{2k+1}{k-1} P_k(\cos \psi), \quad 3.3.10$$

it can be substituted into equation(3.3.7) to obtain

$$\int_{\psi=\psi_0}^{\pi} [S(\psi) - \sum_{k=2}^{\ell} \frac{2k+1}{k-1} P_k(\cos \psi)] P_i(\cos \psi) \sin \psi d\psi = Q_i^\ell(\psi_0) \quad 3.3.11$$

or equivalently

$$Q_i^\ell(\psi_0) = \int_{\psi=\psi_0}^{\pi} [S(\psi) P_i(\cos \psi) \sin \psi d\psi] - \int_{\psi=\psi_0}^{\pi} \sum_{k=2}^{\ell} \frac{2k+1}{k-1} P_k(\cos \psi) P_i(\cos \psi) \sin \psi d\psi. \quad 3.3.12$$

Thus, from equation(3.3.9):

$$Q_i^\ell(\psi_0) = \int_{\psi=\psi_0}^{\pi} [S(\psi) P_i(\cos \psi) \sin \psi d\psi] - \sum_{k=2}^{\ell} \frac{2k+1}{k-1} e_{ik}(\psi_0). \quad 3.3.13$$

The first term on the right-hand side is known as the "Molodenskij's truncation coefficient" [Vanicek and Krakiwsky, 1982]. Paul [1973] has written an efficient algorithm to compute the truncation coefficients. With the truncation coefficients computed, the $Q_i^\ell(\psi_0)$ can then be calculated from equation(3.3.13). The coefficient t_k which determined by substituting equations (3.3.13) into (3.3.9), can be used in equations (3.3.2) and (3.3.1) to obtain the modified spheroidal kernel.

3.4 The Topographic Effect

When solving for the geodetic boundary value problem, it is assumed that no masses should lie outside the geoid. So in other words, the masses outside the geoid have to be removed somehow by condensing them onto the geoid. However, the removal of the masses changes the gravity potential at the surface of the earth. That is, the observed gravity at a point on the surface of the earth is changed. This influence is known as the topographical attraction effect δg_t , and has to be corrected for before the Stokes formula is applied.

To show how these influences take place, let us take for example a value g of the surface gravity at point Q_A which is reduced to the geoid value g_G at the point Q_G (See Figure 3.3) using the free-air gravity gradient $\partial g / \partial H$ and the orthometric height H (expressed in metres):

$$\delta g_F = -\frac{\partial g}{\partial H} H \doteq -\frac{\partial \gamma}{\partial H} H \doteq 0.3086 H \text{ (mGal)}, \quad 3.4.1$$

where the actual gradient is unknown and is replaced by the normal vertical gradient $\partial \gamma / \partial H$.

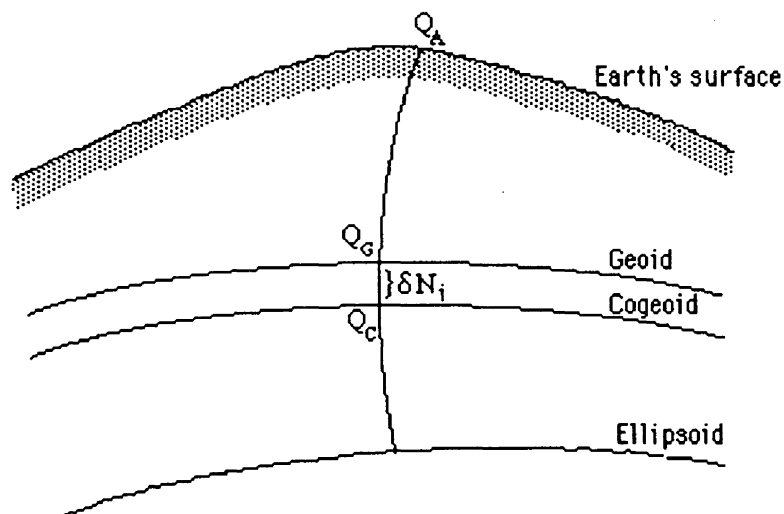


Figure 3.3: The Relationship Between the Geoid, the Cogeoid and the Ellipsoid.

Once the gravity is reduced onto the geoid, it is now necessary to remove all the masses above the geoid. In order to do this, let us approximate locally the geoid by a tangential plane. Assuming that the density σ of the topographical masses is constant, assign ℓ to be the horizontal distance between the point Q_A where the correction is to be made for the topographic effect and the point Q_B where the mass is squashed. This is illustrated in Figure 3.4. The heights for point Q_A and Q_B are indicated by H_A and H_B , respectively.

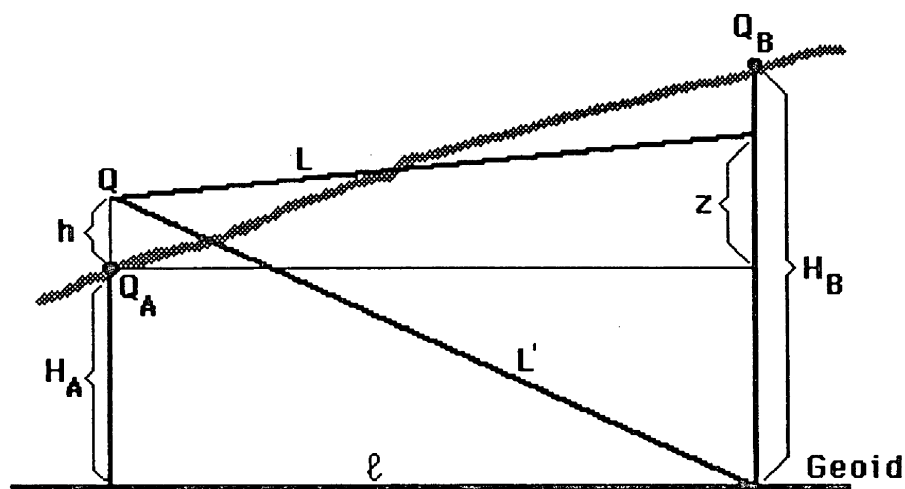


Figure 3.4: The Topographic Effect on the Computation Point [from Vaníček and Kleusberg (1987, p.88)].

Suppose that somewhere below Q_B , with height equal to $H_A + z$ is located a mass element dm :

$$dm = \rho \ell d\alpha d\ell dz, \quad 3.4.2$$

where ℓ is the distance, α is the azimuth and z is the height, reckoned at the geoid below Q_A . The gravity potential effect at Q by this mass would be:

$$dw = Gdm / L, \quad 3.4.3$$

where L is the distance from Q to the point mass. When this mass element is removed by compressing it down onto the geoid, it causes the gravity potential at point Q to change to

$$dw' = Gdm / L' . \quad 3.4.4$$

The observer at point Q will then feel a gravity change equal to the negative vertical gradient of the difference between dw and dw' :

$$\delta g_t = - \frac{\partial}{\partial h} G(dw' - dw)_{h=0} . \quad 3.4.5$$

By integrating over all the mass elements, the total change in gravitational attraction will be obtained. The approximation of equation(3.4.5) is simply stated below without proof:

$$\delta g_t = \frac{G\sigma}{2} \int_{\alpha=0}^{2\pi} \int_{l=0}^{\infty} (H_B^2 - H_A^2) \ell^{-2} dl d\alpha , \quad 3.4.6$$

where α is the azimuth. Interested reader may refer to Vanicek et al. [1986].

Since the data obtained can never be in a continuous form, equation(3.4.6) is then replaced by a discretized form:

$$\delta g_t = \frac{G\sigma R^2}{2} \sum_i (\bar{H}_i^2 - H_A^2) / \ell_i^2 \cos \phi_i a_i^2 , \quad 3.4.7$$

where the bar denotes the mean value and ℓ_i is the distance between the i^{th} cell and the point of interest. The notation " a " is the size of the cell(5') in radian and the notation " H_i " is the topographical height. The summation is extended over all the 5' by 5' cells.

3.5 The Indirect Effect

When we condense the topographic masses mathematically onto the geoid surface, the actual mass distribution is then changed, and hence the geoid changes. Thus, the surface we compute using Stokes's formula is not the geoid, but a different surface called "the cogeoid". The vertical displacement between the geoid and the cogeoid is known as the "indirect effect", δN_{ID} of the geoidal height (See Figure 3.3).

Various authors have mentioned ways to compute the indirect effect for the geoid undulations [Vanicek et al (1986), Wichiencharoen (1982), Heiskanen and Moritz (1985), etc]. One of the methods used in Vanicek et al. [1986] is illustrated in Figure 3.5.

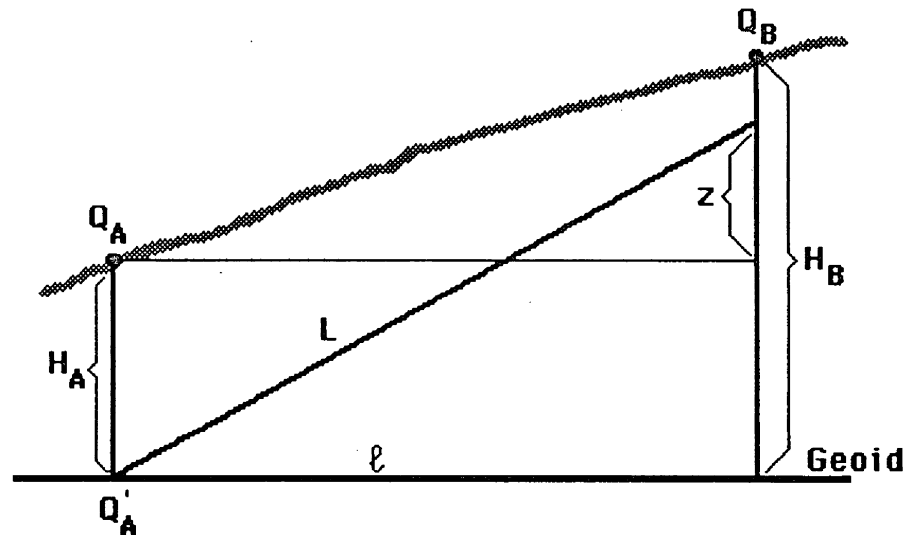


Figure 3.5: The Indirect Effect on the Computation Point [from Vanicek et al.(1986)].

Using the same procedure as in the topographic effect, the gravitational potential at Q'_A (the projection of Q_A) on the geoid, which is affected by a small mass element below Q_B , will be:

$$W_I^* = G\sigma \int_{\alpha=0}^{2\pi} \int_{\ell=0}^{\infty} \int_{y=0}^{H_B} L^{-1} \ell \, d\ell \, d\alpha \, dz . \quad 3.5.1$$

The same mass condensed onto the geoid has a potential of

$$W_2^* = G\sigma \int_{\alpha=0}^{2\pi} \int_{\ell=0}^{\infty} H_B d\ell d\alpha . \quad 3.5.2$$

The change in the gravitational potential dW_{ID} is then the difference between W_1^* and W_2^*

By taking the difference , one can derive:

$$dW_{ID} = W_1^* - W_2^* \quad 3.5.3$$

$$= -\pi G\sigma H_A^2 - \frac{G\sigma}{6} \int_{\alpha=0}^{2\pi} \int_{\ell=0}^{\infty} \frac{H_B^3 - H_A^3}{\ell^2} d\ell d\alpha . \quad 3.5.4$$

Using Bruns's formula, the indirect effect can be determined:

$$\delta N_{ID} = -\frac{(\pi G\sigma)}{\gamma} H_A^2 - \frac{G\sigma}{6\gamma} \int_{\alpha=0}^{2\pi} \int_{\ell=0}^{\infty} \frac{H_B^3 - H_A^3}{\ell^2} d\ell d\alpha \quad 3.5.5$$

and this correction has to be added to the geoid undulation (evaluated by the Stokes integral), algebraically.

In practice, discrete data are used. Therefore, equation(3.5.5) is rewritten as

$$\delta N_{ID} = -\frac{(\pi G\sigma)}{\gamma} H_A^2 - \frac{G\sigma R^2}{6\gamma} \sum_i (\bar{H}_i^2 - H_A^2) / \ell_i^3 \cos \phi_i a_i^2, \quad 3.5.6$$

where \bar{H}_i, H_A, ℓ_i , are as in equation (3.4.7).

3.6 The Atmospheric Effect

One of the assumptions in solving for the geodetic boundary value problem is that no masses should lie outside the geoid. However, there exist air masses above the earth's surface. The attraction of these air masses on the geoid undulation is known as "the atmospheric effect" and it has to be taken into account in the correction to the free-air gravity anomalies in a similar way as that of the topographic masses.

Ecker and Mittermayer [1969] have investigated this effect and the IAG [1971] has published tables for δg_a as a function of topographical height. It is found that for heights from 0 km to 4 km, the atmospheric effect varies from +0.87 mGal to +0.57 mGal, respectively. From Figure 3.6, it should be noted that the effect of the atmosphere decreases as the height of the point increases.

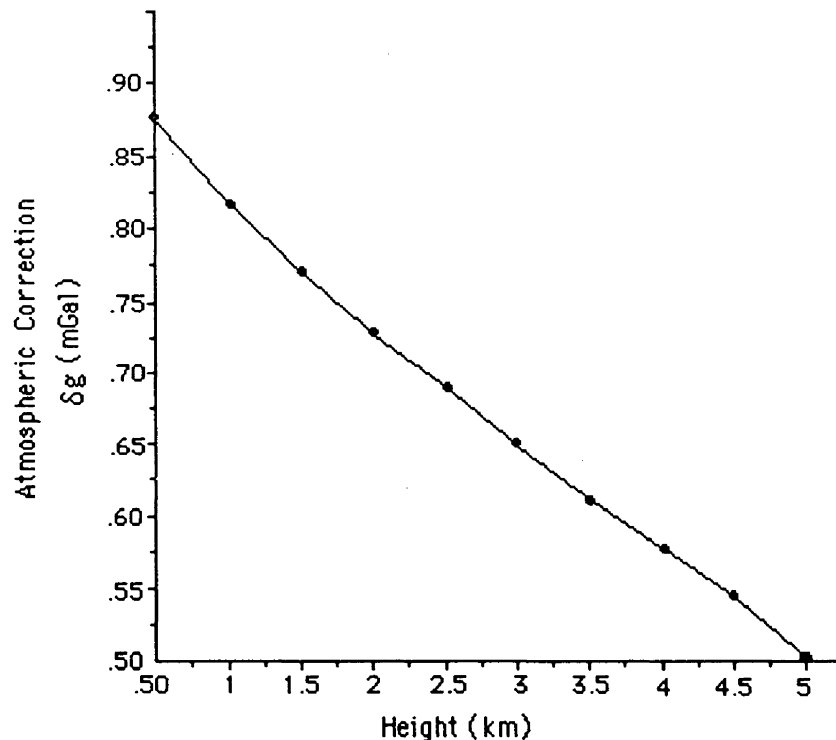


Figure 3.6: The Atmospheric Effect Vs. Height [after IAG (1971)].

CHAPTER FOUR

NUMERICAL INTEGRATION FOR THE UNB APPROACH

4.1 Input Data

In this chapter, only the data structure for the UNB approach is described. Other schemes are used by other people. In order to compare the UNB approach with the ring approach, it is necessary to describe the structure of the input data for both techniques. In the UNB approach as employed by Vanicek et al.[1986], three different types of data are used for the computation, namely: *the point gravity anomalies, the 5 by 5 minute mean gravity anomalies, and the 1 by 1 degree mean gravity anomalies*. Each of these types of data will be discussed separately below.

4.1.1 Point Gravity Anomaly

Two files of point gravity data are provided by the Division of Gravity, Geothermics and Geodynamics of the former Earth Physics Branch of Energy, Mines and Resources Canada [Vanicek and Kleusberg, 1987]. These two files were merged together to form 628,019 records which cover the area (land and sea) from 40° N to 80° N and from 218° E to 320° E [Vanicek et al.(1986)]. Each of these records consists of ϕ , λ , Δg^{ℓ} ,

$\sigma_{\Delta g}^{\ell}$, H , σ_H . The Δg^{ℓ} is the difference between the free-air anomaly and the "Goddard's Earth Model 9" (GEM9) low order harmonic gravity anomaly. The observed value g is referred to the International Gravity Standardization Net 1971 (IGSN71) and γ is referred to the Geodetic Reference System 1980 (GRS80).

The structure of the data as employed by Vanicek et al.[1986] for the GIN program is shown in Figure 4.1. Twenty sequential access files of data have been created with each of the files covering a 10 degree (latitude) by 20 degree (longitude) area, except the rightmost files (east of $\lambda=298^{\circ}$), which are 10 by 22 degrees. Ten minutes of each block is overlaid to the right and upper adjacent blocks (the shaded stripe). The data within each block is arranged in increasing latitude in the northward direction and in increasing longitude in the eastward direction with points of equal latitude.

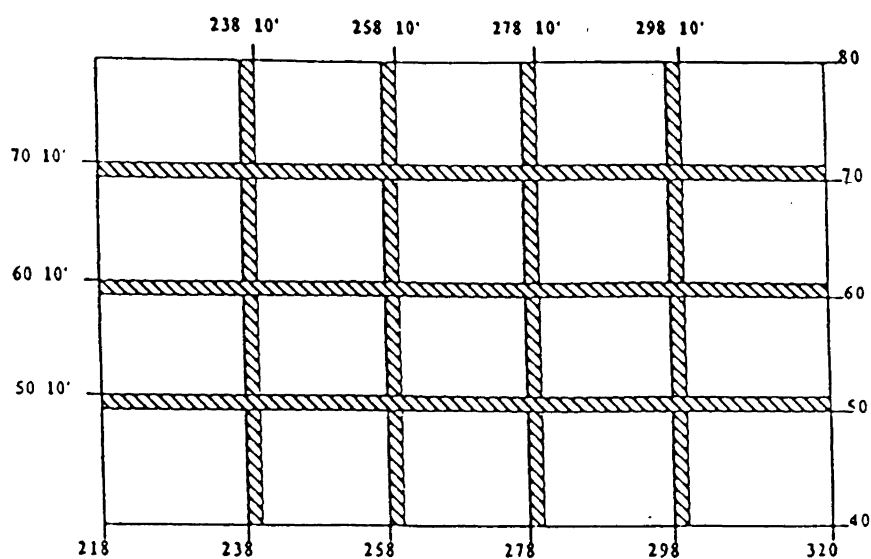


Figure 4.1: Structure of Point Gravity Anomaly Files [from Vanicek et al.(1986, p.40)].

4.1.2 The 5' by 5' Mean Gravity Anomaly

One direct access file has been created for the 5' by 5' mean gravity anomaly. This file has been subdivided into 200, 8° by 8° blocks as shown in Table 4.1. This file covers an area between 40°N and 56°N and between 214° E and 318° E and consists of 9216 records. In order to maintain a rough equi-areality, the size of the cells from 56° N to 76° N is elongated to 5' by 10' (consists of 4608 records). Four degrees of each block is overlapped with the right and upper adjacent blocks. In each block, the records are arranged in the same way as in the point gravity anomaly.

LONGITUDE INTERVAL	LATITUDE INTERVAL
214 - 222	40 - 48
218 - 226	44 - 52
222 - 230	48 - 56
226 - 234	52 - 60
230 - 238	56 - 64
234 - 242	60 - 68
238 - 246	64 - 72
242 - 250	68 - 76
246 - 254	
250 - 258	
254 - 262	
258 - 266	
262 - 270	
266 - 274	
270 - 278	
274 - 282	
278 - 286	
282 - 290	
286 - 294	
290 - 298	
294 - 302	
298 - 306	
302 - 310	
306 - 314	
310 - 318	

Table 4.1: Structure of the 5' by 5' Mean Gravity Anomaly Files [from Vanicek et al. (1986, p.42)].

The 5' by 5' mean gravity anomalies are derived from the point gravity anomalies file using the plain arithmetic means. 3,000 additional means have been predicted by Vanicek et al.[1986] for the empty cells. Each cell contains Δg^{ℓ} (the mean free-air anomaly reduced to GEM9), $\sigma_{\Delta g^{\ell}}$, and H .

4.1.3 The 1 by 1 Degree Mean Gravity Anomaly

The 1 by 1 Degree mean gravity anomaly data used in computing the "UNB Dec.'86" is "*The January 1983 1 by 1 Degree Mean Free-Air Anomaly Data*" which was provided by the Department of Geodetic Science and Surveying of Ohio State University (OSU). The area coverage for the data is: $30^{\circ}\text{N} \leq \phi \leq 80^{\circ}\text{N}$, $190^{\circ}\text{E} \leq \lambda \leq 340^{\circ}\text{E}$. This data set consists of 7701 records, of which 185 hold no information, other than the heights. Using the plain arithmetic mean again, 24 of the 185 1° by 1° mean gravity anomalies have been predicted from existing point gravity anomalies [Vanicek et al., 1986]. Its standard deviation is taken as one half of the absolute value of the predicted mean gravity anomaly minus the GEM9 values and its height remains the same as the original height for the predicted cells. The rest of the 185 records are set with their Δg^{ℓ} equal to zero and $\sigma_{\Delta g^{\ell}}$ equal to 50 mgal [Vanicek and Kleusberg, 1987].

4.2. Numerical Integration

The integration for the Stokes integral was performed analytically over the immediate neighborhood of the computation point. Because of the fact that the data collected are in a discrete form, which is suitable for digital computers, the integration was carried out in three different zones: namely, the innermost zone, the inner zone and the

outer zone. The innermost zone contribution is evaluated using point gravity anomalies and the inner zone contribution is determined employing the 5' by 5' mean gravity anomalies. The outer zone contribution is computed using the 1° by 1° mean gravity anomalies.

4.2.1 The Innermost Zone

The size of the innermost zone is 10' by 10' with its boundaries coinciding with the grid lines of the 5' by 5' gravity anomaly file. The computation point lies inside this zone, but not necessarily in the exact center. The innermost integration is given as follows [Vanicek et al., 1986]:

$$N_{INM} = \frac{R}{4\pi\gamma} \iint_{A_{INM}} S_{\ell}^m \widetilde{\Delta g}^{\ell} d\epsilon, \quad 4.2.1.1$$

where A_{INM} is the area size of the innermost zone and $d\epsilon$ is an element of a spatial angle. By expressing equation(4.2.1.1) in ellipsoidal coordinates ϕ, λ and transforming it onto a (x, y) mapping plane [See Vanicek et al.(1986) for details], this reads

$$N_{INM} = \frac{R}{4\pi\gamma} \int_{x_1}^{x_2} \int_{y_1}^{y_2} S_{\ell}^m(\psi) \widetilde{\Delta g}^{\ell}(x, y) dx dy. \quad 4.2.1.2$$

In the innermost zone, the least-square estimates of the anomaly surface coefficients $\hat{\alpha}_i$, $i=0,1,2,\dots,5$ are determined by fitting all the point gravity anomalies Δg^{ℓ} in the 10' by 10' square to a second-order algebraic surface. If there are not enough Δg^{ℓ} within this square, the number of coefficients is reduced to four. If Δg^{ℓ} are still not enough, the number of coefficients will be reduced further to three and the 5' by 5' mean gravity anomalies will be used instead of the point gravity anomalies [Vanicek and Kleusberg, 1987].

The modified spheroidal Stokes function is approximated by:

$$S_{\ell}^m(\psi, \psi_0) = \frac{2}{\psi} - 3 \ln\left(\frac{\psi}{2}\right) + C(\psi_0), \quad 4.2.1.3$$

where

$$C(\psi_0) = -4 - \sum_{i=2}^{\ell} \frac{2i+1}{i-1} - \sum_{i=0}^{\ell} \frac{2i+1}{2} t_i(\psi_0). \quad 4.2.1.4$$

These two series are then substituted into equation (4.2.1.2). Neglecting the products of non-dominating terms, we get

$$N_{INM} = \sum_{i=1}^8 N_i, \quad 4.2.1.5$$

where N_i is the i^{th} term of the geoidal height contribution to the innermost zone.

4.2.2 The Inner Zone

The inner zone is the area enclosed by a rectangle of dimensions 2° by 2° , minus the innermost zone. The two parallels and the two meridians which bound this zone coincide with the boundaries of the 1° by 1° gravity anomaly file. Mean gravity anomalies of $5'$ by $5'$ (or $5'$ by $10'$) are used in this zone. The integration for the inner zone is written as follows [Vanicek et al., 1986]:

$$N_{IN} = \frac{R}{4\pi\gamma} \iint_{A_{IN}} S_{\ell}^m \widetilde{\Delta g}^{\ell} d\epsilon, \quad 4.2.2.1$$

where A_{IN} is the area size of the inner zone. In practice, equation(4.2.2.1) is expressed as:

$$N_{IN} = \frac{R}{4\pi\gamma} \sum_{i=1}^L S_{\ell}^m(\psi_i) \widetilde{\Delta g}_i^{\ell} \cos\phi_i (5')^2 \quad 4.2.2.2$$

and L is the total number of 5' by 5' cells. $\widetilde{\Delta g}_i^{\ell}$ is the mean gravity anomaly of the 5' by 5' block and $\cos \phi_i (5')^2$ is the area of the i^{th} individual cell in radians. In order to save computation time, the modified spheroidal Stokes function for the inner zone contribution is approximated by a linear form:

$$\widetilde{S} = \beta_0 + \frac{\beta_1}{\psi} + \beta_2 \ln\left(\frac{\psi}{2}\right) + \beta_3 \psi^2 \ln\left(\frac{\psi}{2}\right), \quad 4.2.2.3$$

where the coefficients $(\beta_0, \beta_1, \beta_2, \beta_3)$ are solved by numerical computation. The approximation is obtained in such a way that \widetilde{S} fits the modified Stokes function as well as possible. Tests have been confirmed that the use of this approximation gave an error of less than 1 centimetre [Vanicek and Kleusberg, 1987] in the geoid.

4.2.3 The Outer Zone

Since it is not practical to consider the rest of the earth, the integration is limited within a selected spherical cap of radius (ψ_o) . The outer zone then lies between the outer limit of the spherical cap $(\psi_o = 6^\circ)$ and the outer limit of the inner zone. The 1° by 1° mean gravity anomalies were used in this zone. The geoidal undulation for the outer zone is determined simply by replacing the kernel $S_{\ell}^m(\psi)$ in equation (4.2.2.2) with its value at the center point of the 1° by 1° cell:

$$N_o = \frac{R}{4\pi\gamma} \sum_{i=1}^M S_{\ell}^m(\psi_i) \widetilde{\Delta g}_i^{\ell} \cos \phi_i (1^\circ)^2, \quad 4.2.3.1$$

where M is the total number of 1° by 1° cells, and $\cos \phi_i (1^\circ)^2$ is the area of the cell. Similar to the evaluation of the inner zone, the approximated modified Stokes kernel (equation 4.2.2.3) is used for the computation of the outer zone.

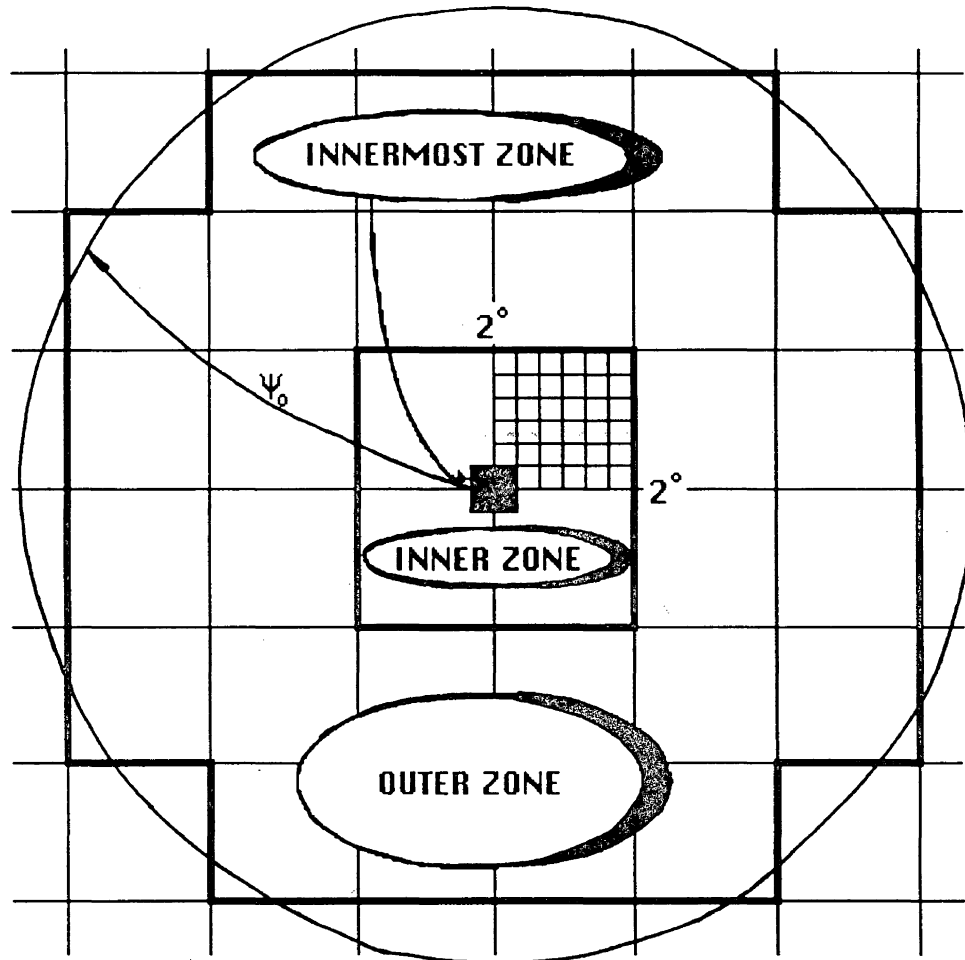


Figure 4.2: The Innermost, the Inner and the Outer Zones [after Vanicek et al (1986, p.21)].

CHAPTER FIVE

RING INTEGRATION METHOD FOR GEOIDAL HEIGHT DIFFERENCE

5.1 Ring Integration Technique for Geoid Computation

The classical method of computing geoidal height is the well known ring integration. It is one of the earliest techniques developed before the coming of electronic computers. The computation is carried out by laying transparent ring templates over gravity maps and the mean values of the gravity anomalies in each of the compartments are estimated. The mean gravity anomalies are then transformed into geoidal height by some means. This method was abandoned for quite some time (due to heavy manual calculations involvement) till the emergence of GPS when new computational techniques required to compare precise geoidal height difference accuracies with GPS-derived ellipsoidal height difference accuracies [Engelis et al.(1985), Gilliland (1986) and Schwarz et al.(1987)]. This ring integration method has been used by Kearsley [1985, 1986a, 1986b, 1988b] for computing the inner zone contribution to geoidal height. His investigation using this approach has shown that a precision of ± 5 cm over 100 km could be achieved. Because of the possibility of achieving high accuracy, "Kearsley's method" was adapted to develop a software that could compute geoidal height differences by supplying the geographical coordinates.

The approach used in this method consists of a paragon of circular rings centered on the point of the interest Q , with lines radiating out from Q to intercept the arcs of the rings to form the compartments as shown in Figure 5.1. Each of these rings will be discussed in the later sections.

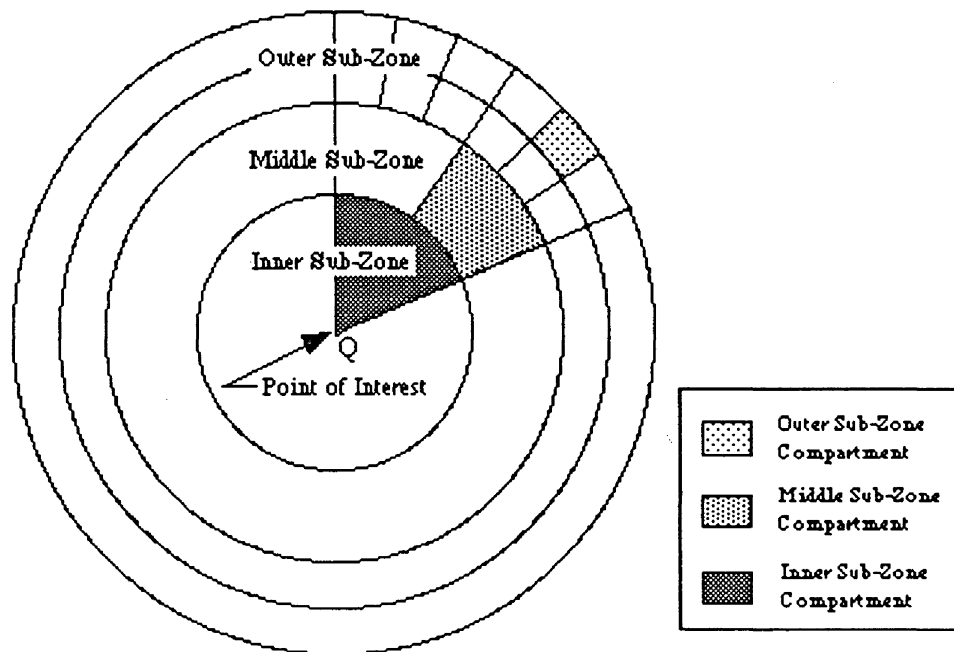


Figure 5.1: The Ring Approach

Similar to the UNB approach, the geoidal height " N " for the ring approach is computed using terrestrial gravity data in a spherical cap (e.g., $\psi_o = 1.0$) surrounding the computation point for the inner zone contribution and from a set of potential coefficients for the remote zone contribution:

$$N = N_R + \delta N_I, \quad 5.1.1$$

where

$$\delta N_I = \frac{R}{4\pi\gamma} \int_{\alpha=0}^{2\pi} \int_{\psi=0}^{\psi_0} \Delta g(\psi, \alpha) S(\psi) \sin\psi \, d\psi \, d\alpha \quad 5.1.2$$

and

$$N_R = \frac{R}{4\pi\gamma} \int_{\alpha=0}^{2\pi} \int_{\psi_0}^{\pi} \Delta g(\psi, \alpha) S(\psi) \sin\psi \, d\psi \, d\alpha. \quad 5.1.3$$

The first term on the right hand side of equation (5.1.1) is the remote(or distant) zone contribution and the second term on the right hand side of equation (5.1.1) is the inner zone contribution. The best way to estimate the remote zone would be to use the result: determined from the perturbations in the orbits of artificial earth satellites. In this research the remote zone contribution is computed using high-order geopotential model such as the Rapp180 model computed by Rapp(1981). According to Engelis et al.[1984], the remote zone can be expressed as:

$$N_R = \frac{R}{2\gamma} \sum_{n=2}^{nmax} Q_n(\psi_0) \Delta g_n(\phi, \lambda), \quad 5.1.4$$

where

- R is the mean radius of the earth;
- γ is the mean value of the gravity;
- Δg is the free-air anomaly;
- Q_n is the Molodenskij truncation function;
- ψ_0 is the spherical cap radius in which the anomalies are given;
- $nmax$ is the maximum degree of the potential coefficients being used;

$\Delta g_n(\phi, \lambda)$ is the n^{th} degree harmonic of the gravity anomalies at latitude(ϕ) and longitude(λ) and it is computed from given potential coefficients (a_{nm}, b_{nm}) as follows:

$$\Delta g_n(\phi, \lambda) = \sum_{m=0}^n [a_{nm} \cos m\lambda + b_{nm} \sin m\lambda] P_{nm}(\cos\phi), \quad 5.1.5$$

where m is the order of the Legendre's function $P_{nm}(\cos\phi)$.

An alternative way to determine N in equation 5.1.1 is to use the geopotential model as a reference solution to which gravity anomalies are reduced [Torge(1980), Vanicek and Krakiwsky(1982), Schwarz et al.(1987) and Kearsley(1988)]:

$$N = \delta N_{\Delta g} + N_{GM}, \quad 5.1.6$$

where

$$\delta N_{\Delta g} = \frac{R}{4\pi\gamma} \int_{\alpha=0}^{2\pi} \int_{\psi=0}^{\psi_0} \Delta g'(\psi, \alpha) S(\psi) \sin\psi \, d\psi \, d\alpha \quad 5.1.7$$

and

$$N_{GM} = \frac{GM}{\gamma R} \sum_{n=2}^{n_{max}} \sum_{m=0}^n [a_{nm} \cos m\lambda + b_{nm} \sin m\lambda] P_{nm}(\cos\phi), \quad 5.1.8$$

with

$$\Delta g'(\psi, \alpha) = \Delta g(\psi, \alpha) - \frac{GM}{R^2} \sum_{n=2}^{n_{max}} \sum_{m=0}^n (n-1) [a_{nm} \cos m\lambda + b_{nm} \sin m\lambda] P_{nm}(\cos\phi). \quad 5.1.9$$

$\Delta g'$ is the reduced gravity anomaly generated by the same model as used in equation (5.1.8) and Δg is the terrestrial gravity anomaly; G is the gravitational constant and M is the mass of the earth. The rest of the notation has been defined previously. The second term on the right hand side of equation(5.1.9) can be computed by transforming the gravity disturbance (δg) to gravity anomaly (Δg) in the subroutine POT written by Tscherning (see Appendix I.9).

The Stokes kernel in equation (5.1.2), however, is fairly difficult to interpolate especially when ψ approaches zero. Because of the non-linearity of Stokes function as discussed in Kearsley's paper [1986a], the use of $F(\psi)$'s function is proposed, (see Figure 5.2) where:

$$F(\psi) = S(\psi) \sin\psi = 2\cos\frac{\psi}{2} \cdot \sin\psi \left[6\sin\frac{\psi}{2} - 1 + \cos\psi \{5 + 3\ell n(\sin\frac{\psi}{2} + \sin^2\frac{\psi}{2})\} \right].$$

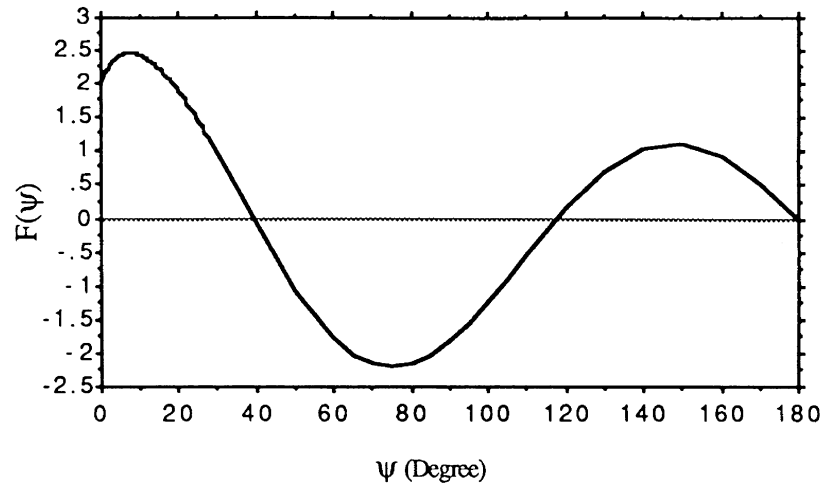


Figure 5.2: The $F(\psi)$'s Function.

Replacing $S(\psi)\sin \psi$ by $F(\psi)$ in equation (5.1.7), we get:

$$\delta N_{\Delta g} = \frac{R}{4\pi\gamma} \int_{\alpha=0}^{2\pi} \int_{\psi=0}^{\psi_0} \Delta g'(\psi, \alpha) F(\psi) d\psi d\alpha \quad 5.1.11$$

which is the foundation for the ring integration technique.

5.2 An Algorithm For Generating the Rings

The inner zone contribution

$$\delta N_{\Delta g} = \frac{R}{4\pi\gamma} \int_{\alpha=0}^{2\pi} \int_{\psi=0}^{\psi_0} \Delta g'(\psi, \alpha) F(\psi) d\psi d\alpha \quad 5.2.1$$

is computed by replacing the geoid with a sphere. Let's introduce a normal to the spherical surface at the point of interest (see Figure 5.3).

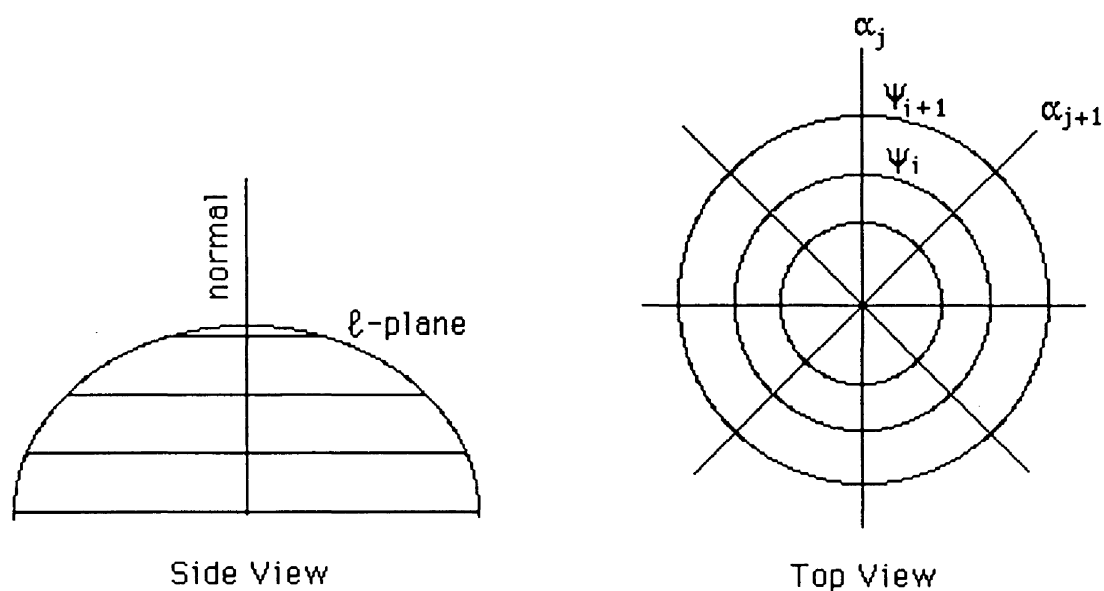


Figure 5.3: Division of Rings and Compartments

This spherical surface is then divided into ℓ rings by introducing $\ell - 1$ planes which are perpendicular to the normal. Each of these rings is then subdivided into equal compartments by planes passing through the normal at a chosen azimuth α . Each of these compartments is formed in such a way that each contributes an equal amount per mGal to the $\delta N_{\Delta g}$.

Let us now denote N_c as the contribution to $\delta N_{\Delta g}$ from one of the compartments:

$$N_c = \frac{R}{4\pi\gamma} \int_{\Delta\alpha_{ij}} \int_{\Delta\psi_{ij}} \widetilde{\Delta g}'(\psi, \alpha) F(\psi) d\psi d\alpha, \quad 5.2.2$$

where $\widetilde{\Delta g}'$ is the mean value of the reduced gravity anomaly in the compartment. $\Delta\psi_i$ and $\Delta\alpha_j$ are the radius and azimuth boundary limits bounding the compartment, respectively (see Figure 5.3). In other words, $\Delta\psi_i = \psi_{i+1} - \psi_i$ and $\Delta\alpha_j = \alpha_{j+1} - \alpha_j$ are the sizes of the compartment. The rest of the parameters are the same as defined previously.

If $\Delta\alpha_j$ is set to a constant (for easy practical evaluation), then equation (5.2.2) can be written as follows:

$$N_c = \xi \int_{\psi_i}^{\psi_{i+1}} \widetilde{\Delta g_{ij}}(\psi, \alpha) F(\psi) d\psi, \quad 5.2.3$$

with

$$\xi = \frac{R}{4\pi\gamma} \Delta\alpha_j. \quad 5.2.4$$

Since $\widetilde{\Delta g_{ij}}$ is the mean value of the reduced gravity anomalies in a compartment, it can be taken out of the integral:

$$N_c = \xi \widetilde{\Delta g_{ij}} \int_{\psi_i}^{\psi_{i+1}} F(\psi) d\psi. \quad 5.2.5$$

Kearsley [1985] solved the integral of equation (5.2.5) as follows:

$$\Phi(\psi) = \int_0^{\psi} F(\psi) d\psi = 1 + 4\sin\frac{\psi}{2} - \cos\psi - A - B - C, \quad 5.2.6$$

where

$$\begin{aligned} A &= 6 \sin^3\left(\frac{\psi}{2}\right), \\ B &= \frac{7}{4} \sin^2\left(\frac{\psi}{2}\right), \\ C &= \frac{3}{2} \sin^2\psi \ln\left[\sin\left(\frac{\psi}{2}\right) + \sin^2\left(\frac{\psi}{2}\right)\right]. \end{aligned}$$

By expanding each of the above terms of equation (5.2.6) into its series and collecting the terms of equal powers together, we arrive at:

$$\Phi(\psi) \doteq 2\psi - \frac{5}{4}\psi^2 - \frac{10}{12}\psi^3 - \frac{3}{2}\psi^2 \ln\left[\frac{\psi}{2} + \frac{\psi^2}{4} - \frac{\psi^3}{24}\right]. \quad 5.2.7$$

According to Kearsley [1985], the terms in ψ^4 or smaller were insignificant for $\psi < 2^\circ$, and could be ignored.

Hence, equation(5.2.5) becomes:

$$N_c = \xi \widetilde{\Delta g}_{ij} \left[\int_{\psi=0}^{\psi_{i+1}} F(\psi) d\psi - \int_{\psi=0}^{\psi_i} F(\psi) d\psi \right] \quad 5.2.8$$

$$= \xi \widetilde{\Delta g}_{ij} [\Phi(\psi_{i+1}) - \Phi(\psi_i)]. \quad 5.2.9$$

In order to generate the rings, a recursive technique is developed [Kearsley, 1985] using the following relationship:

$$\xi \Phi(\psi_{i+1}) = \xi \Phi(\psi_i) + N_c^*, \quad 5.2.10$$

where N_c^* is N_c divided by $\widetilde{\Delta g}_{ij}$ expressed in terms of metres per mGal of $\widetilde{\Delta g}_{ij}$. Since the inner zone is divided into three different sub-zones (see next section), the size of $\Delta\psi$ is different from one sub-zone to another and therefore it is required to solve for (ψ_{i+1}) by substituting equation (5.2.7) into equation (5.2.10):

Step 1: From equation (5.2.10)

$$\xi [\Phi(\psi_{i+1}) - \Phi(\psi_i)] = N_c^*, \quad 5.2.11$$

or equivalently

$$\xi [\Delta\Phi_i] = N_c^*, \quad 5.2.12$$

where $\Delta\Phi_i = \Phi(\psi_{i+1}) - \Phi(\psi_i)$ is the thickness of the compartment in a sub-zone and it is constant within a sub-zone but changes from one sub-zone to another (see Appendix I.6).

Step 2: dividing both sides by ξ :

$$[\Phi(\psi_{i+1}) - \Phi(\psi_i)] = \frac{N_c^*}{\xi}, \quad 5.2.13$$

Step 3: replacing ψ_{i+1} by ψ_k and substituting equation (5.2.7) into equation (5.2.13):

$$\begin{aligned} & 2\psi_k - \frac{5}{4}\psi_k^2 - \frac{10}{12}\psi_k^3 - \frac{3}{2}\psi_k^2 \ln\left[\frac{\psi_k}{2} + \frac{\psi_k^2}{4} - \frac{\psi_k^3}{24}\right] \\ & - 2\psi_i + \frac{5}{4}\psi_i^2 + \frac{10}{12}\psi_i^3 + \frac{3}{2}\psi_i^2 \ln\left[\frac{\psi_i}{2} + \frac{\psi_i^2}{4} - \frac{\psi_i^3}{24}\right] = \frac{N_c^*}{\xi}, \end{aligned} \quad 5.2.14$$

Step 4: collecting i^{th} and k^{th} terms together:

$$\begin{aligned} & 2(\psi_k - \psi_i) - \frac{5}{4}(\psi_k^2 - \psi_i^2) - \frac{10}{12}(\psi_k^3 - \psi_i^3) - \\ & \left(\frac{3}{2} \left(\psi_k^2 \ln\left[\frac{\psi_k}{2} + \frac{\psi_k^2}{4} - \frac{\psi_k^3}{24}\right] - \psi_i^2 \ln\left[\frac{\psi_i}{2} + \frac{\psi_i^2}{4} - \frac{\psi_i^3}{24}\right] \right) \right) = \frac{N_c^*}{\xi}, \end{aligned}$$

5.2.15

Step 5: dividing both sides of equation (5.2.15) by 2 and rearranging the terms:

$$\begin{aligned} & \psi_k = \psi_i + \frac{5}{8}(\psi_k^2 - \psi_i^2) + \frac{10}{24}(\psi_k^3 - \psi_i^3) + \\ & \left(\frac{3}{4} \left(\psi_k^2 \ln\left[\frac{\psi_k}{2} + \frac{\psi_k^2}{4} - \frac{\psi_k^3}{24}\right] - \psi_i^2 \ln\left[\frac{\psi_i}{2} + \frac{\psi_i^2}{4} - \frac{\psi_i^3}{24}\right] \right) \right) + \frac{N_c^*}{2\xi}. \end{aligned}$$

5.2.16

This can be regarded as a recursive formula for solving ψ_k and an approximate value ψ'_k for ψ_k is needed. The way to choose the value ψ'_k is by substituting the leading term of equation (5.2.7) into equation (5.2.13):

$$2(\psi_k - \psi_i) \doteq \frac{N_c^*}{\xi}. \quad 5.2.17$$

Then

$$\psi'_k \doteq \psi_i + \frac{N_c^*}{2\xi}, \quad \text{with } \psi_i = 0.0. \quad 5.2.18$$

N_c^* is selected in such a way that the radial increments $(\psi_{i+1} - \psi_i)$ match the spacing of the point gravity anomalies. For example, if a set of point gravity anomalies whose average spacing is 10 km, and if 10° is chosen for $\Delta\alpha$, then N_c^* needs to be 0.0003 m/mGal in order to generate rings whose radial increments match the average spacing of the point gravity anomalies (see Appendix I.10). The advantage of this approach is that it has a flexibility in matching the compartment size to the distribution of gravity data. Equation (5.2.16) is the basic recursive equation for generating the radii of the rings, which for a selected $\Delta\alpha$, will produce compartments which will contribute N_c for each mGal of $\widetilde{\Delta g}$. It generates the radii of the rings in an increment of small steps (about 10 kilometres) thus allowing the full use of data in the estimation of $\widetilde{\Delta g}$. Kearsley [1985] had tested the accuracy in estimating $\widetilde{\Delta g}$ and concluded that the 2nd., 3rd., and 4th. terms of this equation cannot be neglected. He found out that by neglecting three terms, i.e., if only the approximation in equation (5.2.18) is applied to generate the rings, the cumulative effect at $\psi = 1^\circ$ through the rings is about 6.3 km (more than the actual radius which is computed by equation (5.2.16)). Table 5.1 shows that the thickness of each of the successive rings computed by the above recursive formula is very stable for a sub-zone (see Appendix I.6 and I.7 also).

Table 5.1: The Stability of Thickness $\Delta\Phi_{12}$ of Successive Rings Computed to give a 0.0002 m/mGal contribution to N for 1 mGal per compartment with a 10° apex angle.

Ψ_1 (in degree)	Ψ_2 (in degree)	Φ_1 (in degree)	Φ_2 (in degree)	$\Delta\Phi_{12}$ (in degree)
0.000	0.063	0.000	0.127	0.127
0.063	0.126	0.127	0.254	0.127
0.126	0.188	0.254	0.381	0.127
0.188	0.249	0.381	0.507	0.127
0.249	0.311	0.507	0.634	0.127
0.311	0.372	0.634	0.761	0.127

In this thesis, the inner zone computed by the method of ring integration is divided into three different sub-zones, namely: (1) the inner sub-zone, (2) the middle sub-zone, (3) and the outer sub-zone (see Figure 5.1). The sum of these three sub-zones will be the total contribution of the inner zone to geoidal height. Each of these will be discussed below.

5.2.1 The Inner Sub-Zone

The inner sub-zone is the first ring away from the point of interest (see Figure 5.4).

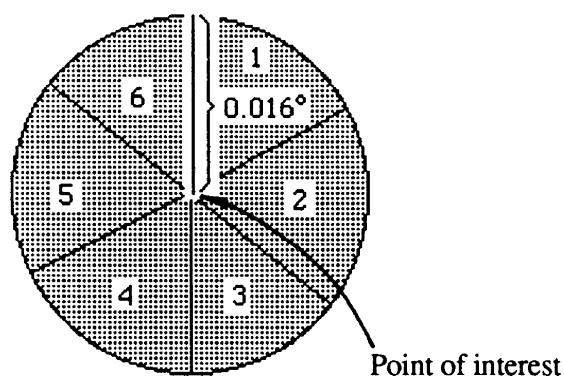


Figure 5.4: The Inner Sub-Zone.

This sub-zone is divided into six compartments and each of these compartments is bounded by $\Delta\alpha_{IM} = 60^\circ$, and $\psi_1 = 0^\circ$ and ψ_2 , where $\psi_2 = 0.016^\circ$ (see Appendix I.7) can be obtained by the recursive technique as mentioned in the previous section with :

$$\xi_{IM} = \frac{R}{4\pi\gamma} \Delta\alpha_{IM} \quad 5.2.1.1$$

and

$R = 6371$ km is the radius of the spherical model of the earth;

$\gamma = 979.9$ Gal is the mean value of the normal gravity over the earth.

The geoidal height contributed by this sub-zone is determined by:

$$N_{IM} = \xi_{IM} \Delta\Phi_{12} \sum_{h=1}^6 \widetilde{\Delta g}_h, \quad 5.2.1.2$$

where h is the index for the compartments; $\widetilde{\Delta g}_h$ is the mean value of the free air gravity anomaly for the h^{th} compartment; $\Delta\Phi_{12} = \Phi_2 - \Phi_1 = 0.032^\circ$ and $\Delta\psi_{21} = 0.016^\circ = 57.6''$ (see Appendix I.6 and I.7). Substituting $\xi_{IM} \Delta\Phi_{12}$ and into equation(5.2.1.2), we arrive at:

$$N_{IM} = (0.0003) \sum_{h=1}^6 \widetilde{\Delta g}_h, \quad 5.2.1.3$$

with $\widetilde{\Delta g}_h$ is in mGal and N_{IM} is in metre. The mean gravity anomaly at the h^{th} compartment is determined in the following steps:

Step 1: first of all, the coordinates of the point which lies in the center of the compartment is determined by obtaining the azimuth(α_m) and the spherical distance(ψ_m):

$$\alpha_m = (\alpha_1 + \alpha_2)/2, \quad 5.2.1.4$$

$$\psi_m = (\psi_1 + \psi_2)/2, \quad 5.2.1.5$$

where $(\alpha_1, \alpha_2, \psi_1, \psi_2)$ are the boundary limits of the compartment (see Figure 5.5).

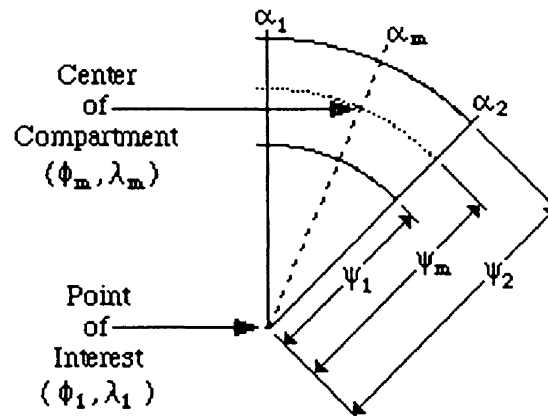


Figure 5.5: Determination of Coordinates for the Center of the Compartment.

Step 2: compute the differences in latitude($\Delta\phi$) and in longitude($\Delta\lambda$) between the point of interest(ϕ_1, λ_1) and the center of the compartment (ϕ_m, λ_m):

$$\Delta\phi = \psi_m \cos(\alpha_m), \quad 5.2.1.6$$

$$\Delta\lambda = \psi_m \sin(\alpha_m), \quad 5.2.1.7$$

Step 3: obtain the coordinates for the center of the compartment:

$$\lambda_m = \Delta\lambda + \lambda_1, \quad 5.2.1.8$$

$$\phi_m = \Delta\phi + \phi_1. \quad 5.2.1.9$$

Step 4: once the coordinates of the center point of the compartment are defined, the boundary limits of the cell are delineated for the prediction of $\widetilde{\Delta g}$. Note that the size of the compartment is different from the size of the cell. The size of the compartment is bounded by the selected $\Delta\alpha$ and $\Delta\psi$ (depending on which sub-zone is to be computed) as shown in Figure 5.6. The prediction point lies in the center of the cell which coincides with the center of the compartment.. However, the size of the cell is a square area (shaded region) which is chosen to be 10' by 10'. If there is no point gravity anomalies inside this cell, the dimension of the cell will increase to 15' by 15', or 20' by 20', or 30' by 30', or 60' by 60' until at least one set of observation is present inside the cell. If there is still no point

gravity anomaly inside the 60' by 60' cell, the computation will skip that cell and move on to the next compartment.

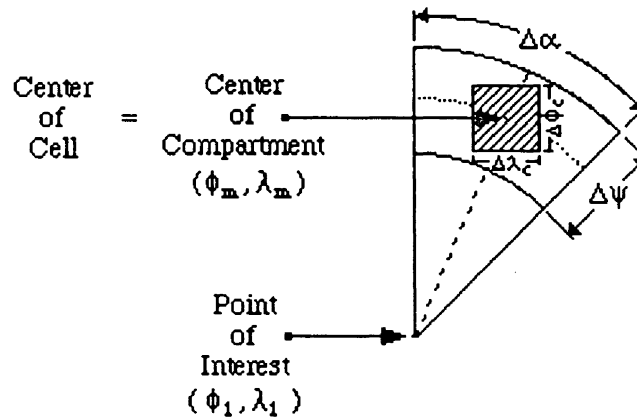


Figure 5.6: Cell (Shaded Area) used for obtaining Δg .

The boundary limits of the cell are defined by the latitudes of the north-east and south-east corners of the cell and the longitudes of the north-west and north-east corners of the cell (see Figure 5.7).

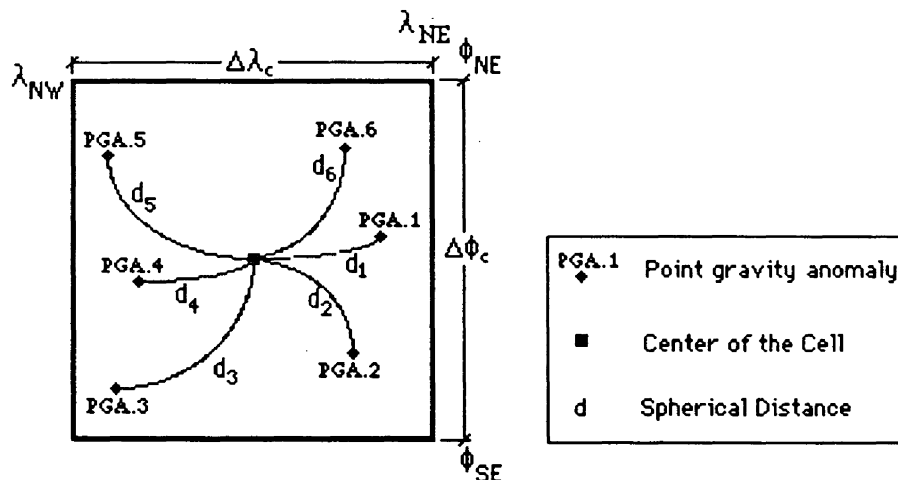


Figure 5.7: The Boundary Limits of the Cell.

They are computed as follows:

$$\phi_{NE} = \phi_m + \Delta\phi_c / 2, \quad 5.2.1.10$$

$$\phi_{SE} = \phi_m - \Delta\phi_c / 2, \quad 5.2.1.11$$

$$\lambda_{NE} = \lambda_m + \Delta\lambda_c / 2, \quad 5.2.1.12$$

$$\lambda_{NW} = \lambda_m - \Delta\lambda_c / 2, \quad 5.2.1.13$$

where $\Delta\phi_c = \Delta\lambda_c = 10', 20', 30',$ or $60'$ as mentioned in the above.

Once the boundary limits are known, the point gravity anomalies within the cell are extracted and arithmetic mean technique is utilized to obtain the mean gravity anomaly at the center of the cell. The spherical distances ($d_i, i=1,2,\dots,n$, where n is the total number of point gravity anomalies within the cell) between the point gravity anomalies within the cell and the center of the cell are determined (see Figure 5.7). They are used to obtain the weight coefficients which utilize in determining the mean gravity anomaly. More about this will be discussed in the next section.

5.2.2 The Middle Sub-Zone

This middle sub-zone is similar to the inner sub-zone but consists of a total of twelve compartments (see Figure 5.8). It lies next to the the inner sub-zone with the point of interest as its center. Its inner boundary is at ψ_2 (as determined from the inner sub-zone) and its outer boundary is at $\psi_3 = 0.047^\circ$ (which will be computed from equation (5.2.15)). $\Delta\alpha_M$ is set to 30° , then

$$\xi_M = \frac{R}{4\pi\gamma} \Delta\alpha_M = \frac{1}{2} \xi_{IM}, \quad 5.2.2.1$$

where R and γ are defined as in the previous subsection.

The contribution to geoid height from this sub-zone is evaluated as follows:

$$N_M = \xi_M \Delta\Phi_{23} \sum_{p=1}^{12} \widetilde{\Delta g}_p, \quad 5.2.2.2$$

where $\widetilde{\Delta g}_p$ is the mean value of the free air gravity anomaly for the p^{th} compartment and

$\Delta\Phi_{23} = \Phi_3 - \Phi_2 = 0.063^\circ$ ($\Delta\psi_{32} = 0.031^\circ = 1' 51.6''$). Substituting ξ_M and $\Delta\Phi_{23}$

into equation(5.2.2.2), we arrive at:

$$N_M = (0.0003) \sum_{p=1}^{12} \widetilde{\Delta g}_p, \quad 5.2.2.3$$

with $\widetilde{\Delta g}_p$ in mGal and N_M in metre. The mean gravity anomaly is determined the same way as for the inner sub-zone.

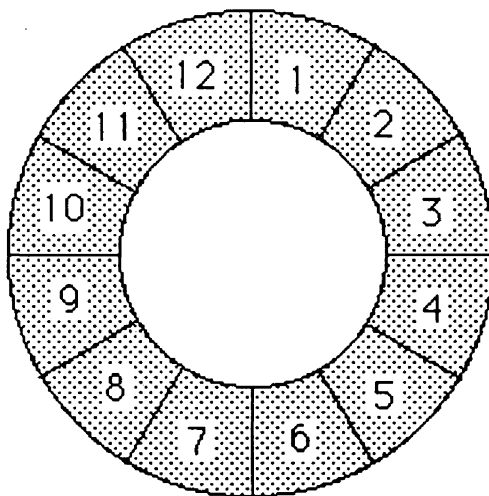


Figure 5.8: The Middle Sub-Zone.

5.2.3 The Outer Sub-Zone

Any rings, apart from the inner and middle sub-zones, which encircle the point of computation are known as outer sub-zone (see Figure 5.9). All these rings compose the outer sub-zone. Each of these rings is subdivided into 36 compartments. The boundary limit of the compartment is bounded by $\Delta\alpha_o = 10^\circ$, ψ_3 and ψ_4 for the first outer ring zone. The second outer ring zone is then bounded by ψ_4 and ψ_5 , and so on. Note that the azimuth boundaries remain the same for the rest of the rings. $\Delta\alpha_o$ is set to 10° , and

$$\xi_o = \frac{R}{4\pi\gamma} \Delta\alpha_o = \frac{1}{6} \xi_{IM}. \quad 5.2.3.1$$

The total geoid height contributions from all these ring are then computed by summing all the geoid height contributions from each of the compartments:

$$N_o = \xi_o \sum_{s=1}^n \sum_{r=1}^{36} \widetilde{\Delta g}_{r,s} \Delta\Phi_s \quad 5.2.3.2$$

where n is total number of the rings up to ψ_o (the limit of the spherical cap size). For example, when n equal to 13, ψ_o will be approximately equal to 1.2° (see Appendix I.7). $\widetilde{\Delta g}_{r,s}$ is the mean value of the free air gravity anomaly for the compartment r,s ; s is the index for the ring. Note that $\Delta\Phi_s$ is inside the summation. This is because $\Delta\Phi_s$ is varying with ψ and can vary to about 8 seconds by the time it reaches 1.2° (see Appendix I.6). However, when these 8 seconds are converted to radian (less than 0.00005 radian difference for $0.14^\circ \leq \psi_o \leq 1.2^\circ$), the effect on N (less than 1.5%) becomes insignificant. Hence $\Delta\Phi_s$ can be assumed to be constant for the outer sub-zone and be taken out of the summation. Equation (5.2.3.2) then can be written as follows:

$$N_o = \xi_o \Delta\Phi \sum_{s=1}^n \sum_{r=1}^{36} \widetilde{\Delta g}_{r,s}, \quad 5.2.3.3$$

where $\Delta\Phi$ is approximately equal to 0.00335 radian (0.192°). The rest of the notations is defined previously.

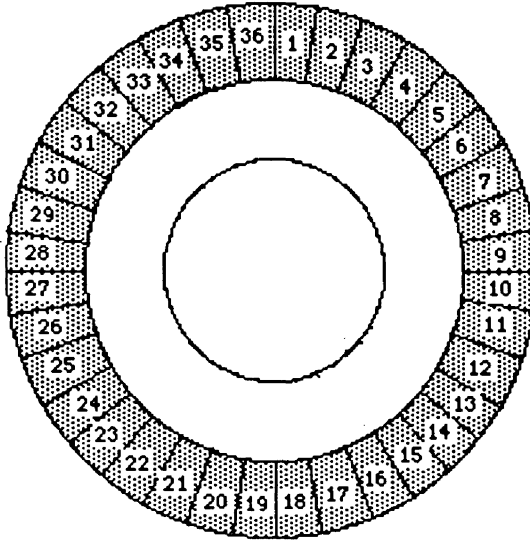


Figure 5.9: The Outer Sub-Zone.

Hence, the sum of the computations from the above three sub-zones will be the contribution of the inner zone to the geoidal height:

$$\delta N_{\Delta g} = N_{IM} + N_M + N_o. \quad 5.2.3.4$$

The above equation (5.2.3.3) can be rewritten as follows:

$$\delta N_{\Delta g} = \xi \Delta \Phi \sum_{i=1}^T \widetilde{\Delta g}_i, \quad 5.2.3.5$$

or equivalently

$$\delta N_{\Delta g} = (0.0003) \sum_{i=1}^T \widetilde{\Delta g}_i, \quad 5.2.3.6$$

where the index T is the total number of compartments within the spherical cap ψ_o . $\widetilde{\Delta g}_i$ is the reduced mean gravity anomaly expressed in mGal and $\delta N_{\Delta g}$ is in metre.

5.2.4 Computation of Geoidal Height Difference

In this subsection, the change in N over line AB , i.e. ΔN , will be discussed. From equation (5.2.3.5), it can be expressed for both points A and B :

$$\delta N_A = \xi \Delta \Phi \sum_{i=1}^T \widetilde{\Delta g}_{i'} , \quad 5.2.4.1a$$

$$\delta N_B = \xi \Delta \Phi \sum_{i=1}^T \widetilde{\Delta g}_i . \quad 5.2.4.1b$$

Therefore, the geoidal height difference $\Delta \delta N_{AB}$ can be computed by taking the difference between equations (5.2.4.1a) and (5.2.4.1b):

$$\begin{aligned} \Delta \delta N_{AB} &= \delta N_B - \delta N_A \\ &= \xi \Delta \Phi \left[\sum_{i=1}^T \widetilde{\Delta g}_i - \sum_{i=1}^T \widetilde{\Delta g}_{i'} \right] . \end{aligned} \quad 5.2.4.2$$

Note that the geoidal height difference is basically computed by taking the difference of the sum of gravity anomalies from all the compartments at each of the endpoints of the line and multiplying it by the constants. The advantages of this approach are its flexibility in selecting constants for matching the compartment size to the density of the data, and its ease and speed, especially with modern computers.

The remote zone contribution to N is computed using equation(5.1.8):

$$N_{GM} = \frac{GM}{\gamma R} \sum_{n=2}^{nmax} \sum_{m=0}^n [a_{nm} \cos m\lambda + b_{nm} \sin m\lambda] P_{nm}(\cos\phi) , \quad 5.1.8$$

where Rapp180 geopotential model is used. N_{GM} is computed at the end points of the baseline and difference is taken to obtain the ΔN_{GM} . The full geoidal height difference is then determined by adding $\Delta \delta N_{\Delta g}$ to ΔN_{GM} .

5.3 Determination of Mean Gravity Anomaly

Determining the shape of the geoid with high accuracy using Stokes formula is not an easy task. One of the problems is that the surface integral in the Stokes equation has to be changed to a finite sum for numerical computation as discussed in the last section. The geoidal height is computed by dividing the spherical cap into a finite number of small surfaces σ_i and in each of these the mean value of the gravity anomaly and of the integral

$$K_i = \xi \Phi = \frac{R}{4\pi\gamma} \iint_{\sigma_i} F(\psi) d\psi d\alpha \quad 5.3.1$$

is determined. Geoidal height contribution for the inner zone is then computed by the following expression:

$$N_I = K \sum_{i=1}^T \widetilde{\Delta g}_i, \quad 5.3.2$$

K is not difficult to enumerate since it is constant. What remains to be determined is the value of $\widetilde{\Delta g}_i$. If all the gravity anomalies around the world were known, the Stokes integration could be evaluated very easily. Unfortunately, there are some areas in which no gravity survey has been done. Hence, the gravity anomalies we have are not continuous but rather discrete. The solution to this problem is by interpolating from the existing gravity anomalies to predict mean gravity anomalies for the unsurveyed areas using statistical methods [Orlin, 1966].

In computing N by means of the Stokes formula, free-air anomalies are most commonly used. The accuracy of $\widetilde{\Delta g}$, i.e., the compartment mean of the free-air anomaly, plays a large part in computing higher accuracy N . In the old days before the computer era, $\widetilde{\Delta g}$ was determined by means of Bouguer anomaly and height maps. With

this method, a huge amount of gravity data was necessary to compute $\widetilde{\Delta g}$ with sufficient accuracy, especially in rough areas. Today this problem - lack of dense gravity data - still exist. There are many ways, such as arithmetic mean [Gilliland, 1989], least squares surface fitting [Vanicek et al., 1986] and least squares collocation [Engelis et al., 1984], which can be used to determine $\widetilde{\Delta g}$. In this thesis, arithmetic mean is used for the prediction of $\widetilde{\Delta g}$.

5.3.1 Arithmetic Mean

Arithmetic mean has been used very frequently in $\widetilde{\Delta g}$ determination by various researchers because of its simplicity [Kassim (1980), Kearsley et al.(1985), Mainville and Veronneau (1989), and Gilliland (1989)]. Two approaches in using arithmetic mean for predicting $\widetilde{\Delta g}$ are considered in here. The first approach is to compute the arithmetic mean value of $\widetilde{\Delta g}$ from the reduced free-air anomalies and the second approach is to compute the arithmetic mean of the Bouguer anomalies and then using the topographic heights to transform to free-air anomaly.

5.3.1.1 Method 1: Arithmetic Mean From Free-Air Anomalies

The approach in here is to compute the arithmetic mean value of Δg from the reduced free-air gravity anomalies. The mean value of the reduced free-air anomaly $\widetilde{\Delta g}_F$ is computed by taking the average value of the free-air anomalies Δg_i within and/or surrounding a compartment:

$$\widetilde{\Delta g}_F = \frac{\sum_{i=1}^n W_i \Delta g_i}{\sum_{i=1}^n W_i}, \quad 5.3.1.1.1$$

where n is the total number of point free-air anomalies in a selected cell, e.g. 10' by 10'; W_i is the weight coefficient and is obtained as the reciprocal of the distance d_i between the points of Δg_i and the prediction point of $\widetilde{\Delta g}$, raised to some power r :

$$W_i = \frac{1}{d_i^r} . \quad 5.3.1.1.2$$

In this thesis, the power r is set to 3.5 as suggested by Sjoberg [Kearsley, 1985] and the gravity anomalies used are the free-air gravity anomalies reduced to Rapp180 geopotential model reference surface.

5.3.1.2 Method 2: Arithmetic Mean From Bouguer Anomalies

In the above mathematical model, free anomalies were used to predict $\widetilde{\Delta g}$. However, the problem in using free-air anomalies is that they vary so rapidly from one location to another location and that it is impossible to obtain satisfactory average value of them to be used in equation(5.3.2). Hence, it is sensible to use different type of anomalies that varies less and so could be averaged to obtain a better representative value of $\widetilde{\Delta g}$. The anomalies to substitute for free-air anomalies in equation(5.3.1.1.1) are the modified Bouguer anomalies. These modified Bouguer anomalies are smoother and they offer much better possibilities for averaging Δg [Vanicek and Krakiwsky, 1982]:

$$\widetilde{\Delta g}_F = \widetilde{\Delta g}_B + 0.1119 \bar{H} , \quad 5.3.1.2.1$$

where \bar{H} is the mean value of height in the selected cell:

$$\bar{H} = \frac{\sum_{i=1}^n H}{n} . \quad 5.3.1.2.2$$

CHAPTER SIX

RESULTS OF THE TESTS

One of the intentions of this thesis is to design a software which could compute the short wavelength contribution to geoidal height difference using terrestrial gravity data and the geodetic coordinates of two points. The contributions from the medium to long wavelengths will be obtained from the subroutine POT written by Tscherning. The first section of this chapter will describe the results obtained from GPS observations, which then will be used as the control data for the comparisons with the results obtained from the ring integration method and the UNB Dec.'86. The second section compares the results from ring integration method with other independent studies and the third section discusses briefly the error analysis.

6.1 The Manitoba GPS Network

The points used as control data for the comparisons were from observations taken from stations during the summer of 1983 in Central Manitoba, using the GPS Macrometer V-1000 receivers under contract for the Geodetic Survey of Canada [Wells (1986), Mainville (1987)]. There were 22 stations observed and 11 of them were connected to the Canadian primary vertical geodetic control network having orthometric heights determined from differential levelling. Figure 6.1 shows the distribution of these 11 GPS stations. With these 11 stations, a set of 52 baselines was produced. However, after testing, one of

these stations was found to be less reliable and was omitted to reduce this set to 42 baselines. Their lengths were ranging from 21 to 134 kilometres. GPS provides the geocentric Cartesian coordinate differences. These coordinate differences were then converted to ellipsoidal height difference(Δh), latitude difference and longitude difference. The orthometric height difference(ΔH) was observed by differential levelling and they are related to ellipsoidal height difference through the following expression:

$$\Delta h_{GPS} = \Delta H_{LEV} + \Delta N_{GPS/LEV}, \quad 6.1.1$$

where $\Delta N_{GPS/LEV}$ is the geoidal height difference derived from GPS and differential levelling. The precision for Δh_{GPS} was estimated to be ± 1.1 ppm and the precision for ΔH_{LEV} was estimated to be ± 3.0 ppm [Mainville, 1987]. The combined precisions from the two sources would, then, give the precision to ± 3.2 ppm for $\Delta N_{GPS/LEV}$. The estimation for the precision of ΔH_{LEV} from Mainville[1987] seem to be somewhat large.

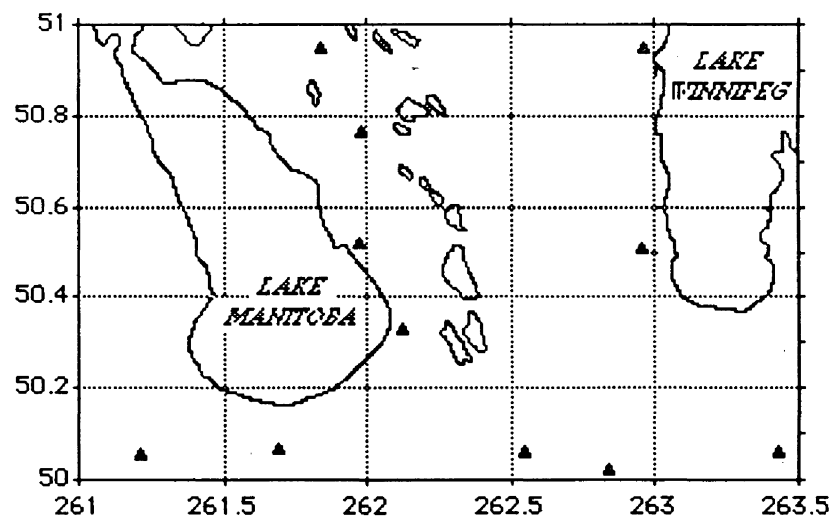


Figure 6.1: Distribution of GPS Stations.

Table 6.1 summaries the results obtained from this GPS Campaign. From Figure 6.2, it is shown that the accuracy of these height differences [Mainville, 1987] deteriorate as the distance between two stations lengthened.

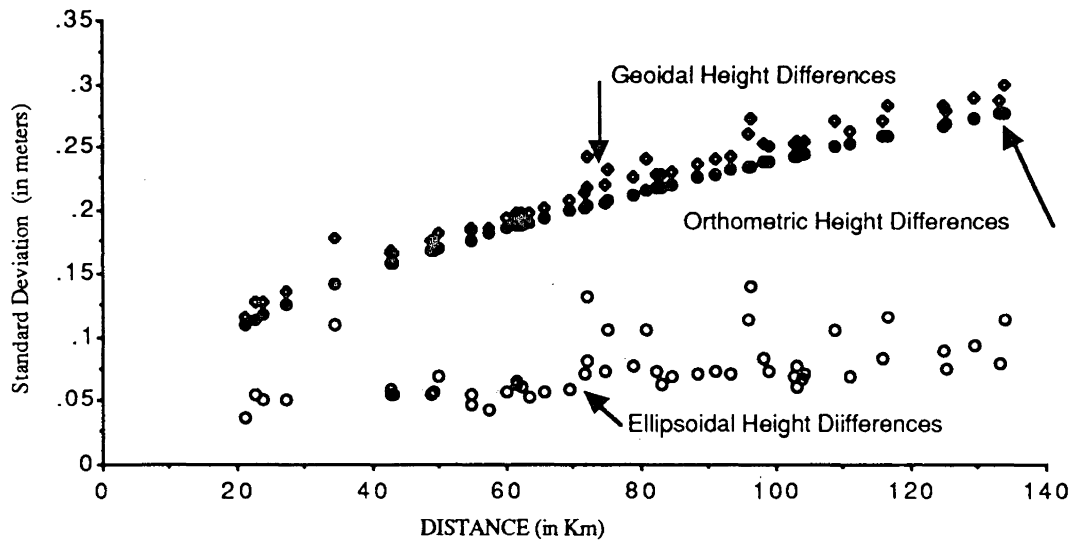


Figure 6.2: Deterioration of Accuracy with respect to Distance.

The error in $\Delta N_{GPS/LEV}$ is mainly contributed from the error in ΔH_{LEV} . Sources of error which affect or may affect the accuracy of heights obtained from GPS have been discussed in Robinson[1990, page 89].

Table 6.1: Results from Manitoba GPS Campaign.

From Station	To Station	Distance (metres)	Azi (Deg)	DHELL (metres)	SDHELL (metres)	DHORT (metres)	SDHORT (metres)	DNGPS (metres)	SDNGPS (metres)
59414	59419	42835.632	264	-13.478	.054	-13.818	.157	.340	.166
59414	59422	63264.550	270	2.292	.053	1.507	.191	.785	.198
59414	774031	115879.659	296	4.599	.083	3.682	.258	.917	.271
59414	774032	60099.078	325	-15.323	.056	-14.979	.186	-.344	.194
59414	82R311	104268.137	341	-24.642	.070	-23.202	.245	-1.440	.255
59414	82R370	98077.694	288	14.751	.083	13.700	.238	1.051	.252
59414	82R382	129579.232	307	14.532	.094	14.466	.273	.066	.289
59419	59422	21152.676	282	15.770	.036	15.325	.110	.445	.116
59419	60404B	116714.955	272	45.673	.116	42.896	.259	2.777	.284
59419	774009	125347.849	325	36.799	.074	37.592	.269	-.793	.279
59419	774031	83040.513	312	18.077	.063	17.500	.219	-.577	.228
59419	774032	54653.119	8	-1.845	.047	-1.161	.177	-.684	.184
59419	82R311	103622.863	4	-11.164	.066	-9.384	.244	-1.780	.253
59419	82R370	61474.039	304	28.229	.063	27.518	.188	.711	.198

59419	82R382	102898.395	324	28.010	.076	28.284	.243	-.274	.255
59422	60404B	95918.573	270	29.903	.113	27.571	.235	2.332	.261
59422	774009	111035.239	333	21.029	.068	22.267	.253	-1.238	.262
59422	774031	65658.204	321	2.307	.056	2.175	.194	.132	.202
59422	774032	57432.930	30	-17.615	.042	-16.486	.182	-1.129	.187
59422	82R311	103092.652	16	-26.934	.061	-24.709	.244	-2.225	.251
59422	82R370	42634.058	314	12.459	.055	12.193	.157	.266	.166
59422	82R382	88307.111	333	12.240	.071	12.959	.226	-.719	.236
60404B	774009	108790.916	23	-8.874	.106	-5.304	.250	-3.570	.272
60404B	774031	75083.356	46	-27.596	.105	-25.396	.208	-2.200	.233
60404B	774032	134078.448	67	-47.518	.114	-44.057	.278	-3.461	.300
60404B	82R370	72030.842	64	-17.444	.132	-15.378	.204	-2.066	.243
60404B	82R382	96176.696	34	-17.663	.139	-14.612	.235	-3.051	.273
774009	774031	48559.933	168	-18.722	.055	-20.092	.167	1.370	.176
774009	774032	93057.963	121	-38.644	.070	-38.753	.232	.109	.242
774009	82R311	79041.027	89	-47.963	.076	-46.976	.213	-.987	.227
774009	82R370	71850.244	163	-8.570	.070	-10.074	.203	1.504	.215
774009	82R382	22730.233	153	-8.789	.055	-9.308	.114	.519	.127
774031	774032	69616.469	90	-19.922	.058	-18.661	.200	-1.261	.208
774031	82R311	84411.431	55	-29.241	.068	-26.884	.221	-2.357	.231
774031	82R370	23857.125	153	10.152	.051	10.018	.117	.134	.128
774031	82R382	27288.879	1	9.933	.050	10.784	.125	-.851	.135
774032	82R311	49242.025	0	-9.319	.056	-8.223	.168	-1.096	.177
774032	82R370	62223.488	251	30.074	.060	28.679	.189	1.395	.199
774032	82R382	74682.196	293	29.855	.072	29.445	.207	.410	.220
82R311	82R370	90849.976	220	39.393	.072	36.902	.229	2.491	.240
82R311	82R382	71899.842	253	39.174	.080	37.668	.204	1.506	.219
82R370	82R382	49644.149	348	-.219	.069	.766	.169	-.985	.183

DHELL = Ellipsoidal Height Difference;
DHORT = Orthometric Height Difference;
DNGPS = GPS/Levelling derived Geoidal Height Difference;

SDHELL = Standard Deviation of DHELL.
SDHORT = Standard Deviation of DHORT.
SDNGPS = Standard Deviation of DNGPS.

The standard deviations of the ellipsoidal height differences were obtained by judging various adjustment results of the GPS data and the standard deviations of the orthometric height differences were estimated from the tolerances $\pm 4, 8$ or $24\text{mm}\sqrt{K}$, where K is the distance in kilometre [Mainville, 1987]. The standard deviations of the geoidal height differences were then obtained by taking the square root of the sum of the variance of Δh and the variance of ΔH .

6.2 Comparison of Results

The area used in our tests is the area where the Manitoba GPS Network lies ($50^\circ < \phi < 51^\circ$, $261^\circ < \lambda < 263.5^\circ$). Because the area has a smooth terrain, it is assumed that the

topographic correction is the same at both end points of the baseline. So that they cancel out in difference. This correction, moreover, is significant in mountainous region. In the succeeding section, comparisons between the results derived from the ring integration approach against those results from other independent methods are carried out. Other independent results used in the comparison are (1) the UNB Dec.'86 results which were computed by Vanicek et al.(1986) and (2) the results from the combination of GPS and spirit levelling. Comparison between (1) and (2) was also carried out. We shall also see how well ΔN can be recovered using the Rapp180 geopotential model alone.

6.2.1 Recovering ΔN_{GM} from Geopotential Model

ΔN_{GM} from geopotential model is computed using a series of spherical harmonic coefficients which were determined from various data such as satellite orbit perturbations, satellite altimeter data, and terrestrial gravity data. In this investigation, the geopotential model used for the test is the Rapp180 model which is complete to degree and order 180. We should first take a look at how well can ΔN be recovered by using the geopotential model (Rapp180) alone.

Figure 6.3 shows how ΔN , computed using geopotential model of various n_{max} , fits the ΔN derived from GPS/Levelling. It is shown, as one would expect that they agree better as n_{max} increases, so that at $n_{max} = 180$ the mean-relative-accuracy is 4.0 ppm while at $n_{max} = 10$ the mean-relative-accuracy is 8.6 ppm. Kearsley[1988] claimed that there is a sharp improvement at $n_{max} = 90$ to about 4 ppm. This has, however, not been the case in this study. There is a little change in the mean-relative-accuracy between $n_{max} = 140$ and $n_{max} = 180$ but starts to deteriorate slowly to 6.3 ppm at $n_{max} = 100$, drops down to 4.1 ppm at $n_{max} = 70$, and deteriorate slowly again to 8.6 ppm at $n_{max} = 10$.

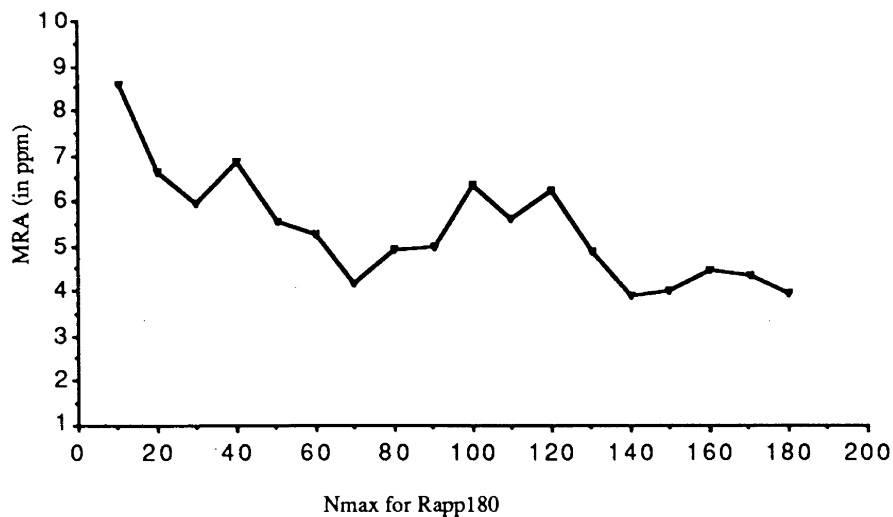


Figure 6.3 : The Recovery of ΔN from Rapp180 Geopotential Model taken to various n_{max} .

6.2.2 Comparison of ΔN between UNB Dec.'86 Solution and GPS/Levelling Solution

Using the technique described in chapters three and four, Vanicek et al. (1986) had produced a detailed geoid for Canada. These geoidal heights were computed on a 10' by 10' geographical grid. A program, called *CndGeoid* was then designed to interpolate N or ΔN at any points in Canada. ΔN is simply computed by taking the difference of N between two points. The results are tabulated in Table 6.2. They are then compared to the results derived from GPS/Levelling. The mean-relative-accuracy obtained between these two methods is 2.26 ppm and the root-mean-square error is 0.19 metres. In here, we can see that the precision for ΔH_{LEV} as quoted by Mainville[1987] does not seem to fit the pattern. Let us compute the precision of ΔN_{UNB} :

$$\sigma_{UNB/GPS}^2 = \sigma_{UNB}^2 + \sigma_{GPS/LEV}^2$$

$$= \sigma_{UNB}^2 + \sigma_{\Delta h}^2 + \sigma_{\Delta H}^2.$$

Solving for σ_{UNB}^2 we obtain:

$$\sigma_{UNB}^2 = \sigma_{UNB/GPS}^2 - \sigma_{\Delta h}^2 - \sigma_{\Delta H}^2,$$

Putting the numbers in, we have

$$\begin{aligned} \sigma_{UNB}^2 &= 2.3_{ppm}^2 - 1.1_{ppm}^2 - 3.0_{ppm}^2 \\ &= -4.92 ppm^2, \end{aligned}$$

which is a negative value. This does not make sense. The test shows that the precision for ΔH_{LEV} quoted by Mainville[1987] seem to be somewhat too large.

Table 6.2: Results of $\Delta N_{GPS/LEV}$ and $\Delta N_{UNB Dec.'86}$

$\Delta N_{GPS/LEV}$ (metres)	$\Delta N_{UNB Dec.'86}$ (metres)	Distance (metres)	Difference (metres)	Difference (ppm)
.34	.58	42835.632	-.24	5.6
.785	.83	63264.55	-.045	0.7
.917	.85	115879.659	.067	0.6
-.344	-.49	60099.078	.146	2.4
-1.44	-1.66	104268.137	.22	2.1
1.051	1.08	98077.694	-.029	0.3
.066	0	129579.232	.066	0.5
.445	.25	21152.676	.195	9.2
2.777	2.7	116714.955	.077	0.7
-.793	-1.12	125347.849	.327	2.6
.577	.27	83040.513	.307	3.7
-.684	-1.07	54653.119	.386	7.0
-1.78	-2.24	103622.863	.46	4.4
.711	.5	61474.039	.211	3.4
-.274	-.58	102898.395	.306	3.0
2.332	2.45	95918.573	-.118	1.2
-1.238	-1.37	111035.239	.132	1.2
.132	.02	65658.204	.112	1.7
-1.129	-1.32	57432.93	.191	3.3
-2.225	-2.49	103092.652	.265	2.6
.266	.25	42634.058	.016	0.4
-.719	-.83	88307.111	.111	1.3
-3.57	-3.85	108790.916	.28	2.6
-2.2	-2.42	75083.356	.22	2.9
-3.461	-3.76	134078.448	.299	2.2
-2.066	-2.2	72030.842	.134	1.9
-3.051	-3.28	96176.696	.229	2.4
1.37	1.4	48559.933	-.03	0.6
.109	.06	93057.963	.049	0.5
-.987	-1.12	79041.027	.133	1.7
1.504	1.63	71850.244	-.126	1.8
.519	.54	22730.233	-.021	0.9
-1.261	-1.34	69616.469	.079	1.1
-2.357	-2.52	84411.431	.163	1.9
.134	.23	23857.125	-.096	4.0
-.851	-.85	27288.879	-.001	0.0
-1.096	-1.18	49242.025	.084	1.7
1.395	1.57	62223.488	-.175	2.8
.41	.49	74682.196	-.08	1.1
2.491	2.75	90849.976	-.259	2.9
1.506	1.66	71899.842	-.154	2.1
-.985	-1.08	49644.149	.095	1.9

6.2.3 Comparison of ΔN between Ring Integration Solution and GPS/Levelling Solution

The use of the ring integration approach is to find the short wavelength features in ΔN from local gravity while the geopotential model will provide the medium to long wavelength contribution. The approach to compute the contribution to ΔN from the medium to long wavelength component is depending on how one handles the inner zone contribution, i.e., whether one should use the "reduced" gravity anomalies or the "unreduced" gravity anomalies. Tests have been carried out to answer this question.

6.2.3.1 Comparison between ΔN using the "Reduced" and the "Unreduced" gravity anomalies.

Approach 1:

As was mentioned in section 5.1, there are two alternative ways to obtain N or ΔN . If the "unreduced free-air anomalies" are to be used to compute the short wavelength contribution to ΔN , the error in ΔN caused by neglecting the gravity anomalies beyond the spherical cap of radius ψ_0 should be considered. From equation (5.1.1), the ΔN can be expressed as follows:

$$\Delta N = \Delta\delta N_I + \Delta N_R, \quad 6.2.3.1.1$$

where $\Delta\delta N_I$ is computed using the Ring integration; N_R is computed using the Molodenskij truncation coefficients and ΔN_R is simply calculated by taking the difference between the N_R at the end points of the baseline. In order to test for optimum cap size, Kearsley's routine [1988] was adopted. $\Delta\delta N_I$ was computed for different spherical cap of radius, ranging from 0.1° to 1.2° in an increment of about 0.1° . These $\Delta\delta N_I$ were then added to ΔN_R (summed to $n_{max} = 180$) to obtain the full ΔN . 42 full geoidal height

differences were computed and were compared with ΔN derived from GPS/Levelling. The results are plotted in Figure 6.4 (solid black circles) which shows that the optimum cap size to be combined with Rapp180 geopotential model is at $\psi_o = 0.6^\circ$. The mean-relative accuracy is 1.8 ppm and its root-mean-square error is 0.15 metres.

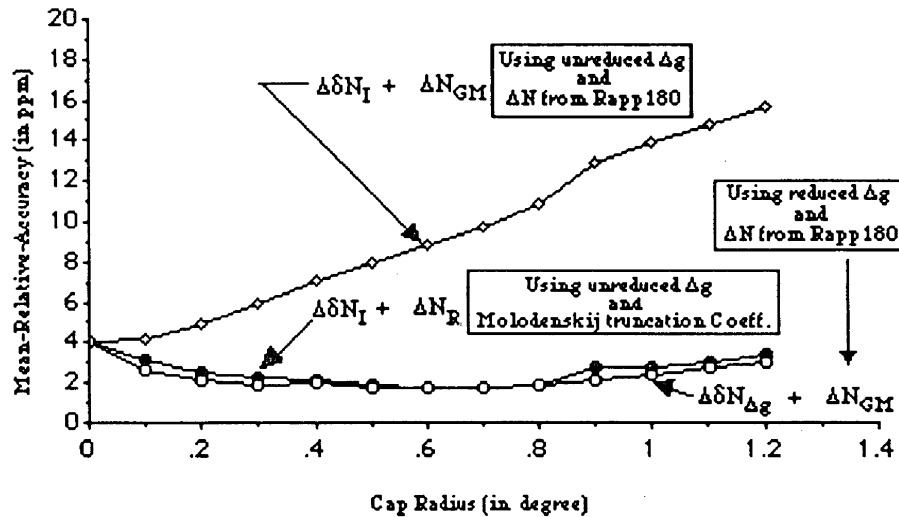


Figure 6.4: Comparisons Between ΔN Using reduced Δg and unreduced Δg in Manitoba ($n_{max} = 180$).

Approach 2:

If one wishes to use equation (5.1.6), then the Δg_n , which is obtained from spherical harmonic expansion, should be subtracted from the terrestrial free-air gravity anomalies. The remaining "reduced" free-air gravity anomalies are to be used in equation (5.1.7) to calculate the additional contribution of the ring compartments to get ΔN . These contributions are then added to the ΔN_{GM} computed by the spherical harmonic expansion. The reason for reducing the terrestrial gravity anomalies is to avoid the double counting of the spherical harmonic estimates of the contribution from the ring integration method. ΔN_{GM} was computed using the POT.RED program (this program is the same as the subroutine POT documented in Arsenault [1982] -- see Appendix I.4), while the RININT.RED program (see Appendix I.2) was used to compute the inner zone

contribution. The results from this method were then compared to the ΔN derived from GPS/Levelling as plotted in Figure 6.4 (open circles). It is surprising to see that the optimum cap size for this approach is also at $\psi_o = 0.6^\circ$, with a mean-relative-accuracy of 1.7 ppm and a root-mean-square of 0.14 metres (see Appendix I.8). The fact is that the Rapp180 geopotential model is based upon mean values of Δg for 1° by 1° rectangular blocks whose 1° by 1° block area is much smaller than that of a circle of radius 1° . In other words, the area of the 1° by 1° block is approximately equal to the area of the circle whose radius is 0.6° .

From the curves of Figure 6.4, one can see that the solutions from the above two approaches are close to each other. However, if one uses the "unreduced" gravity anomalies, rather than the "reduced" gravity anomalies, in equation(5.1.7), the value of ΔN deteriorates as is shown on the same Figure 6.4 (the diamond symbols). This is due to the double contribution of gravity signal to ΔN being both in the terrestrial gravity and in the geopotential model. The use of reduced gravity anomalies is, therefore, not necessary, provided that the Molodenskij truncation coefficients $Q(\psi_o)$ are applied correctly. In other words, if one integrates the spherical cap up to a radius of 0.6° , one should use $\psi_o = 0.6^\circ$ in $Q(\psi_o)$. Therefore, it is not whether the reduced or unreduced gravity anomalies are to be used but rather whether the theory is applied correctly or incorrectly.

What's really appealing from these results is the remarkable (1.7 ppm) improvement in ΔN when only a small spherical cap radius ($\psi_o = 0.6^\circ$) is incorporated. The mean-relative-accuracy (with respect to GPS/Levelling solution) from the above two approaches continue to improve until $\psi_o = 0.5^\circ$, more or less stabilizes, then deteriorates to $\psi_o = 1.2^\circ$; (which is the limit caused by the inavailability of gravity data at the time of the testing).

Analysis was also conducted to see how well ΔN from the ring approach can be recovered by fitting it to the GPS solution. In here, the inner zone contribution is computed with various spherical cap sizes (using the reduced gravity anomalies) and combined with the results computed using Rapp180 geopotential model of various n_{max} . In Figure 6.5, it is shown that the higher the n_{max} , the better the solution that can be obtained. From the same figure, it showed also that the best solution can be obtained using spherical cap radius of 0.6° . Hence, from this figure, one can conclude that the best approach to get an optimum solution is by combining a spherical cap size of 0.6° with Rapp180 geopotential model of n_{max} summed up to 180.

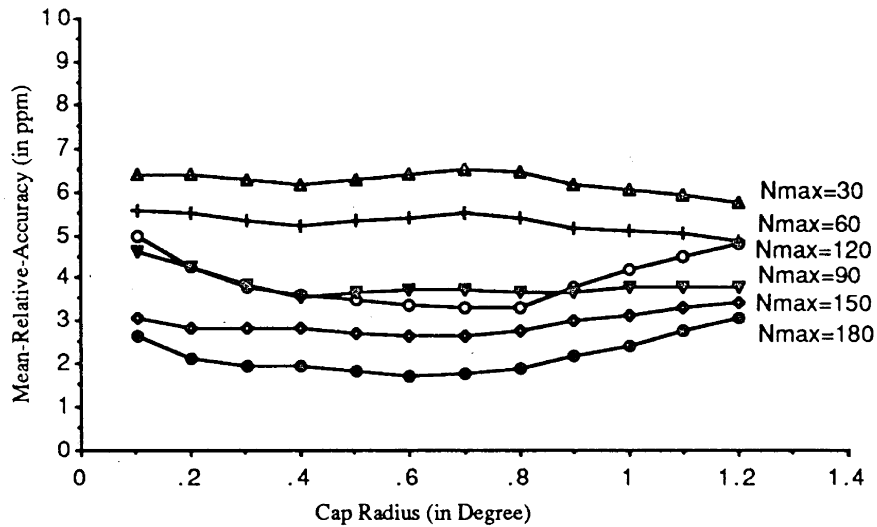


Figure 6.5: Comparison of ΔN Using Combination of Various n_{max} in the Reference Model with Various Spherical Cap Radii. (GPS vs. RING).

6.2.4 Comparison of ΔN Between Ring Integration Solution and UNB Dec.'86 Solution

It is also interesting to see how well the ring integration solution fits the UNB Dec.'86 solution. The analysis was carried out the same way as in the above section.

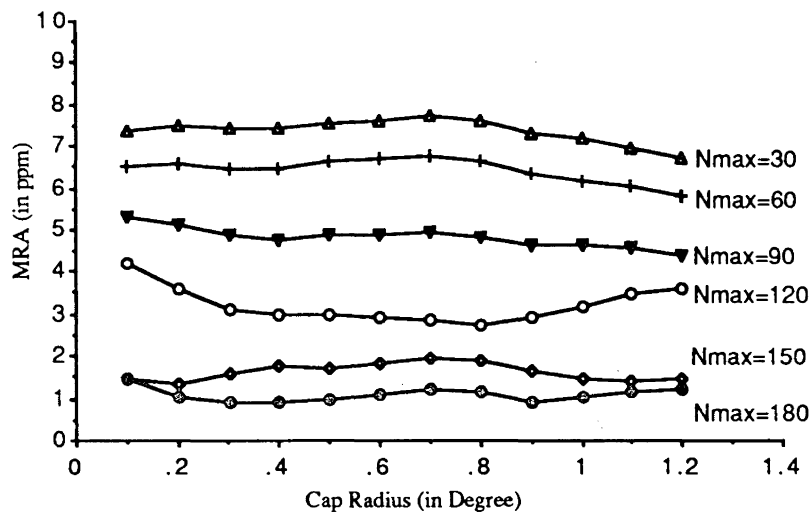


Figure 6.6: Comparison of ΔN Using Combination of Various n_{max} as the Reference Model with Various Spherical Cap Radii. (RING vs. UNB Dec.'86).

From Figure 6.6, the curves also indicate that the higher the n_{max} , the better the agreement to the UNB Dec.'86 solution. As was expected, the solution that used $n_{max} = 180$ has the best agreement. However, the best agreement to the UNB Dec.'86 solution occurred at two minima; one at $\psi_o = 0.4^\circ$ and the other at $\psi_o = 0.9^\circ$. They both have mean-relative-accuracies of 0.92 ppm and root-mean-squares errors of 0.07 metres. Figure 6.7 shows that for n_{max} up to 100, the ring integration solution (using the reduced gravity anomalies) agrees better to the GPS/Levelling solution than it is to the UNB Dec.'86 solution. Then for n_{max} about 100 and up, the ring integration solution agrees better with the UNB Dec.'86 solution than with the GPS/Levelling solution.

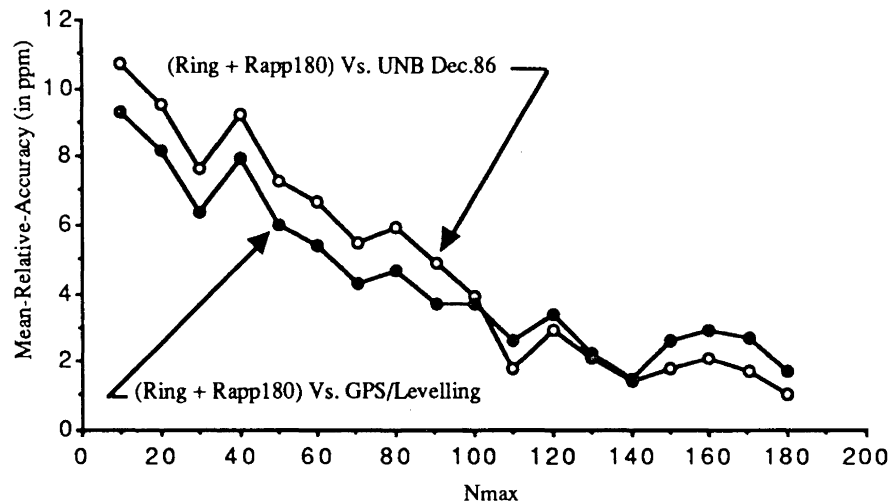


Figure 6.7: The Recovery of ΔN with Various n_{max} .
(Ring is computed with $\psi_o = 0.6$ degree)

6.2.5 Analysis of ΔN with respect to Baseline Lengths.

Further analysis was carried out to see if there was any correlation between ΔN and the baseline lengths. Misclosures were computed as the absolute values of differences between two different solutions. For each of the 42 baselines, the misclosures were plotted against its corresponding baseline lengths (see Figure 6.8). These three plots show no trend between the misclosures and the baseline lengths. In other words, ΔN is independent of the baseline length. Misclosures were also plotted against the azimuths (see Figure 6.9) and these plots also show that ΔN is independent of the azimuth.

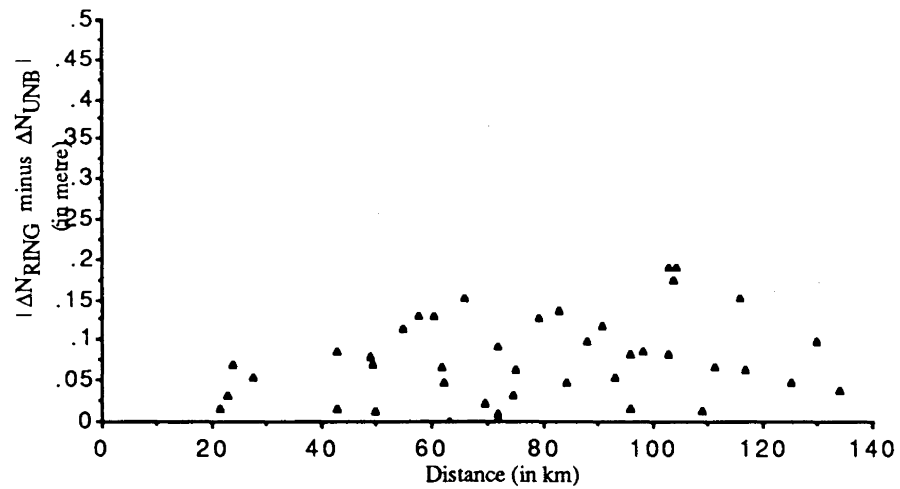
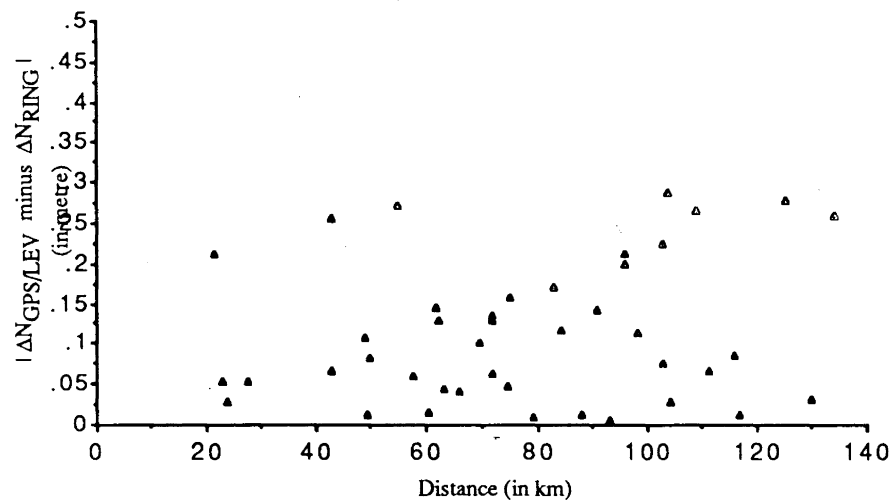
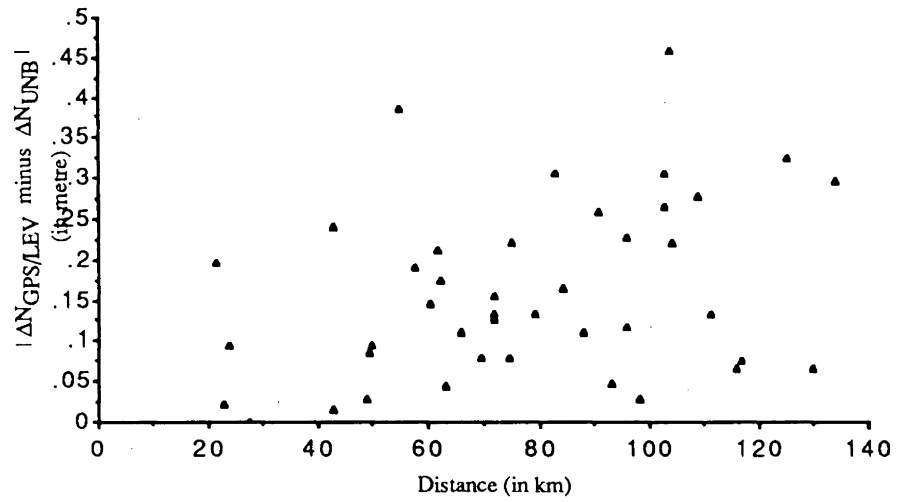


Figure 6.8: Plots of Misclosures against Distances.

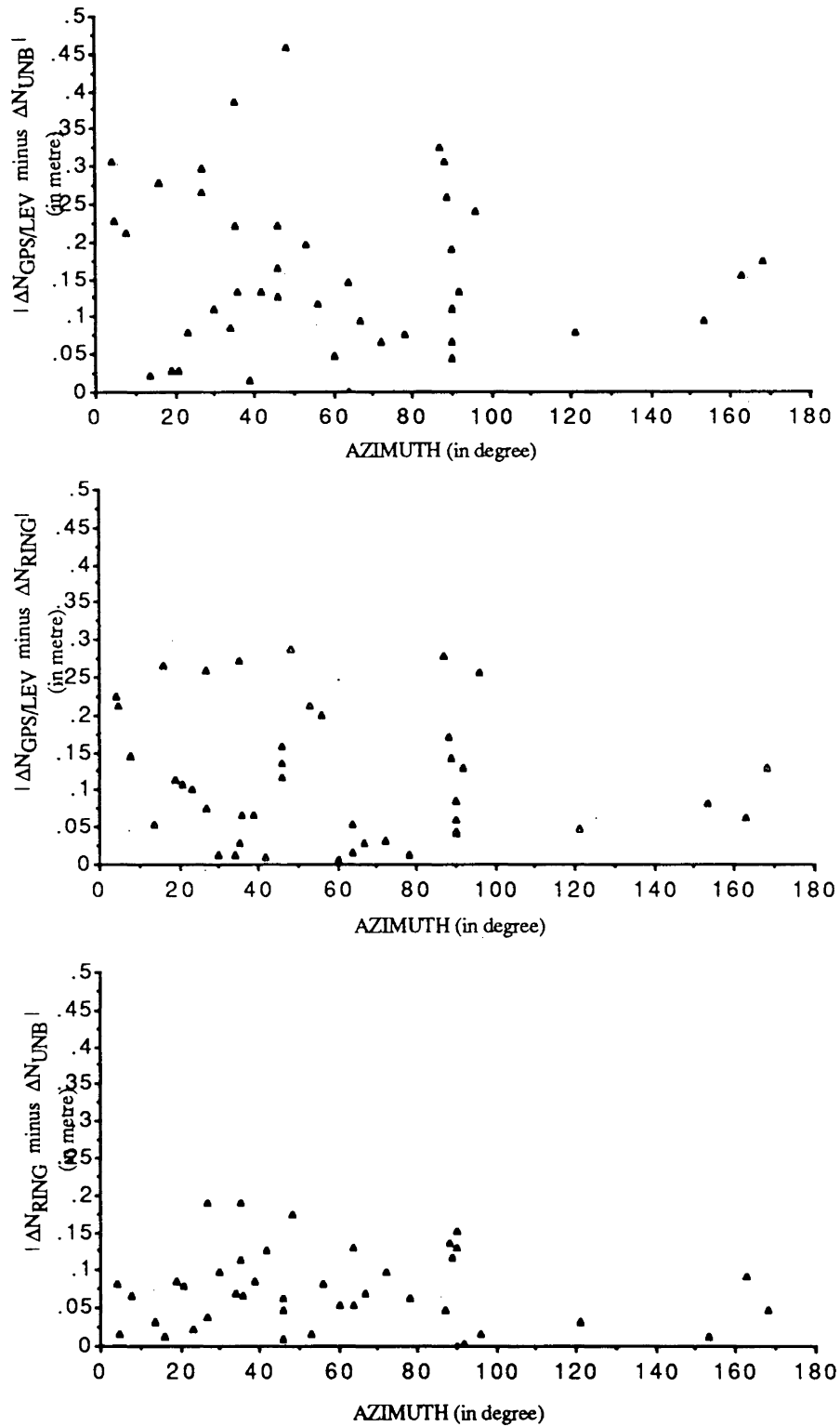


Figure 6.9: Plots of Misclosures against Azimuths.

6.3 Error Analysis

In this section, the errors in geoidal height difference will be presented. The structure of our analysis here is very similar to that of the investigation conducted by Kearsley[1986a, 1986b]. There are basically three types of errors: the random errors, the systematic errors and the errors from the remote zone contribution. Each of these will be discussed separately.

6.3.1 Random Errors

The existence of random error in geoidal height(σ_N) is mostly due to the errors in the mean gravity anomalies($\widetilde{\Delta g}_i$) from every compartment. That is to say, each i^{th} compartment contributes an error:

$$\delta N_i = N_c^* \delta \widetilde{\Delta g}_i. \quad 6.3.1.1$$

to N , where $\delta \widetilde{\Delta g}_i$ is the error in $\widetilde{\Delta g}_i$. Assuming that the correlation between successive $\widetilde{\Delta g}_i$ is zero, then the error in N can be obtained by applying the law of error propagation to the above equation(6.3.1.1):

$$\sigma_N^2 = (N_c^*)^2 \sum_{i=1}^I \sigma_{\widetilde{\Delta g}_i}^2, \quad 6.3.1.2$$

where $\sigma_{\widetilde{\Delta g}_i}^2$ is the variance of the mean gravity anomaly for i^{th} compartment and can be obtained from the following expression:

$$\sigma_{\widetilde{\Delta g}_i}^2 = \frac{\sum_{i=1}^I \sigma_{\Delta g_i}^2}{n} \quad 6.3.1.3$$

and n is the total number of gravity anomalies within the cell. From equation(5.2.4.2), the above procedure can be applied to obtain the error in ΔN_{AB} . However, some of the compartments which were used to predict $\widetilde{\Delta g}$ at point A will be used to predict $\widetilde{\Delta g}$ at point B . These "common" $\widetilde{\Delta g}$ will not affect ΔN and somehow, we need to eliminate them and to sort out only those $\widetilde{\Delta g}$ that are used to evaluate N at point A and not at point B .

The approach to these so called "eliminated $\widetilde{\Delta g}$ " and "sorted $\widetilde{\Delta g}$ " is to apply the "area method". This method estimates the areas of the inner zone which are not common to the computations at either points (see Figure 6.10).

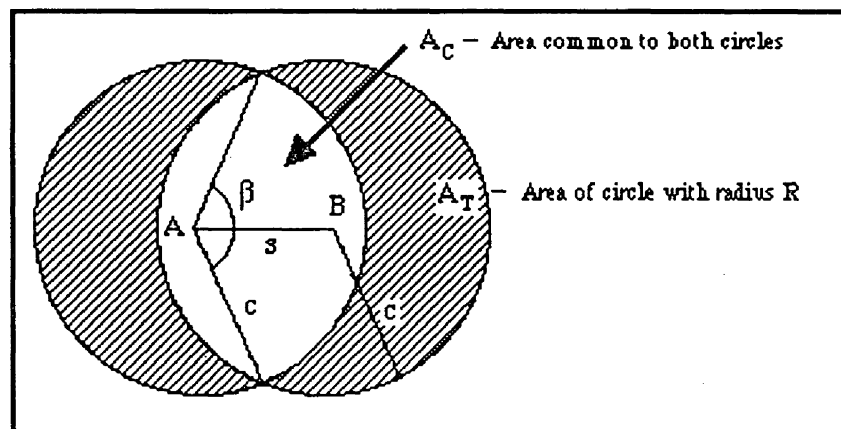


Figure 6.10: The shaded regions show the areas which are not common to the Inner Zones of Points A and B where ΔN is being computed [after Kearsley (1986b, p. 159)].

If A_c is the area common to the inner zones of both points A and B and if A_T is the total area of the inner zone, then the proportion Q of the unshared area (i.e., the area which is not common to both circles) is [Kearsley, 1986a]:

$$Q = 1 - \frac{A_c}{A_T} = 1 - \left[\frac{\beta - \sin\beta}{180^\circ} \right], \quad 6.5.1.4$$

where $\beta = 2 \cos^{-1}\left(\frac{s}{2c}\right)$ and c is the spherical cap radius.

Hence Q is a function of the length of the line or distance s between points A and B . These proportions Q have been calculated for several lengths and are tabulated in Table 6.3.

Table 6.3: The relationships between the proportion Q , the distance s and the spherical cap radius c [after Kearsley (1986b, p. 162)].

c (km)	34	45	56	67	78	89	100	111
ψ_0	0.3°	0.4°	0.5°	0.6°	0.7°	0.8°	0.9°	1.0°
s (km)	Q							
10	0.19	0.14	0.11	0.10	0.08	0.07	0.06	0.06
20	0.38	0.28	0.23	0.19	0.16	0.14	0.13	0.11
30	0.55	0.42	0.34	0.28	0.24	0.21	0.19	0.17
40	0.71	0.55	0.45	0.38	0.32	0.28	0.25	0.23
50	0.86	0.68	0.55	0.47	0.40	0.35	0.31	0.28
60		0.79	0.65	0.55	0.48	0.42	0.38	0.34
70		0.89	0.74	0.64	0.55	0.49	0.44	0.39
80		0.96	0.83	0.71	0.62	0.55	0.50	0.45
90			0.90	0.79	0.69	0.62	0.55	0.50
100			0.96	0.86	0.76	0.68	0.61	0.55
110			1.00	0.91	0.82	0.73	0.66	0.60

When the spherical cap radius increases, Q decreases. Although the proportion of the circle area is smaller when a larger spherical cap radius is applied, the contribution of the error in $\widetilde{\Delta g}$ to the error in ΔN_{AB} will be larger. This is because there are more mean gravity anomalies located in the area of the inner zone whose spherical cap radius is large, than in the area of the inner zone whose spherical cap radius is small. We can also observe that as s increases, Q increases. This indicates that the further the two points are apart, the fewer Δg they share, and hence the larger the error contributed to ΔN_{AB} .

From the above analysis, the error in ΔN_{AB} from $\widetilde{\Delta g}$ that are used only at point A can be computed by rewriting equation (6.3.1.2) as follows:

$$\sigma_{\Delta N}^2 = (N_c^*)^2 [2n' \sigma_{\Delta g_i}^2 (1 - \mu)], \quad 6.3.1.4$$

where $2n'$ is the total number of compartments that are used in the two unshared regions and μ is the correlation coefficient between mean gravity anomalies. n' can be estimated using the area-proportion Q from Table 6.3.

For example, given $\psi_o = 0.6^\circ$, $s = 10$ km, we have:

$$\begin{aligned} n' &= Q \times \text{the total number of compartments within a spherical cap} \\ &= 0.1 \times 234 = 23.4 \doteq 24. \end{aligned}$$

The estimated n' are tabulated in Table 6.4 for various baselines.

Table 6.4: Number of Compartments (n') used to calculate N_A which are not used to compute N_B .

c (km)	34	45	56	67	78	89	100	111
ψ_o	0.3°	0.4°	0.5°	0.6°	0.7°	0.8°	0.9°	1.0°
s (km)	n'							
10	24	23	22	24	22	22	23	25
20	48	46	46	45	44	43	50	46
30	70	69	68	66	65	65	71	71
40	90	90	90	89	87	86	95	96
50	109	111	109	110	108	108	118	116
60		128	129	129	130	129	144	141
70		145	147	150	149	150	167	162
80		156	165	167	168	169	189	187
90			179	185	187	190	208	207
100			191	202	206	209	231	228
110			198	213	222	224	250	249

Assuming that the variance in $\widetilde{\Delta g}_i$ is 9 mGal², the errors in ΔN , i.e., $\sigma_{\Delta N}$, can be estimated using Table 6.4 and equation(6.3.1.4) and they are tabulated in Table 6.5.

Table 6.5: Error in ΔN over various s due to Random Error in $\widetilde{\Delta g}$.

$\sigma_{\Delta N}$ (in cm)						
s (Km)	$\mu = 0$			$\mu = 1$ in 20% of uncoupled $\widetilde{\Delta g}$		
	$\psi_o = 0.5^\circ$	$\psi_o = 0.6^\circ$	$\psi_o = 1.0^\circ$	$\psi_o = 0.5^\circ$	$\psi_o = 0.6^\circ$	$\psi_o = 1.0^\circ$
10	0.6	0.6	0.6	0.5	0.5	0.5
20	0.9	0.7	0.9	0.7	0.7	0.7
30	1.1	1.0	1.1	0.8	0.8	0.8
40	1.2	1.2	1.3	0.9	0.9	1.0
50	1.3	1.3	1.4	1.0	1.0	1.1
60	1.4	1.4	1.5	1.1	1.1	1.2
70	1.5	1.6	1.6	1.2	1.2	1.3
80	1.6	1.6	1.7	1.3	1.3	1.3
90	1.7	1.7	1.8	1.3	1.3	1.4
100	1.8	1.8	1.9	1.4	1.4	1.5
110	1.8	1.9	2.0	1.4	1.4	1.6

6.3.2 Systematic Errors

The error in ΔN will be caused by the systematic error in $\widetilde{\Delta g}$, too. Since gravity anomalies are calculated based on the choice of datums of networks (e.g. gravity network, vertical network and horizontal network) used in the free-air reduction procedure, they can be influenced by the systematic errors caused by the inconsistency of the local datums with respect to the global datums. The effects on ΔN by some of these systematic error sources were analyzed in details by Heck [1990]. In here, a brief discussion on them will be revisited.

6.3.2.1 Error caused by Gravity Datum Inconsistency

Absolute or relative gravity measurements are made on the surface of the earth. Corrections, such as drift, atmospheric attraction, earth and ocean tides, etc., are then applied to reduce these measured gravity values to nominal gravity values. In practise, absolute and relative gravity are combined together, through the establishment of global network known as the International Gravity Standardization Net 1971 (IGSN 71). This is the reference datum that is used to tie local gravity surveys to a global homogeneous network. However, regional biases of about 0.2 mGal [Heck, 1990] have been detected in the absolute gravity values. These regional biases will affected other absolute values of regional gravity surveys that were tied to some IGSN 71 stations which, in turn, will introduce systematic errors(< 0.2 mGal) in gravity anomalies.

6.3.2.2 Error Caused By Vertical Datum Inconsistency

Differential levelling determines height differences between pairs of points. These observed height differences are then converted into orthometric, dynamic or normal height differences through the application of appropriate corrections [Vanicek and Krakiwsky, 1982]. Orthometric height is then determined by connecting height differences with the reference bench marks which define the vertical datum. If all the heights are connected to one common datum, then a consistency of heights will be obtained. However, in Canada, more than one datum have been used [Robinson, 1990]. Vertical datum has been established by tide gauge observations in coastal regions. It was assumed that at one time the mean sea-level theoretically coincided with the geoid (which is the reference surface for heights) but later realized that the two surfaces are separated by the sea surface topography amounting up to 1-2 m on the oceans [Heck, 1990]. The use of

inconsistent vertical datum can cause a bias of ± 0.5 mGal [Heck, 1990] in the terrestrial gravity anomalies. Thus, the effect of this bias would propagate as systematic errors in ΔN .

6.3.2.3 Error Caused By Horizontal Datum Inconsistency

The horizontal coordinates of a gravity station are defined in term of ellipsoidal (geodetic) latitude and longitude. These coordinates are normally referred to a local horizontal datum which was defined using astronomical observations at one or several fundamental points in the beginning of this century. Since then, more observations have been obtained using modern instruments. However, datum such as the North American Datum 27 (NAD27) is no longer valid today due to a shift of coordinates. Because of the shift of coordinates, the geodetic datum has to be redefined and coordinates from old datum have to be transformed to the new datum (NAD83). In order to perform this transformation, the parameter differences (ΔX_o , ΔY_o , ΔZ_o , Δa , Δf) between the two datums are required [Vanicek and Krakiwsky, 1982]:

$$\begin{bmatrix} \phi_2 \\ \lambda_2 \\ h_2 \end{bmatrix} = \begin{bmatrix} \phi_1 \\ \lambda_1 \\ h_1 \end{bmatrix} - J^{-1} \left(\begin{bmatrix} \Delta X_o \\ \Delta Y_o \\ \Delta Z_o \end{bmatrix} + B \begin{bmatrix} \Delta a \\ \Delta f \end{bmatrix} \right), \quad 6.3.2.3.1$$

where

$$J^{-1} = \begin{bmatrix} -\sin\phi\cos\lambda/(M+h) & -\sin\phi\sin\lambda/(M+h) & \cos\phi/(M+h) \\ -\sin\lambda/[(N+h)\cos\phi] & \cos\lambda/[(N+h)\cos\phi] & 0 \\ \cos\phi\cos\lambda & \cos\phi\sin\lambda & \sin\phi \end{bmatrix}, \quad 6.3.2.3.2$$

$$B = \begin{bmatrix} N\cos\phi\cos\lambda/a & M\sin^2\phi\cos\phi\cos\lambda/(1-f) \\ N\cos\phi\sin\lambda/a & M\sin^2\phi\cos\phi\sin\lambda/(1-f) \\ N(1-f)^2\sin\phi/a & (M\sin^2\phi-2N)\sin\phi/(1-f) \end{bmatrix}, \quad 6.3.2.3.3$$

M and N are the radii of curvature; f is the flattening; a is the major-semi axis of the ellipsoid and $(X_o, \Delta Y_o, \Delta Z_o)$ are the datum translation components. From equation(6.3.2.3.1), we can obtain $d\phi$ (the shift of the ellipsoidal latitude ϕ). This $d\phi$ will induce the change in the normal gravity $d\gamma$ using the approximate formula [Heck,1990]:

$$d\gamma = \gamma_a f^* \sin 2\phi d\phi, \quad 6.3.2.3.4$$

where $\gamma_a f^* = 5.172 \times 10^{-2} \text{ m/s}^2$. The change in the normal gravity will, in turn, affect the gravity anomaly through the following equation:

$$\Delta g_{FA} = g_s - \gamma_o - 0.3086H_p, \quad 6.3.2.3.5$$

where g_s is the observed gravity on the surface of the earth; γ_o is the normal gravity computed using equation(2.2.2); and H_p is the orthometric height at point p . However, the maximum value for $d\phi$, for transforming NAD27 to NAD83(GRS80), is about 1" [Vanicek, 1991]. Assuming $\phi = 45^\circ$, $d\gamma$ will be $26 \times 10^{-6} \text{ mGal}$ which has a very small effect on ΔN .

Using the law of the propagation of systematic errors, one can estimate the size of the systematic error in $\widetilde{\Delta g}$ and see how much ΔN can be influenced from the following equation:

$$\epsilon_{\Delta N} = n' N_c^* \epsilon_{\widetilde{\Delta g}}, \quad 6.3.2.3.6$$

If there is a bias of 1.0 mGal in the gravity set which was used to compute only N_A , the errors in ΔN for a 110 km baseline computed using $\psi_o = 0.6^\circ$ can be as large as 6.4 cm. The error in ΔN is computed for various distances and is tabulated in Table 6.6. The systematic error increases as the baseline length increases. If one has to achieve $\epsilon_{\Delta N}$ below

5 cm over 110 km, then $\varepsilon_{\widetilde{\Delta g}}$ (using spherical cap radius of $\psi_o = 0.6^\circ$) would need to be less than 0.8 mGal.

Table 6.6: Error in ΔN due to Systematic Error in $\widetilde{\Delta g}$. Assuming $\varepsilon_{\widetilde{\Delta g}}$ of 1.0 mGal presents between gravity data used exclusively for N_A and that used exclusively for N_B .

S (Km)	$\varepsilon_{\Delta N}$ (in cm)		
	$\psi_o = 0.5^\circ$	$\psi_o = 0.6^\circ$	$\psi_o = 1.0^\circ$
10	0.7	0.7	0.8
20	1.4	1.4	1.4
30	2.0	2.0	2.1
40	2.7	2.7	2.9
50	3.3	3.3	3.5
60	3.9	3.9	4.2
70	4.4	4.5	4.9
80	5.0	5.0	5.6
90	5.4	5.6	6.2
100	5.7	6.1	6.8
110	5.9	6.4	7.5

6.3.3 Errors from the Remote Zone Contribution

As was mentioned in the previous section, Rapp180 geopotential model with degree and order to 180 had been used to compute the remote zone contribution to ΔN . Two error sources, such as (1) the errors due to the geopotential coefficient errors, and (2) errors due to the truncation of the infinite series to n_{max} have been discussed by Engelis et al. [1985]. They show that the total contribution from these two error sources can be about 3 cm for baseline of only 20 km, i.e., 1.5 ppm. The comparison of the results (combination of ΔN from Rapp180 geopotential model with ΔN from ring integration) with ΔN derived from GPS/Levelling (1.7 ppm) agreed.

CHAPTER SEVEN

SUMMARY, CONCLUSIONS AND RECOMMENDATIONS

Two sets of programs, namely (RININT.RED with POT.RED) and (RININT.UNRED with POT.UNRED), which have been developed to determine geoidal height difference by simply inserting the latitude and longitude of two points. Program RININT.RED computed the short wavelength contribution to ΔN using the "reduced" free-air gravity anomalies. The contribution to ΔN from medium to long wavelength was computed using the program POT.RED. The results from these two programs were then added together to obtain a full geoidal height difference. Program RININT.UNRED also computed the short wavelength contribution to ΔN but using the "unreduced" free-air gravity anomalies. The corresponding program to compute the medium to long wavelength contribution to ΔN was program POT.UNRED. A full geoidal height difference was then obtained by adding the results from these two contributions.

The Ring Integration approach consists of rings centering upon the point of computation and lines radiating out from the point of computation. The intersections of these rings and lines formed compartments which are used to evaluate the inner zone contribution of the geoidal height difference. The area between concentric circles of radius up to 1.2° is divided into three sub-zones. The inner sub-zone and the middle sub-zone consists of six and twelve compartments respectively, while the outer sub-zone consists of 36 compartments in each of the 13 rings. The inner and the outer radii of each ring are

selected so that the mean gravity anomaly for a sector of a ring, formed by a pair of radial lines subtending an angle, will contribute 0.0003 m/mGal to N . These methods has been outlined in chapter five. The remote zone contribution (using programs POT.RED or POT.UNRED) were computed from the high order geopotential model (RAPP180) to degree and order of 180.

The computation methods and the type of data used in the UNB approach have been shown in chapters three and four. Its results had been compared with the Ring Integration method in chapter six. The dissimilarities between the Ring Integration approach and the Stokes approach were summarized as followed:

- a) In this investigation, the software which was used to obtain the short wavelength contribution computes the geoidal height difference directly. In the UNB approach, the program, named "GIN" [Chang et al.,1986], used to obtain the short wavelength contribution, computes only the geoidal height. Geoidal heights at each end of the line were then differenced to obtain the geoidal height difference.
- b) The UNB approach uses the Stokes function while the Ring Integration approach used the F -function.
- c) In the UNB approach, pre-computed mean gravity anomalies which were stored in a grid form were used to compute N , while in the Ring Integration approach, mean gravity anomalies interpolated at the time of the computation using weighted arithmetic mean technique, were employed to determine ΔN .
- d) GEM9 geopotential model of degree and order to 20 were used in the UNB approach as the reference surface where terrestrial gravity anomalies were reduced,

while RAPP180 geopotential model of degree and order to 180 were used in the Ring Integration approach for the reference surface.

- e) In the UNB approach, the integration had to be carried out to a cap size of 6.0° radius to obtain an accurate N while in the Ring Integration approach, an integration over a cap size of 0.6° radius was good enough to obtain a reasonable ΔN .
- f) In the UNB approach, corrections such as the terrain effects, the indirect effects and the atmospheric effects have been included in the evaluation of N . In the Ring Integration approach, none of these have been incorporated.
- g) The database for the UNB approach consists of point gravity anomalies, pre-computed 5 by 5 minute mean Δg and 1 by 1 degree mean Δg , while the database for the Ring Integration approach includes only the point gravity anomalies.

The results from the Ring Integration approach have been tested by comparing against those values which were derived from a combination of GPS and spirit levelling, and against those values (UNB Dec.'86) which were derived from the UNB method. From the comparisons, a root-mean-square difference of 0.14 metre was obtained between the GPS/Levelling method and the Ring Integration method using a cap size of 0.6° radius. However, the root-mean-square difference between the UNB method and the GPS/Levelling method had a value of 0.19 metre. Despite the fact that the root-mean-square difference (with respect to GPS/Levelling) for the Ring Integration shows a better value than the UNB method, it does not indicate which of the two methods is better. This is because there are errors that are present in ΔN from GPS/Levelling. In the comparisons, we assumed that the error in GPS/levelling derived geoidal height difference, the error in RAPP180 derived geoidal height difference and the error in GEM9 derived geoidal height difference were negligible. In fact, the error in GPS/Levelling derived geoidal height

difference was estimated to be about 3.2 ppm [Mainville, 1987] and the errors contributed from RAPP180 and GEM9 geopotential models were proved to be 1 metre [Lachapelle and Rapp, 1982] and 1.75 metres [Vanicek and Kleusberg, 1987], respectively.

Nevertheless, the results of the comparisons certainly encourage one that the Ring Integration approach is capable of producing ΔN whose precision at least matches those produced by the UNB method and those produced by the GPS/Levelling method. An agreement of 1.7 ppm in mean-relative-accuracy with respect to GPS/Levelling solutions was achieved considering a small 0.6° integration of gravity anomalies was incorporated in the evaluation of ΔN . Using a spherical cap radius of 0.4° , a 0.92 ppm in mean-relative-accuracy with respect to UNB solutions was achieved.

From the comparisons of the results, it is observed that the cap size radius (ψ_o) and the n_{max} value which is used for computing the remote zone, play significant roles in geoidal height determination. The results computed from the Ring Integration approach agrees better to the results obtained from GPS/Levelling as n_{max} increases. By trial and error, the optimum solution can be obtained by using the combination a spherical cap radius of $\psi_o = 0.6^\circ$ with $n_{max} = 180$. The results also show that ΔN derived from RAPP180 geopotential coefficients could be improved by taking the effect of detailed terrestrial gravity in a cap size radius of 0.6° into account. When ΔN is computed only from the RAPP180 geopotential model alone, the agreement with GPS/Levelling is 4.0 ppm at best.

Since the method of Ring Integration is simply the summation of mean gravity anomalies ($\widetilde{\Delta g}$) and scaling it by 0.0003 m/mGal, the technique for predicting mean Δg for the compartments also played an important role in the determination of geoidal height difference. The choice of the method for predicting mean Δg , however, depends on the spacing of the point gravity anomalies in the data file that is available. Although, in this

thesis the method used to evaluate mean Δg was the arithmetic weighted mean, there were several prediction methods, such as least-squares collocation and polynomial surface fittings [Kassim,1980], that could be used to obtain the mean gravity anomalies for the compartments. It is thus recommended that further research should be conducted to investigate these methods for producing mean Δg .

Other than the prediction method used, the errors in the free-air anomalies need special attention and are by far the largest component affecting ΔN . The effect on ΔN from these errors (i.e., random errors and systematic errors) have been estimated in chapter six. It was shown that a random error of 3 mGal in $\widetilde{\Delta g}$ could contribute an error of about ± 6 mm in ΔN for distances of 10 km to about ± 20 mm in ΔN for distances of 110 km. Analysis has also shown that a systematic error of 1.0 mGal in $\widetilde{\Delta g}$ could give an error of about ± 10 mm for distances of 10 km to about ± 80 mm for distances of 110 km. The errors in ΔN resulting from systematic errors in $\widetilde{\Delta g}$ seem to be large. It is suggested that further investigation be conducted to study the effect of the errors in Δg on ΔN using the Ring Integration approach.

The advantage of the Ring Integration method is its flexibility in matching the compartment size to the density of the data. The thickness of the rings was generated in small steps, thus allowing the full use of the available data in the averaging of Δg . The method is simple to understand and is easy to program. Nevertheless, the disadvantage is that the mean gravity anomalies obtained for the compartments at one point were different and therefore could not be reused at the other points in the evaluation of N , whereas in the UNB approach, the mean gravity anomalies are stored in grid form and hence they could be reused for computation at other points. The other disadvantage is that the Ring Integration approach takes longer time to produce ΔN , while in the UNB approach, N is available on a grid and it is easily interpolated so that ΔN can be obtained in almost no time whatever.

REFERENCES

- Agajelu, Sammy I. [1976]. "The Influence of the Short Wavelength features of the Earth's Gravity Field on Low Orbiting Satellites." Department of Geodetic Science, Report No. 246, The Ohio State University, Columbus.
- Alamdari, Mehdi Najafi. [1981]. "Local Evaluation of the Geoid from Gravity Data." M.Sc.E. thesis, Department of Surveying Engineering, University of New Brunswick, Fredericton.
- Anderson, E. G. [1975]. "Atmospheric Effects in Physical Geodesy." UNISURV G, No. 23, The School of Surveying, University of New South Wales, Sydney, Australia, pp 23-41.
- Arsenault, T. [1982]. "Computer Program Library User's Guide." Department of Surveying Engineering Technical Report 86, University of New Brunswick, Fredericton.
- Beers, Larry Delano [1971]. "The Earth's Gravity Field from a Combination of Satellite and Terrestrial Gravity Data." Ph.D. dissertation, Hawaii Institute of Geophysics, University of Hawaii, USA.
- Biro, Peter [1983]. *Time Variation of Height and Gravity*, Herbert Wichmann Verlag, Karlsruhe, Hungary.
- Carrera, G. [1984]. "Heights on a Deforming Earth." Department of Surveying Engineering Technical Report 107, University of New Brunswick, Fredericton.
- Chang, R.G., N. Christou and H. Fashir [1986]. "Software for Geoid Computation." Department of Surveying Engineering, Technical Memorandum TM-10, University of New Brunswick, Fredericton.
- Ecker, E. and E. Mittermayer [1969]. "Gravity Corrections for the Influences of the Atmosphere." *Boll. Geoph. Teor. Appl.*, XI, pp. 70-79.
- Encyclopædia Britannica [1978]. "Surveying." Volume 17, 15th. Edition, Helen Hemingway Benton Publisher, Chicago, p. 828.
- Engelis, T., R. Rapp and C.C. Tscherning [1984]. "The Precise Computation of Geoid Undulation Differences with Comparison to Results Obtained from the Global Positioning System." *Geophysical Research Letters*, Volume 1, No. 9, pp. 821-824.
- Engelis, T., R. Rapp, and Y. Bock [1985]. "Measuring Orthometric Height Differences with GPS and Gravity Data." *Manuscripta Geodaetica*, Volume 10, pp. 187-194.

- Gilliland, J.R. [1986]. "Heights and G.P.S." *The Australian Surveyor*, Volume 33, No.4, December.
- Gilliland, J.R. [1989]. "A Gravimetric Geoid of Australia" *The Australian Surveyor*, Volume 34, No.7, September.
- Heck, B. [1990]. "An Evaluation of Some Systematic Error Sources Affecting Terrestrial Gravity Anomalies." *Bulletin Geodesique*, Volume 64, pp. 88-108.
- Heiskanen, W. A., and H. Moritz [1985]. *Physical Geodesy*. W. H. Freeman and Company, San Francisco and London.
- Hung, Pen-Shan [1986]. "Evaluation of the Plumbline Curvature Effect on the Deflection of the Vertical." Department of Surveying Engineering Technical Report 121, University of New Brunswick, Fredericton.
- International Association of Geodesy [1971]. *Geodetic Reference System 1967*, IAG Special Publication No. 3, Paris, France.
- Kassim, Faud A. [1980]. "An Evaluation of Three Techniques for the Prediction of Gravity Anomalies in Canada." Department of Surveying Engineering Technical Report 73, University of New Brunswick, Fredericton.
- Kearsley, A.H.W. [1985]. "Toward the Optimum evaluation of the Inner Zone Contribution to Geoidal heights." *Aust. J. Geod. Photo. Surv.*, No.42, pp. 75-98.
- Kearsley, A.H.W. [1986a]. "Data Requirements for Determining Precise Relative Geoid Heights From Gravimetry." *Journal of Geophysical Research*, Volume 91, No.B9, pp. 9193-9201, August.
- Kearsley, A.H.W. [1986b]. "The Determination of Precise Geoid Height Differences Using Ring Integration." Anno XLV, *Bollettino Di Geodesia E Scienze Affini*, N.2.
- Kearsley, A.H.W. [1988a]. "The Determination of the Geoid-Ellipsoid Separation for GPS Levelling." *The Australian Surveyor*, Volume 34, No.1, March.
- Kearsley, A.H.W. [1988b]. "Tests on the Recovery of Precise Geoid Height Differences From Gravimetry." *Journal of Geophysical Research*, Volume 93, No.B6, pp. 6559-6570, June.
- Kearsley, A.H.W., M. G. Sideris, Jan Krynski, Rene Forsberg and K.P. Schwarz [1985]. "White Sands Revisited a Comparison of Techniques to Predict Deflections of the Vertical." UCSE Reports #30007, Division of Surveying Engineering, University of Calgary, Calgary, Alberta.
- Lachapelle, G. [1975]. "Determination of the Geoid Using Heterogeneous Data." *Mitteilungen der geodatischen Institute der Technischen Universitat Graz*, Folge 19, Graz.

- Lachapelle, G. [1978a]. "Estimation of the Geoid and Deflection Components in Canada." Collected Papers Geodetic Survey, Surveys and Mapping Branch, Energy, Mines and Resource Canada, pp. 157-181.
- Lachapelle, G. [1978b]. "Evaluation of 1 X 1 Degree Mean Free-Air Gravity anomalies in North America." Collected Papers Geodetic Survey, Surveys and Mapping Branch, Energy, Mines and Resource Canada, pp. 183-213.
- Lachapelle, G. [1978c]. "Status of the Redefinition of the Vertical Reference System in Canada." Collected Papers Geodetic Survey, Surveys and Mapping Branch, Energy, Mines and Resource Canada, pp. 215-228.
- Lachapelle, G. [1980]. "Earth's Gravity Field in Surveying." Geodetic Seminal on the Impact of Redefinition and New Technology on the Surveying Profession, *Canadian Institute of Surveying*, pp. 81-102.
- Lachapelle, G. and R. Rapp [1982]. "Estimation of Disturbing Potential Components with Emphasis on North America." CIS Centennial Convention 1982 Proceeding. *Canadian Institute of Surveying*, Ottawa.
- Laskowski, Piotr [1983]. "The Effect of Vertical Datum Inconsistencies on the Determination of Gravity Related Quantities." Department of Geodetic Science, Report No. 349, The Ohio State University, Columbus.
- Mainville, A. [1987]. "Intercomparison of Various Geoid Computation Methods at GPS Stations." Paper presented at the Association of Geodesy Meeting, Vancouver.
- Mainville, A. and M. Veronneau [1989]. "Creating a Gravity Grid Over Canada Using Bouguer Anomalies and a Digital Elevation Model." Paper presented at the Canadian Geophysical Union Annual Meeting, Montreal.
- Mather, R.S. [1975]. "Mean Sea Level and the Definition of the Geoid." UNISURV G, No. 23, The School of Surveying, University of New South Wales, Sydney, Australia, pp. 68-79.
- Merry, Charles [1975]. "Studies toward an Astrogravimetric Geoid for Canada." Ph.D. dissertation, Department of Surveying Engineering, University of New Brunswick, Fredericton.
- Mitchell, H.L. [1988]. "G.P.S. Heighting in Australia: An Introduction." *The Australian Surveyor*, Volume 34, No.1, March.
- Molodenskij, M.S., V.F. Eremeev and M.I. Yurkina [1962]. "Methods for the Study of the External Gravitational Field and the Figure of the Earth." English translation by Israel Program for Scientific Translations, Jerusalem, U.S. Department of Commerce, Washington, D.C., U.S.A.
- Moritz, Helmut [1980]. "Geodetic Reference System 1980." *Bulletin Geodesique*, Volume 54, No.3, pp. 395-405.

- Moritz, Helmut [1983]. "Local Geoid Determination in Mountain Regions." Department of Geodetic Science, Report No. 352, The Ohio State University, Columbus.
- Nassar, Mohamed M. [1977]. "Gravity Field and Levelled Heights in Canada." Department of Surveying Engineering Technical Report 41, University of New Brunswick, Fredericton.
- Nassar, Mohamed M. and P. Vanicek [1975]. "Levelling and Gravity." Department of Surveying Engineering Technical Report 33, University of New Brunswick, Fredericton.
- Orlin, H (ED.) [1966]. *Extension of Gravity Anomalies to Unsurveyed Areas*. American Geophysical Union Monograph 9, Washington, D.C., U.S.A.
- Paul, M.K. [1973]. "A Method of Evaluating the Truncation Error Coefficients for Geoidal Height." *Bulletin Geodesique*, Volume 57, pp. 413-425.
- Pick, M., J. Picha and V. Vyskocil [1973]. *Theory of the Earth's Gravity Field*. Elsevier, Amsterdam.
- Rapp, R. [1980]. "A Comparison of Altimeter and Gravimetric Geoids in the Tonga Trench and Indian Ocean Areas." *Bulletin Geodesique*. Volume 54, pp. 149-163.
- Rapp, R. [1981]. "The Earth's Gravity Field to Degree and Order 180 Using Seasat Altimeter Data, Terrestrial Gravity, and Other Data." Department of Geodetic Science, Report No. 322, The Ohio State University, Columbus.
- Rapp, R. and M. Kadir [1988]. "A preliminary Geoid for the State of Tennessee." *Surveying and Mapping*, Volume 48, No. 4, December.
- Robinson, G.L. [1991]. "Verification of Gravimetric Geoidal Models by a Combination of GPS and Orthometric Heights." M.Sc.E. thesis, Department of Surveying Engineering, University of New Brunswick, Fredericton.
- Schwarz, K.P. and M.G. Sideris [1985]. "Precise Geoid Heights and their Use in GPS Interferometry." Contract Report 85-004, Geodetic Survey of Canada, Energy, Mines and Resources, Canada, September.
- Schwarz, K.P., M.G. Sideris, and R. Forsberg [1987]. "Orthometric Heights Without Levelling." *Journal of Surveying Engineering*, American Society of Civil Engineers, Volume 113, No. 1, pp. 28-40.
- Sideris, M.G. [1984]. "Computation of Gravimetric Terrain Corrections Using Fast Fourier Transform Techniques." UCSE Reports #20007, Division of Surveying Engineering, University of Calgary, Calgary, Alberta.
- Sjoberg, L. and S.H. Stocki [1985]. "The Accuracy of Geoid Undulations Determined by Modification of Stokes' Formula Using GEM9 Potential Coefficients." Anno XLIV, *Bollettino Di Geodesia E Scienze Affini*, N.3.
- Torge, Wolfgang [1980]. *Geodesy*. Walter de Gruyter & Co., Berlin, Germany, 254 pages.

- Tscherning, C.C., R.H. Rapp and C. Goad [1983]. "A Comparison of Methods for Computing Gravimetric Quantities From High Degree Spherical Harmonic Expansions." *Manuscripta Geodaetica*, Volume 8, pp. 249-272.
- Uotila, Urho A. [1977]. "The Changing World of Geodetic Science." Department of Geodetic Science, Report No. 250, The Ohio State University, Columbus.
- Vanicek, P. [1971]. "Physical Geodesy." Department of Surveying Engineering Lecture Notes 21, University of New Brunswick, Fredericton.
- Vanicek, P. [1991]. Private Communication. University of New Brunswick, Fredericton.
- Vanicek, P. and A. Kleusberg [1986]. "Towards a New Combined Geoid for Canada." Anno XLV, *Bollettino Di Geodesia E Scienze Affini*, N.2.
- Vanicek, P. and A. Kleusberg [1987]. "The Canadian Geoid-Stokesian Approach." *Manuscripta Geodaetica*, Volume 12, No.2, pp. 86-98.
- Vanicek, P. and E.J. Krakiwsky [1982]. *Geodesy: the Concepts*. North-Holland Publishing Company, Amsterdam, 691 pages.
- Vanicek, P., A. Kleusberg, R.G. Chang, H. Fashir, N. Chrisou, M. Hofman, T. Kling and T. Arsenault [1986]. "The Canadian Geoid." Department of Surveying Engineering Technical Report 122, University of New Brunswick, Fredericton.
- Vanicek, P., C. Zhang and P. Ong [1990]. "Computation of a File of Geoidal Heights Using Molodenskij's Truncation Method." Department of Surveying Engineering Technical Report 147, University of New Brunswick, Fredericton.
- Wells, D.E. (ED.) [1986]. *Guide to GPS Positioning*. Canadian GPS Associates, University of New Brunswick Graphic Services, Fredericton.
- Wells, D.E. and E.J. Krakiwsky [1971]. "The Method of Least Squares." Department of Surveying Engineering Lecture Notes 18, University of New Brunswick, Fredericton.
- Wichiencharoen, Chugiat [1982]. "The Indirect Effects on the Computation of Geoid Undulations." Department of Geodetic Science, Report No. 336, The Ohio State University, Columbus.

APPENDICES

APPENDIX I.1

Description of Programs

There were several programs that have been developed by the author for the purpose of studying the geoidal height difference computed using the ring integration approach. However, only four of them will be discussed in this section. Two of these four programs, namely (1) RININT.RED and (2) RININT.UNRED, are used for computing the short wavelength contribution to geoidal height difference while the other two programs, namely (3) POT.RED and (4) POT.UNRED, are used for computing the medium to long wavelength contribution to geoidal height difference. The geoidal height difference which was computed from the program RININT.RED has to be added to the geoidal height difference computed from program POT.RED, in order to obtain a full geoidal height difference. Likewise, the result obtained from program RININT.UNRED has to be added to the result obtained from program POT.UNRED. So that these two sets of the programs are used in pairs. These four programs have been written in standard FORTRAN. The first two programs run on both Macintosh(MAC) Plus computer and IBM mainframe while the latter two run only on the mainframe. Originally, both RININT.RED and RININT.UNRED programs were designed to run on MAC Plus. Due to the limitation of the MAC plus memory, the programs were transferred to the IBM mainframe. It was discovered later that not only the small size of the MAC plus memory is the limiting factor but also its speed. It was very much faster for the programs to be run on the IBM mainframe than on MAC plus computer. For the MAC plus, the program took about 3 hours to compute seven ΔN while for the IBM mainframe, the program took less than a minute. The author, thus, decided to conduct the testing on the IBM mainframe.

1.1 The RININT.RED Program

The RININT.RED program computes geoidal height difference for the inner zone contribution using the reduced free-air gravity anomalies. This program and the data set, which contains the reduced free-air anomalies, and its associated coordinates (latitude, longitude and elevation), are stored on a floppy diskette and on the UNB IBM Mainframe. The program is self-documented and is available from the author.

The algorithms used in this program are based on the techniques presented in the previous chapter. This program consists of the main program and 9 subroutines. Two of these subroutines are called by the main program and the rest are called via other subroutines. Each of these subroutines was verified separately, and the final (main) program was tested by merging all the subroutines together. The main program calls the subroutine READP to read the data set from a data file and stores them in memory. It, then, reads the two geodetic end points of a baseline from another file. Subroutine THICK is then called to compute the thickness of the ring. That is, it is called to delineate the inner sub-zone, the middle sub-zone and the outer sub-zone. To compute the sum of N from all the compartments for a sub-zone, subroutine CRING is called. This subroutine calls five other subroutines: CAP, GRAMID, SURBND, EXTR and AMEAN. It is called at least three times to compute N for the three sub-zones. The first and the second calls on subroutine CRING are for the inner sub-zone and the middle sub-zone contributions, respectively. The third and the subsequent calls are for the outer sub-zone contribution. The contributions from these three sub-zones are then added up to obtain the short wavelength contribution to N_1 for the first end point of the baseline. This process is repeated for the second end point of the baseline to obtain N_2 and the difference ($N_2 - N_1$)

between these values will be the short wavelength contribution to geoidal height difference across this baseline.

Subroutine GRAMID is called by subroutine CRING to determine the coordinates of the point which lies in the center of the compartment using the following steps:

Step 1: obtain the azimuth(α_m) and the spherical distance(ψ_m) for the center of the compartment:

$$\alpha_m = (\alpha_1 + \alpha_2)/2 \quad 1.1$$

$$\psi_m = (\psi_1 + \psi_2)/2 \quad 1.2$$

where ($\alpha_1, \alpha_2, \psi_1, \psi_2$) are the boundary limits of the compartment (See Figure 1).

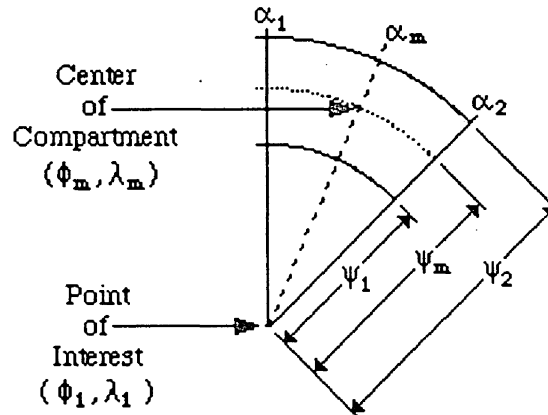


Figure 1: Determination of Coordinates for the Center of the Compartment.

Step 2: compute the differences in latitude($\Delta\phi$) and in longitude($\Delta\lambda$) between the point of interest(ϕ_1, λ_1) and the center of the compartment (ϕ_m, λ_m):

$$\Delta\phi = \psi_m \cos(\alpha_m), \quad 1.3$$

$$\Delta\lambda = \psi_m \sin(\alpha_m), \quad 1.4$$

Step 3: obtain the coordinates for the center of the compartment:

$$\lambda_m = \Delta\lambda + \lambda_1, \quad 1.5$$

$$\phi_m = \Delta\phi + \phi_1. \quad 1.6$$

Subroutine SURBND is called to delineate the boundary limit of the cell for the prediction of $\widetilde{\Delta g}$. It has been discussed in chapter five that the size of the compartment was different from the size of the cell. This section, the two will be differentiated. The size of the compartment is bounded by the selected $\Delta\alpha$ and $\Delta\psi$ (depending on which sub-zone is to be computed) as shown in Figure 2. The prediction point lies in the center of the cell which coincides with the center of the compartment.. However, the size of the cell is a square area (shaded region) which is chosen to be 10' by 10'. If there is no point gravity anomalies inside this cell, the dimension of the cell will increase to 15' by 15', or 20' by 20', or 30' by 30', or 60' by 60' until at least one set of observation is present inside the cell. If there is still no point gravity anomaly inside the 60' by 60' cell, the computation will skip that cell and move on to the next compartment.

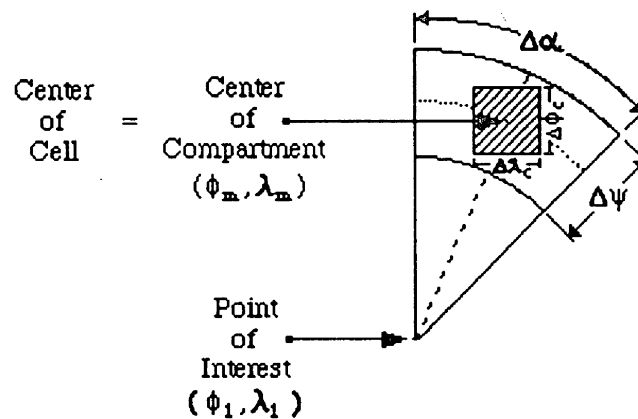


Figure 2: Cell (Shaded Area) Used for Predicting $\widetilde{\Delta g}$.

The boundary limits of the cell are defined by the latitudes of the north-east and south-east corners of the cell and the longitudes of the north-west and north-east corners of the cell (See Figure 3).

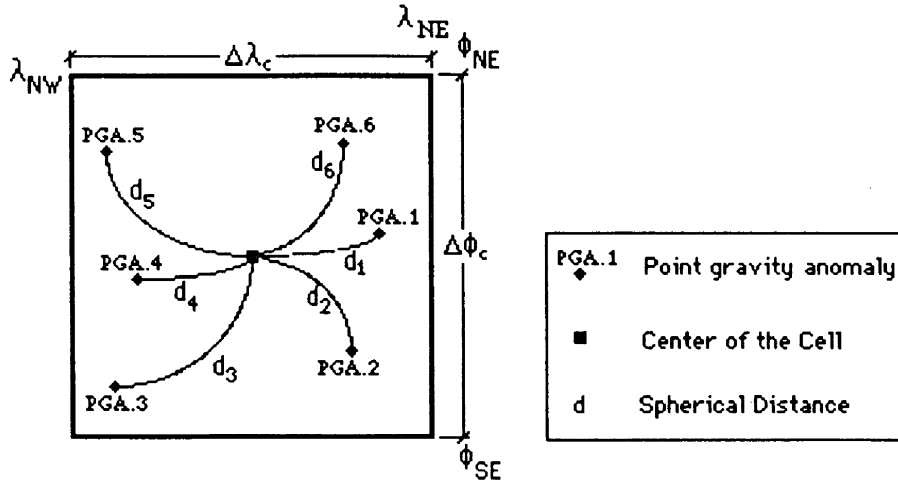


Figure 3: The Boundary Limits of the Cell.

They are computed as follows:

$$\phi_{NE} = \phi_m + \Delta\phi_c / 2, \quad 1.7$$

$$\phi_{SE} = \phi_m - \Delta\phi_c / 2, \quad 1.8$$

$$\lambda_{SE} = \lambda_m + \Delta\lambda_c / 2, \quad 1.9$$

$$\lambda_{NW} = \lambda_m - \Delta\lambda_c / 2, \quad 1.10$$

where $\Delta\phi_c = \Delta\lambda_c = 10', 20', 30',$ or $60'$ as mentioned in the above.

Once the boundary limits are known, subroutine EXTR is called to extract all the point gravity anomalies, including its associated coordinates, within the square cell and to reassign them into new arrays. Of all the subroutines, this subroutine is the most time consuming part. This is because for each cell, 4793 set of data have to be scanned through and to determine one of the ΔN between two points, contributions from 828 cells (for $\psi_o = 1.0^\circ$) have to be computed.

Arithmetic mean technique (as described in the above section) is utilized in subroutine AMEAN to predict the mean gravity anomaly at the center of the cell. Subroutine CPSI is called by Subroutine AMEAN to compute the spherical distances(ψ_i ,

$i=1,2,\dots,n$, where n is the total number of point gravity anomalies within the cell) between the point gravity anomalies within the cell and the center of the cell (See Figure 3).

1.2 The RININT.UNRED Program

This program computes ΔN using the unreduced Δg as described in chapter 5.1. The procedures are written basically the same as the RININT.RED program. A set of data file is used in this program, namely: DATA.UNRED. The DATA.UNRED file consists of the unreduced free-air gravity anomalies, the bouguer anomalies, and their associated coordinates (latitudes, longitudes and elevations).

Instead of reading the reduced free-air anomalies, subroutine READP reads in the Bouguer anomalies and stores them into arrays. Subroutine EXTR is then called to extract the topographic heights within the cell and reset them into different arrays. Once the topographic heights are extracted, they are transferred to subroutine AMEAN to compute the mean value (arithmetic mean) of the height in that cell. This mean value and the mean value of the Bouguer gravity anomaly (computed in subroutine AMEAN) are then used to determine the mean value of the free-air anomalies for equation (5.1.2).

APPENDIX I.2

Program RININT.RED

```

//RINGRED JOB '*-RESEARCH',NONEWS
/*JOBPARM S=30,L=5,R=2048,PRINT=ALL
//      EXEC FORTVCLG,REGION=2048K,
//      PARM.FORT='NOXREF,NOMAP,OPTIMIZE(3) '
//FORT.SYSIN DD *
C*****
C*
C* PROGRAM NAME   : RININT.RED
C* FUNCTION      : GEOIDAL HEIGHT COMPUTATION
C* COMPILER      : FORTRAN 77
C* AUTHOR        : ARTHUR TSEN
C* HISTORY       : JULY 31, 1991 - VERSION 1.0
C* REFERENCE     : KEARSLEY'S PAPERS(1985,1986a,1986b,1988)
C*
C* This program is designed to compute geoidal height
C* difference using Kearsley's method.
C*
C* DELTA G' is used for the integration, i.e.,
C*      DELTA G' = DELTA G - DELTA G",
C* where DELTA G" is computed from the Geopotential Coefficients
C* (RAPP180) and DELTA G is the terrestrial gravity anomaly.
C*
C* MAIN Program
C*
C* CALLS:
C*      Subroutine READP
C*      Subroutine THICK
C*      Subroutine CRING
C*
C* Input parameters:
C*      LATD1, LATM1, LATS1: the geodetic latitude of the first
C*                          point in degree, minute and seconds
C*      LONGD1, LONGM1, LONGS1: the geodetic longitude of the first
C*                          point in degree, minute and seconds
C*      LATD2, LATM2, LATS2: the geodetic latitude of the second
C*                          point in degree, minute and seconds
C*      LONGD2, LONGM2, LONGS2: the geodetic longitude of the second
C*                          point in degree, minute and seconds.
C*
C* Output parameters:
C*      LATD1, LATM1, LATS1: the geodetic latitude of the first
C*                          point in degree, minute and seconds
C*      LONGD1, LONGM1, LONGS1: the geodetic longitude of the first
C*                          point in degree, minute and seconds
C*      LATD2, LATM2, LATS2: the geodetic latitude of the second
C*                          point in degree, minute and seconds
C*      LONGD2, LONGM2, LONGS2: the geodetic longitude of the second
C*                          point in degree, minute and seconds
C*      GDIFF: height difference between two points
C*              across the baseline.
C*
C*****

```

```

      IMPLICIT REAL*8 (A-H,O-Z)
      CHARACTER*6 STA
      INTEGER NUM1,SS,CAPSIZE
      INTEGER LATD1, LATM1, LONGD1, LONGM1
      REAL*8 LATS1, LONGS1
      INTEGER LATD2, LATM2, LONGD2, LONGM2
      REAL*8 LATS2, LONGS2
      REAL*8 P(4800), D(4800), DG(4800)
      REAL*8 H(4800)
C
C*****
C*
C* Subroutine READP is called to read in the reduced point
C* gravity anomalies (PGA) and its associated coordinates.
C*
C* Output parameters:
C* DG: arrays of reduced point gravity anomalies in mGals.
C* P,D: its associated latitudes and longitudes in decimal
C* degree.
C* H: its associated heights in meters.
C*
C* NUM1: total number of reduced PGA in data file.
C*
C*****
C
      CALL READP (P,D,H,DG,NUM1)
C
      PI = DARCOS (-1.D0)
      WRITE (6,500)
      WRITE (6,501)
C
C*****
C*
C* Read in the geographical coordinates of the terminal points
C* of the line.
C*
C*****
C
      999 READ (11,502,END=900) LATD1,LATM1,LATS1, LONGD1, LONGM1, LONGS1,
      $ LATD2,LATM2,LATS2, LONGD2, LONGM2, LONGS2
C
C*****
C*
C* Converts degree, minute, second into decimal degree.
C*
C*****
C
      PHI1 =DFLOAT (LATD1) + DFLOAT (LATM1)/(60.D0) + LATS1/(3600.D0)
      XDLAM1 =DFLOAT (LONGD1) + DFLOAT (LONGM1)/(60.D0) + LONGS1/(3600.D0)
C
      PHI2 =DFLOAT (LATD2) + DFLOAT (LATM2)/(60.D0) + LATS2/(3600.D0)
      XDLAM2 =DFLOAT (LONGD2) + DFLOAT (LONGM2)/(60.D0) + LONGS2/(3600.D0)
C

```

```

C*****
C*
C*   Converts Longitude West to Longitude East (decimal degree).   *
C*
C*****

      DLAM1 = 360.D0 - XDLAM1
      DLAM2 = 360.D0 - XDLAM2

C*****
C*
C*   Initialization of Parameters.
C*
C*****
C
      TGRAV = 0.D0
      XTRING1 = 0.D0
      XTRING2 = 0.D0
      PSIO = 0.D0
      SS = 0

C
C*****
C*
C*   CN: Contribution of 0.0003 meter per mGals in a compartment.   *
C*   R: Major-semi axis of the earth.
C*   G: the normal gravity of the ellipsoid.
C*
C*****
C
      CN = 0.0003D00
      R = 6378137.D0
      G = 979764.4656D0
      PHI = PHI1
      DLAM = DLAM1
700  CONTINUE

C
C*****
C*
C*   Subroutine THICK is called to compute the outer radius of the   *
C*   ring for the inner sub-zone.
C*
C*   Subroutine CRING is called to compute the total contribution    *
C*   to geoidal height for the inner sub-zone.  There are total    *
C*   of 6 compartments in this sub-zone.
C*
C*****
C
      DALF1 = 60.D0
      SK1 = (R*DALF1)/(720.D0*G)
      CALL THICK(SK1,CN,PSIO,PSI1)

C
      CALL CRING(6,0.D0,PSI1,PHI,DLAM,NUM1,
$             P,D,H,DG,TRINGA)

C

```

```

C*****
C*
C* Subroutine THICK is called to compute the outer radius of the *
C* ring for the middle sub-zone. *
C*
C* Subroutine CRING is called to compute the total contribution *
C* to geoidal height for the middle sub-zone. There are total *
C* of 12 compartments in this sub-zone. *
C*
C*****
C
      DALF2 = 30.D0
      SK2 = (R*DALF2)/(720.D0*G)
      CALL THICK(SK2,CN,PSI1,PSI2)
C
      CALL CRING(12,PSI1,PSI2,PHI,DLAM,NUM1,
$           P,D,H,DG,TRINGB)
C
C*****
C*
C* Subroutine THICK is called to compute the outer radii of the *
C* ring for the outer sub-zone. *
C*
C* Subroutine CRING is called to compute the total contribution *
C* to geoidal height for the outer sub-zone. There are 36 *
C* compartments between the inner radius and the outer radius *
C* of the rings. *
C*
C* If CAPSIZE = 5, Then spherical cap size is 0.5 degree. *
C* If CAPSIZE = 6, Then spherical cap size is 0.6 degree. *
C* If CAPSIZE =11, Then spherical cap size is 1.0 degree. *
C* If CAPSIZE =13, Then spherical cap size is 1.2 degree. *
C*
C*****
C
      DALF3 = 10.D0
      SK3 = (R*DALF3)/(720.D0*G)
      TRA = 0.D0
C
      CAPSIZE = 11
      DO 300 I2 = 1,CAPSIZE
      CALL THICK(SK3,CN,PSI2,PSI3)
C
      CALL CRING(36,PSI2,PSI3,PHI,DLAM,NUM1,
$           P,D,H,DG,TRINGC)
      TRA = TRA + TRINGC
      PSI2 = PSI3
300 CONTINUE
C
      TGRAV = TRINGA + TRINGB + TRA
C
      IF (SS.EQ.0)THEN
          XTRING1 = TGRAV
      ELSE
          XTRING2 = TGRAV
      ENDIF
      SS = SS + 1

```

```

C*****
C*
C*   If 'SS' less than 2, then start computing geoidal height   *
C*   for the second point.  If 'SS' greater than 2, then take  *
C*   the difference of the geoidal heights between the two points. *
C*
C*****
C
      IF (SS.LT.2) THEN
          PHI = PHI2
          DLAM = DLAM2
          GO TO 700
      ELSE
CC      GDIFF = XTRING2 - XTRING1
          GDIFF = (XTRING2 - XTRING1)*CN
      ENDIF
C
C*****
C*
C*   Print out the geoidal height difference between two points   *
C*   and its associated coordinates.                               *
C*
C*****
C
      WRITE(6,250) LATD1, LATM1, LATS1, LONGD1, LONGM1, LONGS1,
$           LATD2, LATM2, LATS2, LONGD2, LONGM2, LONGS2,
$           GDIFF
C
      GO TO 999
C
C*****
C*
C*   Format Statements.                                           *
C*
C*****
C
250  FORMAT(2X,4(2(I3,1X),F9.6,2X),2X,F8.3)
500  FORMAT(20X,'COMPUTATION OF GEOIDAL HEIGHT DIFFERENCES',/,
$     20X,'    USING THE RING INTEGRATION METHOD    ')
501  FORMAT(2X,'PHI1 (DMS)',5X,'          LAMDA1 (DMS)',
$     7X,'PHI2 (DMS)',5X,'          LAMDA2 (DMS)',
$     7X,'DN (METRES)',/)
502  FORMAT(2(2(I3,1X),F9.6),2(2(I3,1X),F9.6))
900  STOP
      END
C

```



```

C*****
C*
C*   SOURCE FILE: CRING
C*
C*   CALLED BY:   MAIN Program
C*
C*   CALLS:      Subroutine CAP
C*               Subroutine GRAMID
C*               Subroutine SURBND
C*               Subroutine EXTR
C*               Subroutine AMEAN
C*
C*   PURPOSE:    This subroutine CRING computes the total gravity
C*               anomalies of all the compartments for one ring.
C*
C*   Input parameters:
C*       NC: the total number of compartments in a ring
C*       BPSI0: the inner radius of the ring in radian
C*       BPSI1: the outer radius of the ring in radian
C*       YPHI,YDLAM: The lat. and long. coordinates of the point of
C*                   interest in decimal degree
C*       XNUM2: The total number of reduced PGA in data file
C*       P,D: The lat. and long. of PGA in decimal degree
C*       H: The height of PGA in meters
C*       DG: the reduced PGA in mGals.
C*
C*   Output paramters:
C*       TRING1: The sum of the mean gravity anomalies from
C*               all the compartments in a ring.
C*
C*   Other parameters:
C*       AZI: The initial boundary of the compartment in
C*            radian
C*       XAZI: The end boundary of the compartment in radian.
C*       CAZI: The size of the compartment in radian
C*       FPHI,FDLAM: The lat. and long. coordinates of the point at
C*                   the center of the compartment
C*       DIM: The size of the cell for computing the mean
C*            gravity anomaly.
C*****
C
$   SUBROUTINE CRING(NC,BPSI0,BPSI1,YPHI,YDLAM,XNUM2,
      P,D,H,DG,TRING1)
      IMPLICIT REAL*8 (A-H, O-Z)
      INTEGER XNUM2
      INTEGER XNUM, NUM2, NC
      REAL*8 P (XNUM2), D (XNUM2), DG (XNUM2), H (XNUM2)
      REAL*8 YP2 (500), YD2 (500), YDG2 (500), YH2 (500)
      PI = DARCOS (-1.D0)
C

```

```

C*****
C*
C*   Setting input parameters into another variables.
C*
C*****
C
      APSI0 = BPSI0
      APSI1 = BPSI1
      XPHI = YPHI
      XDLAM = YDLAM
      NUM2 = XNUM2
C
C*****
C*
C*   Initialization of variables.
C*
C*****
C
      TRING1 = 0.D0
      AZI = 0.D0
C
      CAZI = 2.D0*PI/DFLOAT(NC)
      CALL CAP(APSI0,API)
      CALL CAP(APSI1,APJ)
      APJI = APJ - API
C
      DO 100 J = 1,NC
          XAZI = AZI + CAZI
          FPFI = 0.D0
          FDLAM = 0.D0
C
C*****
C*
C*   Subroutine GRAMID is called to compute the coordinates of the
C*   center of the compartment.
C*
C*****
C
      CALL GRAMID(AZI,XAZI,APSI0,APSI1,XPHI,XDLAM,FPFI,FDLAM)
C
      K9 = 0
      DIM = 10.D0
115      XPHIN = 0.D0
          XPHIS = 0.D0
          XDLAMW = 0.D0
          XDLAME = 0.D0
          XNUM = 0
          ANOINT1=0.D0
C
      DO 300 J1 = 1,500
          YP2(J1) = 0.D0
          YD2(J1) = 0.D0
          YDG2(J1) = 0.D0
          YH2(J1) = 0.D0
C
300      CONTINUE
C

```

```

C*****
C*
C* Subroutine SURBND is called to delineate the boundaries for *
C* cell. *
C* *
C*****
C
C      CALL SURBND (FPHI, FDLAM, DIM, XPHIN, XPHIS, XDLAMW, XDLAME)
C
C*****
C*
C* Subroutine EXTR is called to extract all the PGA, together *
C* with its associated coordinates, within the cell size defined *
C* by the boundaries computed from subroutine SURBND. *
C* *
C*****
C
C      CALL EXTR (NUM2, XPHIN, XPHIS, XDLAMW, XDLAME, P, D, H, DG,
C              $      YP2, YD2, YH2, YDG2, XNUM)
C
C*****
C*
C* If there is at least one set of PGA exists within the *
C* cell, then subroutine AMEAN is called to predict the mean *
C* gravity anomaly within that cell. If there is no PGA within *
C* the cell, then the cell size (DIM) will be enlarged to a *
C* (15' by 15'), or to (30' by 30'), or to (60' by 60') cell *
C* whichever cell contains at least one set of record. If there *
C* is still no PGA found within the 60' by 60' cell, then the *
C* computation for that particular cell is simply skipped. *
C* *
C*****
C
C      IF (XNUM .GT. 0) THEN
C          CALL AMEAN (XNUM, FPHI, FDLAM, YP2, YD2, YH2, YDG2, ANOINT1)
C          GO TO 113
C      ENDIF
C
C      IF ((K9 .EQ. 0) .AND. (XNUM.LE.0)) THEN
C          DIM = 15.D0
C          K9 = K9 + 1
C          GO TO 115
C      ENDIF
C
C      IF ((K9 .EQ. 1) .AND. (XNUM.LE.0)) THEN
C          DIM = 20.D0
C          K9 = K9 + 1
C          GO TO 115
C      ENDIF
C
C      IF ((K9 .EQ. 2) .AND. (XNUM.LE.0)) THEN
C          DIM = 30.D0
C          K9 = K9 + 1
C          GO TO 115
C      ENDIF
C
C

```

```
      IF ((K9 .EQ. 3) .AND. (XNUM .LE. 0)) THEN
        DIM = 60.D0
        K9 = K9 + 1
        GO TO 115
      ENDIF
C
      IF ((K9 .EQ. 4) .AND. (XNUM .LE. 0)) THEN
        GO TO 111
      ENDIF
C
C113  TRING1 = TRING1 + ANOINT1*APJI
113   TRING1 = TRING1 + ANOINT1
111   CONTINUE
      AZI = XAZI
C
100   CONTINUE
      RETURN
      END
```

```

C*****
C*
C*   SOURCE FILE: CAP
C*
C*   CALLED BY:   CRING
C*
C*   PURPOSE:     This subroutine CAP computes the  $\Phi$  which
C*                will be use to compute the geoidal heights.
C*
C*   Input parameter:
C*   XPSI:        The radius of the ring.
C*
C*   Output parameter:
C*   XFIL :       The  $\Phi$ 
C*
C*****
C
SUBROUTINE CAP(XPSI,XFIL)
IMPLICIT REAL*8(A-H,O-Z)
C
PART1 = XPSI * 2.D0
PART2 = (5.D0/4.D0)*(XPSI**2)
PART3 = (10.D0/12.D0)*(XPSI**3)
PART4 = (3.D0/2.D0)*(XPSI**2)
IF (XPSI .NE. 0.D0) THEN
PART5 = DLOG(XPSI/2.D0 + XPSI**2/4.D0 - XPSI**3/24.D0)
ELSE
PART5 = 0.D0
ENDIF
XFIL = PART1 - PART2 - PART3 - PART4*PART5
RETURN
END
C
C
SUBROUTINE CAP(XPSI,XFIL)
CC IMPLICIT REAL*8(A-H,O-Z)
C
CC PART1 = 4.D0*(DSIN(XPSI/2.D0))
CC PART2 = DCOS(XPSI)
CC PART3 = 6.D0*(DSIN(XPSI/2.D0)**3)
CC PART4 = (7.D0/4.D0)*(DSIN(XPSI/2.D0)**2)
CC PART5 = (3.D0/2.D0)*(DSIN(XPSI)**2)
CC IF (XPSI .NE. 0.D0) THEN
CC PART6 = DLOG(DSIN(XPSI/2.D0) + (DSIN(XPSI/2.D0)**2))
CC ELSE
CC PART6 = 0.D0
CC ENDIF
CC XFIL = 1.D0+PART1-PART2-PART3-PART4-(PART5*PART6)
CC RETURN
CC END
C

```

```

C*****
C*
C*   SOURCE FILE: THICK
C*
C*   CALLED BY:   MAIN PROGRAM
C*
C*   PURPOSE:    This subroutine THICK computes the spherical
C*               distance (radius) of the ring or the thickness
C*               of the compartments.
C*
C*   Input parameters:
C*       SSK1: a scale that use to determine the size of
C*             the ring (See MAIN program)
C*       XCN: = 0.0003 m/mGal per compartment
C*       PSIA: the inner radius of the ring in radian.
C*
C*   Output parameters:
C*       PSIB: the outer radius of the ring in radian.
C*
C*****
C
C   SUBROUTINE THICK(SSK1,XCN,PSIA,PSIB)
C   IMPLICIT REAL*8 (A-H,O-Z)
C
C   PSI2P = PSIA + XCN / (2.D0 * SSK1)
C   TERM2 = (5.D0/8.D0)*(PSI2P**2 - PSIA**2)
C   TERM3 = (10.D0/24.D0)*(PSI2P**3 - PSIA**3)
C   TERM4A = (PSI2P**2)*DLOG( (PSI2P/2.D0) +
$   (PSI2P**2/4.D0) - (PSI2P**3/24.D0) )
C   IF (PSIA .NE. 0.D0) THEN
C       TERM4B = (PSIA**2)*DLOG( (PSIA/2.D0) +
$   (PSIA**2/4.D0) - (PSIA**3/24.D0) )
C   ELSE
C       TERM4B = 0.D0
C   ENDIF
C   TERM4 = (3.D0/4.D0) * (TERM4A - TERM4B)
C   TERM5 = XCN / (2.D0 * SSK1)
C   PSIB = PSIA + TERM2 + TERM3 + TERM4 + TERM5
C   RETURN
C   END
C

```

```

C*****
C*
C*   SOURCE FILE: AMEAN
C*
C*   CALLED BY:   Subroutine CRING
C*
C*   CALLS:      Subroutine CPSI
C*
C*   PURPOSE:    This subroutine AMEAN computes the mean gravity
C*               anomaly within a compartment using the weighted
C*               arithmetic mean.
C*
C*   Input parameters:
C*       XNUM:   the total number of extracted reduced PGA
C*               within the boundaries of the cell.
C*       GPHI,GDLAM: the lat. and long. coordinates of the center of
C*               cell in decimal degree.
C*       DGEXTR:  array of extracted reduced PGA within the cell
C*               in mGals.
C*       PEXTR,DEXTR: its associated lat. and long. coordinates
C*               in decimal degree.
C*       HEXTR:   its associated heights in meters
C*
C*   Output parameters:
C*       TOGR:   the mean gravity anomaly within the cell.
C*
C*   Other parameters:
C*       DLO:   array of spherical distances (in decimal degree)
C*               between the point at the center of the cell and
C*               the PGA points.
C*****
SUBROUTINE AMEAN(XNUM,GPHI,GDLAM,PEXTR,DEXTR,HEXTR,DGEXTR,TOGR)
IMPLICIT REAL*8 (A-H,O-Z)
INTEGER XNUM
REAL*8 PEXTR(XNUM), DEXTR(XNUM), DGEXTR(XNUM)
REAL*8 DLO(500), HEXTR(XNUM)

C
BTEST = 0.D0
TOGR = 0.D0
SUMDLO = 0.D0

C
DO 200 MN = 1,500
DLO(MN) = 0.D0
200 CONTINUE

C
CALL CPSI(DLO,PEXTR,DEXTR,GPHI,GDLAM,XNUM)

C
DO 100 MM = 1,XNUM
BTEST = BTEST + DGEXTR(MM) / (DLO(MM)**3.5)
SUMDLO = SUMDLO + (1.D0/DLO(MM)**3.5)
100 CONTINUE

C
TOGR = BTEST /SUMDLO

C
RETURN
END

```

```

C*****
C*
C*   SOURCE FILE: CPSI
C*
C*   CALLED BY:   Subroutine AMEAN
C*
C*   PURPOSE:     This subroutine CPSI computes the spherical
C*                distances between the point at the center of the
C*                cell and the PGA extracted within the cell.
C*
C*   Input parameters:
C*       XNUM:    the total number of extracted reduced PGA
C*                within the boundaries of the cell
C*   PEXTR,DEXTR: the lat. and long. coordinates of the extracted
C*                PGA stations in decimal degree
C*   HPHI, HDLAM: the lat. and long. coordinates of the center of
C*                the cell in decimal degree.
C*
C*   Output parameters:
C*       YLO:    array of spherical distances in decimal degree.
C*
C*****
C
C   SUBROUTINE CPSI (YLO, PEXTR, DEXTR, HPHI, HDLAM, XNUM)
C   IMPLICIT REAL*8 (A-H,O-Z)
C   INTEGER XNUM
C   REAL*8 PEXTR(XNUM), DEXTR(XNUM), YLO(500)
C   REAL*8 SINP, COSP, COSL, PP, DD, APSI
C
C   PI = DARCOS(-1.D0)
C   RAD = PI/180.D0
C   PHI = HPHI*RAD
C   DLAM = HDLAM*RAD
C   SINP = DSIN(PHI)
C   COSP = DCOS(PHI)
C
C   DO 100 I =1, XNUM
C       PP = PEXTR(I)*RAD
C       DD = DEXTR(I)*RAD
C
C   SIND = DSIN(PP)
C   COSD = DCOS(PP)
C   COSL = DCOS(DABS(DD-DLAM))
C
C   APSI = DARCOS(SINP*SIND + COSP*COSD*COSL)
C
C   YLO(I) = APSI*(180.D0/PI)
C
C 100 CONTINUE
C   RETURN
C   END
C

```



```

C*****
C*
C*   SOURCE FILE: READP
C*
C*   CALLED BY:   MAIN Program
C*
C*   PURPOSE:    This subroutine READP reads the reduced gravity
C*               anomalies, together with its associated coordi-
C*               nates, from file DATA.RED and stores them
C*               into memories.
C*
C*   Input parameters:
C*       NONE
C*
C*   Output parameters:
C*       RDELG1:   array of PGA in mGals.
C*       PHIX:     array of latitudes of PGA stations in decimal
C*               degree.
C*       DLAMX:    array of longitudes of PGA stations in decimal
C*               degree.
C*       H:        array of heights of PGA stations in meters.
C*       K:        the total number of PGA in DATA.RED file.
C*
C*****
C
C       SUBROUTINE READP (PHIX,DLAMX,H,RDELG1,K)
C
C       IMPLICIT REAL*8 (A-H,O-Z)
C       REAL*8 PDEG1,DLDEG1
C       INTEGER K
C       REAL*8 ELSTAL
C       REAL*8 PHIX(4800),DLAMX(4800)
C       REAL*8 DLAME,H(4800)
C       REAL*8 DELG,DELG1,DELG2,DIST
C       REAL*8 RDELG1(4800)
C
C*****
C*
C*   Initializing PGA record fields.
C*
C*****
C
C       K = 0
C       DO 20 L=1,4800
C           PHIX(L)=0.D0
C           DLAMX(L)=0.D0
C           RDELG1(L)=0.D0
C           H(L) = 0.D0
C 20   CONTINUE
C

```

```

C*****
C*
C*      Reading in record fields.
C*
C*****
C
  50  READ (10, 88, END=100) PDEG1, DLDEG1, ELSTA1, DELG, DELG2, DELG1, DIST
  88  FORMAT (2X, F13.8, 2X, F13.8, 2X, F6.2, 3 (2X, F6.1), 2X, F9.3)
C
C*****
C*
C*      Redefining the fields.
C*
C*****
C
      K=K+1
      RDELG1 (K) = DELG1
      H(K) = ELSTA1
C
      PHIX(K) = PDEG1
      IF (DLDEG1.LT.0) THEN
          DLAME = DLDEG1
          DLAMX(K) = DLAME + 360.D0
      ELSE
          DLAME = DLDEG1
          DLAMX(K) = DLAME
      ENDIF
      GO TO 50
C
  100  RETURN
      END
C

```

```

C*****
C*
C*   SOURCE FILE: SURBND
C*
C*   CALLED BY:   Subroutine CRING
C*
C*   PURPOSE:     This subroutine SURBND computes the boundaries
C*                limits of a cell for the prediction of mean
C*                gravity anomaly.
C*
C*   Input parameters:
C*     PHI,DLAM:  the lat. and long. coordinates of the center
C*                of the compartment
C*     XNX:       the size of the cell.
C*
C*   Output parameters:
C*     PHIN:     the latitude of the north-east corner
C*     PHIS:     the latitude of the south-east corner
C*     DLAMW:    the longitude of the north-west corner
C*     DLAME:    the longitude of the south-east corner.
C*
C*****
C
SUBROUTINE SURBND (PHI, DLAM, XNX, PHIN, PHIS, DLAMW, DLAME)
IMPLICIT REAL*8 (A-H,O-Z)
XNXD = (XNX/2.0)/60.D0
PHIN = PHI + XNXD
PHIS = PHI - XNXD
DLAMW = DLAM - XNXD
DLAME = DLAM + XNXD
RETURN
END
C

```

```

C*****
C*
C*   SOURCE FILE: EXTR
C*
C*   CALLED BY:   Subroutine CRING
C*
C*   PURPOSE:     This subroutine SURBND extracts the reduced
C*                PGA and its associated coordinates and heights
C*                within the boundaries limits defined by
C*                subroutine SURBND.
C*
C*   Input parameters:
C*       NK:      the total number of PGA in data file
C*       PHIN:    the latitude of the north-east corner
C*       PHIS:    the latitude of the south-east corner
C*       DLAMW:   the longitude of the north-west corner
C*       DLAME:   the longitude of the south-east corner
C*       DG:      the PGA in mGals
C*       P,D:     its associated lat. and long. coordinates
C*                in decimal degree
C*       H:       its associated height in meters.
C*
C*   Output parameters:
C*       YDG1:    the extracted PGA (in mGals) within the cell
C*       YP1,YD1: its associated lat. and long. coordinates
C*                in decimal degree
C*       YH1:     its associated height in meters
C*       NUM1:    the total number of PGA within the cell.
C*
C*****
C
C   SUBROUTINE EXTR(NK,PHINN,PHISS,DLAMW,DLAME,P,D,H,DG,
C   $              YP1,YD1,YH1,YDG1,NUM1)
C   IMPLICIT REAL*8 (A-H,O-Z)
C
C   INTEGER NK,NUM1
C   DIMENSION P(NK), D(NK), DG(NK), H(NK)
C   DIMENSION YP1(NK), YD1(NK), YDG1(NK), YH1(NK)
C
C   NUM1 = 0
C   DO 100 I = 1,NK
C   $   IF (( P(I) .LE. PHINN) .AND. (P(I) .GE. PHISS) .AND.
C   $       ( D(I) .LE. DLAME) .AND. (D(I) .GE. DLAMW)) THEN
C       NUM1 = NUM1 + 1
C       YP1(NUM1) = P(I)
C       YD1(NUM1) = D(I)
C       YDG1(NUM1) = DG(I)
C       YH1(NUM1) = H(I)
C   $   ENDIF
C   100 CONTINUE
C   WRITE(6,1000) NUM1
C1000  FORMAT(5X,'NUM1 = ',I4)
C   RETURN
C   END
C

```

```

C*****
C*
C*   SOURCE FILE: GRAMID
C*
C*   CALLED BY:   Subroutine CRING
C*
C*   PURPOSE:     This subroutine GRAMID computes the coordinates
C*                of the point which lies in the center of the
C*                compartment. The latitude and the longitude
C*                that come out from this subroutine are in
C*                decimal degree.
C*
C*   Input parameters:
C*     AZI1:       the initial boundary of the compartment in
C*                radian
C*     AZI2:       the end boundary of the compartment in radian
C*     XPSI1:      the inner radius of the ring in radian
C*     XPSI2:      the outer radius of the ring in radian
C*   PHI1,DLAM1:  the lat. and long. coordinates of the point of
C*                interest in decimal degree.
C*
C*   Output parameters:
C*     PHI2,DLAM2: the lat. and long. coordinates of the center of
C*                compartment in decimal degree.
C*
C*****
C
SUBROUTINE GRAMID(AZI1,AZI2,XPSI1,XPSI2,PHI1,DLAM1,PHI2,DLAM2)
IMPLICIT REAL*8 (A-H, O-Z)
PI = DARCOS(-1.D0)
C
      AZIMID = (AZI2 + AZI1)/2.D0
      PSIMID = (XPSI2 + XPSI1)/2.D0
      DLAT = DCOS(AZIMID) * PSIMID
      DLONG = DSIN(AZIMID) * PSIMID
      XDLAT = DLAT * (180.D0/PI)
      XDLONG = DLONG * (180.D0/PI)
      PHI2 = XDLAT + PHI1
      DLAM2 = XDLONG + DLAM1
      RETURN
      END
C
//GO.FT10F001 DD *
/INCLUDE DATA.RED
//GO.FT11F001 DD *
/INCLUDE INPUTD
//*GO.FT12F001 DD DSN=UNBPLOT.AT.RININT6.OUT,SPACE=(TRK,(10,10),RLSE),
/* DCB=(LRECL=80,RECFM=FB,BLKSIZE=3200),
/* DISP=(NEW,CATLG,DELETE),UNIT=DASD
//

```

APPENDIX I.3

Program RININT.UNRED

```

//RININT JOB '*-RESEARCH',NONEWS
/*JOBPARM S=30,L=5,R=2048,PRINT=ALL
/*SERVICE -4
/**
//      EXEC FORTVCLG,REGION=2048K,
//      PARM.FORT='NOXREF,NOMAP,OPTIMIZE(3)'
//FORT.SYSIN DD *
C
C*****
C*
C* PROGRAM NAME      : RININT.UNRED
C* FUNCTION          : GEOIDAL HEIGHT COMPUTATION
C* COMPILER          : FORTRAN 77
C* AUTHOR            : ARTHUR TSEN
C* HISTORY            : AUGUST 2, 1991 - VERSION 1.0
C* REFERENCE         : KEARSLEY'S PAPERS (1985,1986a,1986b,1988)
C*
C* This program is designed to compute geoidal height
C* difference using the unreduced free-air gravity anomaly.
C*
C*****
C*
C*   MAIN Program
C*
C*   CALLS: Subroutine READP
C*           Subroutine THICK
C*           Subroutine CRING
C*
C*   Input Parameters:
C*     LATD1,LATM1,LATS1 : the geodetic latitude of the first
C*                          point in degree, minute, and second
C*     LONGD1, LONGM1, LONGS1: the geodetic longitude of the first
C*                          point in degree, minute, and second
C*     LATD2,LATM2,LATS2 : the geodetic latitude of the second
C*                          point in degree, minute, and second
C*     LONGD2, LONGM2, LONGS2: the geodetic longitude of the second
C*                          point in degree, minute, and second.
C*
C*   Output parameters:
C*     LATD1,LATM1,LATS1 : the geodetic latitude of the first
C*                          point in degree, minute, and second
C*     LONGD1, LONGM1, LONGS1: the geodetic longitude of the first
C*                          point in degree, minute, and second
C*     LATD2,LATM2,LATS2 : the geodetic latitude of the second
C*                          point in degree, minute, and second
C*     LONGD2, LONGM2, LONGS2: the geodetic longitude of the second
C*                          point in degree, minute, and second
C*
C*           GDIFF: geoidal height difference between two
C*                   points across the baseline.
C*
C*****
C

```

```

      IMPLICIT REAL*8 (A-H,O-Z)
      CHARACTER*6 STA
      INTEGER NUM1, CAPSIZE
      INTEGER LATD1, LATM1, LONGD1, LONGM1
      REAL*8 LATS1, LONGS1
      INTEGER LATD2, LATM2, LONGD2, LONGM2
      REAL*8 LATS2, LONGS2
      REAL*8 P(4800), D(4800)
      REAL*8 H(4800), BG(4800)

C
C*****
C*
C* Subroutine READP is called to read in the point bouguer
C* gravity anomalies (BGA) and its associated coordinates.
C*
C* Output parameters:
C* BG: arrays of point bouguer gravity anomalies in mGals.
C* P,D: its associated latitudes and longitudes in decimal
C* degree.
C* H: its associated heights in meters.
C*
C* NUM1: total number of BGA in data file.
C*
C*****
C
      CALL READP (P,D,BG,H,NUM1)
      PI = DARCOS (-1.D0)
      WRITE (6,500)
      WRITE (6,501)

C
C*****
C*
C* Read in the geographical coordinates of the terminal points
C* of the line.
C*
C*****
C
      999 READ (11,502,END=900) LATD1,LATM1,LATS1,LONGD1,LONGM1,LONGS1,
      $ LATD2,LATM2,LATS2,LONGD2,LONGM2,LONGS2

C
C*****
C*
C* Converts degrees, minutes, seconds into decimal degree.
C*
C*****
C
      PHI1 =DFLOAT (LATD1) + DFLOAT (LATM1) / (60.D0) + LATS1 / (3600.D0)
      XDLAM1 =DFLOAT (LONGD1) + DFLOAT (LONGM1) / (60.D0) + LONGS1 / (3600.D0)

C
      PHI2 =DFLOAT (LATD2) + DFLOAT (LATM2) / (60.D0) + LATS2 / (3600.D0)
      XDLAM2 =DFLOAT (LONGD2) + DFLOAT (LONGM2) / (60.D0) + LONGS2 / (3600.D0)

C

```

```

C*****
C*
C*   Converts Longitude West to Longitude East (decimal degree).   *
C*                                                                 *
C*****
C
      DLAM1 = 360.D0 - XDLAM1
      DLAM2 = 360.D0 - XDLAM2
C
C*****
C*
C*   Initialization of Parameters.                                  *
C*                                                                 *
C*****
C
      TGRAV = 0.D0
      XTRING1 = 0.D0
      XTRING2 = 0.D0
      SS = 0
      PSIO = 0.D0
C
C*****
C*
C*   CN: Contribution of 0.0003 meter per mGals in a compartment. *
C*   R: Major-semi axis of the earth.                             *
C*   G: the normal gravity of the ellipsoid.                       *
C*                                                                 *
C*****
C
      CN = 0.0003D00
      R = 6378137.D0
      G = 979764.4656D0
      PHI = PHI1
      DLAM = DLAM1
700  CONTINUE
C
C*****
C*
C*   Subroutine THICK is called to compute the outer radius of the *
C*   ring for the inner sub-zone.                                  *
C*                                                                 *
C*   Subroutine CRING is called to compute the total contribution *
C*   to geoidal height for the inner sub-zone.  There are total  *
C*   of 6 compartments in this sub-zone.                          *
C*                                                                 *
C*****
C
      DALF1 = 60.D0
      SK1 = (R*DALF1)/(720.D0*G)
      CALL THICK(SK1,CN,PSIO,PSI1)
C
      CALL CRING(6,0.D0,PSI1,PHI,DLAM,NUM1,
$           P,D,BG,H,TRINGA)
C

```



```

C*****
C*
C* Subroutine THICK is called to compute the outer radius of the *
C* ring for the middle sub-zone. *
C* *
C* Subroutine CRING is called to compute the total contribution *
C* to geoidal height for the middle sub-zone. There are total *
C* of 12 compartments in this sub-zone. *
C* *
C*****
C
      DALF2 = 30.D0
      SK2 = (R*DALF2)/(720.D0*G)
      CALL THICK(SK2,CN,PSI1,PSI2)
C
      CALL CRING(12,PSI1,PSI2,PHI,DLAM,NUM1,
$           P,D,BG,H,TRINGB)
C
C*****
C*
C* Subroutine THICK is called to compute the outer radii of the *
C* ring for the outer sub-zone. *
C* *
C* Subroutine CRING is called to compute the total contribution *
C* to geoidal height for the outer sub-zone. There are 36 *
C* compartments between the inner radius and the outer radius *
C* of the rings. *
C* *
C* If CAPSIZE = 5, Then spherical cap size is 0.5 degree. *
C* If CAPSIZE = 6, Then spherical cap size is 0.6 degree. *
C* If CAPSIZE =11, Then spherical cap size is 1.0 degree. *
C* If CAPSIZE =13, Then spherical cap size is 1.2 degree. *
C* *
C*****
      DALF3 = 10.D0
      SK3 = (R*DALF3)/(720.D0*G)
      TRA = 0.D0
C
      CAPSIZE = 11
      DO 300 I2 = 1,CAPSIZE
      CALL THICK(SK3,CN,PSI2,PSI3)
C
      CALL CRING(36,PSI2,PSI3,PHI,DLAM,NUM1,
$           P,D,BG,H,TRINGC)
      TRA = TRA + TRINGC
      PSI2 = PSI3
300 CONTINUE
C
      TGRAV = TRINGA + TRINGB + TRA
C
      IF (SS.EQ.0) THEN
          XTRING1 = TGRAV
      ELSE
          XTRING2 = TGRAV
      ENDIF
C
      SS = SS + 1

```

```

C*****
C*
C*   If 'SS' less than 2, then start computing geoidal height   *
C*   for the second point.  If 'SS' greater than 2, then take  *
C*   the difference of the geoidal heights between the two points. *
C*                                                                 *
C*****
C
      IF (SS.LT.2)THEN
          PHI = PHI2
          DLAM = DLAM2
          GO TO 700
      ELSE
C
          GDIFF = XTRING2 - XTRING1
          GDIFF = (XTRING2 - XTRING1) * CN
      ENDIF
C
C*****
C*
C*   Print out the geoidal height difference between two points   *
C*   and its associated coordinates.                               *
C*                                                                 *
C*****
C
      WRITE (6,250) LATD1, LATM1, LATS1, LONGD1, LONGM1, LONGS1,
$              LATD2, LATM2, LATS2, LONGD2, LONGM2, LONGS2,
$              GDIFF
C
      GO TO 999
C
C*****
C*
C*   Format Statements.                                           *
C*                                                                 *
C*****
C
250  FORMAT(2X,4(2(I3,1X),F9.6,2X),2X,F8.3)
500  FORMAT(20X,'COMPUTATION OF GEOIDAL HEIGHT DIFFERENCES',/,
$      20X,'    USING THE RING INTEGRATION METHOD    ',//)
501  FORMAT(2X,'PHI1 (DMS) ',5X,'          LAMDA1 (DMS) ',
$      7X,'PHI2 (DMS) ',5X,'          LAMDA2 (DMS) ',
$      7X,'DN (METRES) ',/)
502  FORMAT(2(2(I3,1X),F9.6),2(2(I3,1X),F9.6))
900  STOP
      END
C

```

```

C*****
C*
C*   SOURCE FILE: CRING
C*
C*   CALLED BY:   MAIN Program
C*
C*   CALLS:       Subroutine CAP
C*                Subroutine GRAMID
C*                Subroutine SURBND
C*                Subroutine EXTR
C*                Subroutine AMEAN
C*
C*   PURPOSE:     This subroutine CRING computes the total gravity
C*                anomalies of all the compartments for one ring.
C*
C*   Input parameters:
C*       NC: the total number of compartments in a ring.
C*       BPSI0: the inner radius of the ring in radian.
C*       BPSI1: the outer radius of the ring in radian.
C*       YPHI,YDLAM: The lat. and long. coordinates of the point of
C*                interest in decimal degree.
C*       XNUM2: The total number of BGA in data file.
C*       P,D: The lat. and long. of BGA in decimal degree.
C*       H: The height of PGA in meters.
C*       BG: the BGA in mGals.
C*
C*   Output paramters:
C*       TRING1: The sum of the mean gravity anomalies from
C*                all the compartments in a ring.
C*
C*   Other parameters:
C*       AZI: The initial boundary of the compartment in
C*                radian.
C*       XAZI: The end boundary of the compartment in radian.
C*       CAZI: The size of the compartment in radian.
C*       FPHI,FDLAM: The lat. and long. coordinates of the point at
C*                the center of the compartment.
C*       DIM: The size of the cell for computing the mean
C*                gravity anomaly.
C*
C*****
C
C   SUBROUTINE CRING (NC,BPSI0,BPSI1,YPHI,YDLAM,XNUM2,
C   $               P,D,BG,H,TRING1)
C   IMPLICIT REAL*8 (A-H, O-Z)
C   INTEGER XNUM2,XNUM,NUM2,NC
C   REAL*8 P (XNUM2),D (XNUM2),BG (XNUM2),H (XNUM2)
C   REAL*8 YP2 (500),YD2 (500),YBG2 (500),YH2 (500)
C   PI = DARCOS (-1.D0)
C

```

```

C*****
C*
C*   Setting input parameters into another variables.
C*
C*****
C
      APSI0 = BPSI0
      APSI1 = BPSI1
      XPHI = YPHI
      XDLAM = YDLAM
      NUM2 = XNUM2
C
C*****
C*
C*   Initialization of variables.
C*
C*****
C
      TRING1 = 0.D0
      AZI = 0.D0
      CAZI = 2.D0*PI/DFLOAT(NC)
      CALL CAP(APSI0,API)
      CALL CAP(APSI1,APJ)
      APJI = APJ - API
C
      DO 100 J = 1,NC
          XAZI = AZI + CAZI
          FPFI = 0.D0
          FDLAM = 0.D0
C
C*****
C*
C*   Subroutine GRAMID is called to compute the coordinates of the
C*   center of the compartment.
C*
C*****
C
      CALL GRAMID(AZI,XAZI,APSI0,APSI1,XPHI,XDLAM,FPFI,FDLAM)
C
      K9 = 0
      DIM = 10.D0
115      XPHIN = 0.D0
          XPHIS = 0.D0
          XDLAMW = 0.D0
          XDLAME = 0.D0
          XNUM = 0
          ANOINT1=0.D0
C
      DO 300 J1 = 1,500
          YP2(J1) = 0.D0
          YD2(J1) = 0.D0
          YBG2(J1) = 0.D0
          YH2(J1) = 0.D0
C
300      CONTINUE
C

```

```

C*****
C*
C* Subroutine SURBND is called to delineate the boundaries for *
C* cell. *
C* *
C*****
C
      CALL SURBND (FPHI,FDLAM,DIM,XPHIN,XPHIS,XDLAMW,XDLAME)
C
C*****
C*
C* Subroutine EXTR is called to extract all the BGA, together *
C* with its associated coordinates, within the cell size defined *
C* by the boundaries computed from subroutine SURBND. *
C* *
C*****
C
      CALL EXTR (NUM2,XPHIN,XPHIS,XDLAMW,XDLAME,P,D,BG,
      $          H,YP2,YD2,YBG2,YH2,XNUM)
C
C*****
C*
C* If there is at least one set of BGA is existing within the *
C* cell, then subroutine AMEAN is called to predict the mean *
C* gravity anomaly within that cell. If there is no BGA within *
C* the cell, then the cell size (DIM) will be enlarged to a *
C* (15' by 15'), or to (30' by 30'), or to (60' by 60') cell *
C* whichever cell contains at least one set of record. If there *
C* is still no BGA found within the 60' by 60' cell, then the *
C* computation for that particular cell is simply skipped. *
C* *
C*****
C
      IF (XNUM .GT. 0) THEN
C
          CALL AMEAN (XNUM,FPHI,FDLAM,YP2,YD2,YBG2,YH2,ANOINT)
          GO TO 113
          ENDIF
C
      IF ((K9.EQ.0) .AND. (XNUM.LE.0)) THEN
          DIM = 15.D0
          K9 = K9 + 1
          GO TO 115
          ENDIF
C
      IF ((K9.EQ.1) .AND. (XNUM.LE.0)) THEN
          DIM = 20.D0
          K9 = K9 + 1
          GO TO 115
          ENDIF
C
      IF ((K9.EQ.2) .AND. (XNUM.LE.0)) THEN
          DIM = 30.D0
          K9 = K9 + 1
          GO TO 115
          ENDIF
C

```

```
IF ((K9.EQ.3).AND.(XNUM.LE.0)) THEN
  DIM = 60.D0
  K9 = K9 + 1
  GO TO 115
ENDIF
C
IF ((K9.EQ.4).AND.(XNUM.EQ.0)) THEN
  GO TO 111
ENDIF
C
C113 TRING1 = TRING1 + ANOINT1*APJI
113 TRING1 = TRING1 + ANOINT
111 CONTINUE
AZI = XAZI
C
100 CONTINUE
RETURN
END
C
```

```

C*****
C*
C*   SOURCE FILE: CAP
C*
C*   CALLED BY:   CRING
C*
C*   PURPOSE:     This subroutine CAP computes the  $\Phi$  which
C*                will be used to compute the geoidal heights.
C*
C*   Input parameter:
C*   XPSI:        The radius of the ring.
C*
C*   Output parameter:
C*   XFIL:        The  $\Phi$ 
C*****
C
C   SUBROUTINE CAP(XPSI,XFIL)
C   IMPLICIT REAL*8(A-H,O-Z)
C
C       PART1 = XPSI * 2.D0
C       PART2 = (5.D0/4.D0)*(XPSI**2)
C       PART3 = (10.D0/12.D0)*(XPSI**3)
C       PART4 = (3.D0/2.D0)*(XPSI**2)
C       IF (XPSI .NE. 0.D0) THEN
C       PART5 = DLOG(XPSI/2.D0 + XPSI**2/4.D0 - XPSI**3/24.D0)
C       ELSE
C           PART5 = 0.D0
C       ENDIF
C       XFIL = PART1 - PART2 - PART3 - PART4*PART5
C   RETURN
C   END
C

```

```

C*****
C*
C*   SOURCE FILE: THICK
C*
C*   CALLED BY:   MAIN Program
C*
C*   PURPOSE:     This subroutine THICK computes the spherical
C*                distance (radius) of the ring or the thickness
C*                of the compartments.
C*
C*   Input parameters:
C*       SSK1: a scale that use to determine the size of
C*            the ring (See MAIN program).
C*       XCN: = 0.0003 m/mGal per compartment.
C*       PSIA: the inner radius of the ring in radian.
C*
C*   Output parameters:
C*       PSIB: the outer radius of the ring in radian.
C*
C*****
C
C       SUBROUTINE THICK(SSK1,XCN,PSIA,PSIB)
C       IMPLICIT REAL*8 (A-H,O-Z)
C
C       PSI2P = PSIA + XCN / (2.D0 * SSK1)
C       TERM2 = (5.D0/8.D0)*(PSI2P**2 - PSIA**2)
C       TERM3 = (10.D0/24.D0)*(PSI2P**3 - PSIA**3)
C       TERM4A = (PSI2P**2)*DLOG( (PSI2P/2.D0) +
$       (PSI2P**2/4.D0) - (PSI2P**3/24.D0) )
C       IF (PSIA .NE. 0.D0) THEN
C           TERM4B = (PSIA**2)*DLOG( (PSIA/2.D0) +
$           (PSIA**2/4.D0) - (PSIA**3/24.D0) )
C       ELSE
C           TERM4B = 0.D0
C       ENDIF
C       TERM4 = (3.D0/4.D0) * (TERM4A - TERM4B)
C       TERM5 = XCN / (2.D0 * SSK1)
C       PSIB = PSIA + TERM2 + TERM3 + TERM4 + TERM5
C       RETURN
C       END
C

```



```

C*****
C*
C*   SOURCE FILE: AMEAN
C*
C*   CALLED BY:   Subroutine CRING
C*
C*   CALLS:       Subroutine CPSI
C*
C*   PURPOSE:     This subroutine AMEAN computes the mean gravity
C*                anomaly within a compartment using the weighted
C*                arithmetic mean.
C*
C*   Input parameters:
C*       XNUM:    the total number of extracted BGA
C*                within the boundaries of the cell.
C*       GPHI,GDLAM: the lat. and long. coordinates of the center of
C*                cell in decimal degree.
C*       DGEXTR:   array of extracted BGA within the cell in mGals.
C*       PEXTR,DEXTR: its associated lat. and long. coordinates
C*                in decimal degree.
C*       HEXTR:    its associated heights in meters
C*
C*   Output parameters:
C*       TOGR:     the mean gravity anomaly within the cell.
C*
C*   Other parameters:
C*       DLO:      array of spherical distances (in decimal degree)
C*                between the point at the center of the cell and
C*                the BGA points.
C*****
SUBROUTINE AMEAN (XNUM, GPHI, GDLAM, PEXTR, DEXTR, DGEXTR, HEXTR, TOGR)
IMPLICIT REAL*8 (A-H, O-Z)
INTEGER XNUM
REAL*8 PEXTR (XNUM), DEXTR (XNUM), DGEXTR (XNUM), DLO (500), HEXTR (XNUM)

C
      HTOT = 0.D0
      HMEAN = 0.D0
      BTEST = 0.D0
      TOGR = 0.D0
      SUMDLO = 0.D0

C
      DO 200 MN = 1, 500
          DLO (MN) = 0.D0
200  CONTINUE

C
      CALL CPSI (DLO, PEXTR, DEXTR, GPHI, GDLAM, XNUM)
      DO 100 MM = 1, XNUM
          HTOT = HTOT + HEXTR (MM)
          BTEST = BTEST + DGEXTR (MM) / (DLO (MM) ** 3.5)
          SUMDLO = SUMDLO + (1.D0 / DLO (MM) ** 3.5)
100  CONTINUE

C
      HMEAN = HTOT / DFLOAT (XNUM)
      TOGR = BTEST / SUMDLO + 0.1119D0 * HMEAN
      RETURN
      END

```

```

C*****
C*
C*   SOURCE FILE: CPSI
C*
C*   CALLED BY:   Subroutine AMEAN
C*
C*   PURPOSE:     This subroutine CPSI computes the spherical
C*                distances between the point at the center of the
C*                cell and the PGA extracted within the cell.
C*
C*   Input parameters:
C*       XNUM:    the total number of extracted BGA within the
C*                boundaries of the cell.
C*   PEXTR,DEXTR: the lat. and long. coordinates of the extracted
C*                BGA stations in decimal degree.
C*   HPHI, HDLAM: the lat. and long. coordinates of the center of
C*                the cell in decimal degree.
C*
C*   Output parameters:
C*       YLO:    array of spherical distances in decimal degree.
C*
C*****
C
SUBROUTINE CPSI (YLO, PEXTR, DEXTR, HPHI, HDLAM, XNUM)
IMPLICIT REAL*8 (A-H, O-Z)
INTEGER XNUM
REAL*8 PEXTR(XNUM), DEXTR(XNUM), YLO(500)
REAL*8 SINP, COSP, COSL, PP, DD, APSI

C
PI = DARCOS(-1.D0)
RAD = PI/180.D0
PHI = HPHI*RAD
DLAM = HDLAM*RAD
SINP = DSIN(PHI)
COSP = DCOS(PHI)

C
DO 100 I = 1, XNUM
    PP = PEXTR(I)*RAD
    DD = DEXTR(I)*RAD

C
SIND = DSIN(PP)
COSD = DCOS(PP)
COSL = DCOS(DABS(DD-DLAM))

C
APSI = DARCOS(SINP*SIND + COSP*COSD*COSL)

C
YLO(I) = APSI*(180.D0/PI)

C
100 CONTINUE
RETURN
END
C

```

```

C*****
C*
C*   SOURCE FILE: READP
C*
C*   CALLED BY:   MAIN Program
C*
C*   PURPOSE:     This subroutine READP reads the bouguer gravity
C*                anomalies, together with its associated coordi-
C*                nates, from file DATA.UNRED and stores them
C*                into memories.
C*
C*   Input parameters:
C*       NONE
C*
C*   Output parameters:
C*       BA:       array of BGA in mGals.
C*       PHIX:     array of latitudes of BGA stations in decimal
C*                degree.
C*       DLAMX:    array of longitudes of BGA stations in decimal
C*                degree.
C*       H:        array of heights of BGA stations in meters.
C*       K:        the total number of BGA in DATA.UNRED file.
C*
C*****
C
C       SUBROUTINE READP (PHIX,DLAMX,BA,H,K)
C
C       IMPLICIT REAL*8 (A-H,O-Z)
C       INTEGER YR1,PID1,PDEG1,DLDEG1
C       INTEGER TERAC1,GRAVA1,FACC1,BACC1
C       INTEGER K
C       INTEGER CACC1, EACC1
C       INTEGER DEPWL, DEPT1, DEPAC1
C       CHARACTER*6 STAID1
C       REAL*8 PMIN1,DLMIN1,TERCO1,GRAV1
C       REAL*8 ELSTA1
C       REAL*8 PHIX(4800),DLAMX(4800)
C       REAL*8 H(4800),BA(4800)
C       REAL*8 FAL,BA1
C
C*****
C*
C*       Initializing BGA record fields.
C*
C*****
C
C       K = 0
C       DO 20 L=1,4800
C           PHIX(L)=0.DO
C           DLAMX(L)=0.DO
C           BA(L) = 0.DO
C           H(L) = 0.DO
C 20    CONTINUE
C

```

```

C*****
C*
C*      Reading in record fields.
C*
C*****
C
  50      READ(10,88,END=100)YR1,PID1,STAID1,PDEG1,PMIN1,
        $          DLDEG1,DLMIN1,
        $          CACC1,ELSTAL,EACC1,DEPW1,DEPT1,DEPAC1,
        $          TERCO1,TERAC1,GRAV1,GRAVA1,FA1,FACC1,
        $          BA1,BACC1
  88      FORMAT(I2,I3,A6,I3,F6.2,I4,F6.2,I2,F7.2,I2,I5,I1,I1,F4.1,I2,F8.1,
        $          I2,F6.1,I2,F6.1,I2)
C
C*****
C*
C*      Redefining the fields.
C*
C*****
C
      K=K+1
      BA(K) = BA1
      H(K) = ELSTAL
C
      PHIX(K) = DBLE(PDEG1) + PMIN1/60.D0
      IF (DLDEG1.LT.0)THEN
          DLAME = DBLE(DLDEG1) - DLMIN1/60.D0
          DLAMX(K) = DLAME + 360.D0
      ELSE
          DLAME = DBLE(DLDEG1) + DLMIN1/60.D0
          DLAMX(K) = DLAME
      ENDIF
      GO TO 50
C
  100     RETURN
        END
C

```

```

C*****
C*
C*   SOURCE FILE: SURBND
C*
C*   CALLED BY:   Subroutine CRING
C*
C*   PURPOSE:     This subroutine SURBND computes the boundaries
C*                limits of a cell for the prediction of mean
C*                gravity anomaly.
C*
C*   Input parameters:
C*     PHI,DLAM:  the lat. and long. coordinates of the center
C*                of the compartment
C*     XNX:       the size of the cell.
C*
C*   Output parameters:
C*     PHIN:     the latitude of the north-east corner
C*     PHIS:     the latitude of the south-east corner
C*     DLAMW:    the longitude of the north-west corner
C*     DLAME:    the longitude of the south-east corner.
C*
C*****
C
      SUBROUTINE SURBND (PHI,DLAM,XNX,PHIN,PHIS,DLAMW,DLAME)
      IMPLICIT REAL*8 (A-H,O-Z)
      XNXD = (XNX/2.0)/60.D0
      PHIN = PHI + XNXD
      PHIS = PHI - XNXD
      DLAMW = DLAM - XNXD
      DLAME = DLAM + XNXD
      RETURN
      END

```

C

```

C*****
C*
C* SOURCE FILE: EXTR
C*
C* CALLED BY: Subroutine CRING
C*
C* PURPOSE: This subroutine SURBND extracts the reduced
C* PGA and its associated coordinates and heights
C* within the boundaries limits defined by
C* subroutine SURBND.
C*
C* Input parameters:
C* NK: the total number of BGA in data file
C* PHIN: the latitude of the north-east corner
C* PHIS: the latitude of the south-east corner
C* DLAMW: the longitude of the north-west corner
C* DLAME: the longitude of the south-east corner
C* BA: the BGA in mGals
C* P,D: its associated lat. and long. coordinates
C* in decimal degree
C* H: its associated height in meters.
C*
C* Output parameters:
C* YBA1: the extracted BGA (in mGals) within the cell
C* YP1,YD1: its associated lat. and long. coordinates
C* in decimal degree
C* YH1: its associated height in meters
C* NUM1: the total number of BGA within the cell.
C*
C*****
C
SUBROUTINE EXTR(NK,PHINN,PHISS,DLAMW,DLAME,P,D,BA,H,
$ YP1,YD1,YBA1,YH1,NUM1)
IMPLICIT REAL*8 (A-H,O-Z)

C
INTEGER NUM1,NK
DIMENSION P(NK), D(NK), H(NK), BA(NK)
DIMENSION YP1(NK), YD1(NK), YBA1(NK), YH1(NK)

C
NUM1 = 0
DO 100 I = 1,NK
IF (( P(I) .LE. PHINN) .AND. (P(I) .GE. PHISS) .AND.
$ ( D(I) .LE. DLAME) .AND. (D(I) .GE. DLAMW)) THEN
NUM1 = NUM1 + 1
YP1(NUM1) = P(I)
YD1(NUM1) = D(I)
YBA1(NUM1) = BA(I)
YH1(NUM1) = H(I)
ENDIF
100 CONTINUE
C WRITE(6,1000) NUM1
C1000 FORMAT(5X,'NUM1 = ',I4)
RETURN
END
C

```

```

C*****
C*
C*   SOURCE FILE: GRAMID
C*
C*   CALLED BY:   Subroutine CRING
C*
C*   PURPOSE:     This subroutine GRAMID computes the coordinates
C*                of the point which lies in the center of the
C*                compartment. The latitude and the longitude
C*                that come out from this subroutine are in
C*                decimal degree.
C*
C*   Input parameters:
C*     AZI1:      the initial boundary of the compartment in
C*                radian
C*     AZI2:      the end boundary of the compartment in radian
C*     XPSI1:     the inner radius of the ring in radian
C*     XPSI2:     the outer radius of the ring in radian
C*   PHI1,DLAM1: the lat. and long. coordinates of the point of
C*                interest in decimal degree.
C*
C*   Output parameters:
C*   PHI2,DLAM2: the lat. and long. coordinates of the center of
C*                compartment in decimal degree.
C*
C*****
C
C   SUBROUTINE GRAMID(AZI1,AZI2,XPSI1,XPSI2,PHI1,DLAM1,
C   $              PHI2,DLAM2)
C   IMPLICIT REAL*8 (A-H, O-Z)
C   PI = DARCOS(-1.D0)
C
C   AZIMID = (AZI2 + AZI1)/2.D0
C   PSIMID = (XPSI2 + XPSI1)/2.D0
C   DLAT = DCOS(AZIMID) * PSIMID
C   DLONG = DSIN(AZIMID) * PSIMID
C   XDLAT = DLAT * (180.D0/PI)
C   XDLONG = DLONG * (180.D0/PI)
C   PHI2 = XDLAT + PHI1
C   DLAM2 = XDLONG + DLAM1
C   RETURN
C   END
C
C   //GO.FT10F001 DD *
C   /INCLUDE DATA.UNRED
C   //GO.FT11F001 DD *
C   /INCLUDE INPUTD
C   //*GO.FT12F001 DD DSN=UNBLOT.AT.RININT6.OUT,SPACE=(TRK,(10,10),RLSE),
C   /**          DCB=(LRECL=80,RECFM=FB,BLKSIZE=3200),
C   /**          DISP=(NEW,CATLG,DELETE),UNIT=DASD
C   //

```

APPENDIX I.4

Program POT.RED

```

//RAPP180 JOB '*-RESEARCH',NONEWS
/*JOBPARM M=1,L=9,R=2048
/*SERVICE NONPRIME
/*SETUP SLOT=5172 VOLUME=SE0001
//*
// EXEC FORTVCLG,
// PARM.FORT='NOXREF,NOMAP,OPTIMIZE(3)'
//FORT.SYSIN DD *
C*****
C*
C* PROGRAM NAME : POT.RED *
C* FUNCTION : GEOIDAL HEIGHT COMPUTATION *
C* COMPILER : FORTRAN 77 *
C* AUTHOR : ARTHUR TSEN *
C* HISTORY : JULY 31, 1991 - VERSION 1.0 *
C* REFERENCE : KEARSLEY'S PAPERS(1985,1986a,1986b,1988) *
C*
C* This program is designed to compute geoidal height *
C* from the Geopotential Coefficients (Rapp180) and to *
C* be used in conjunction with RININT.RED. *
C*
C*****
C*
C* MAIN Program *
C*
C* CALLS: *
C* Subroutine POT1 (Store in MAINFRAME) *
C*
C* Input parameters: *
C* STAT: Name of Station *
C* HT: Height of Station in meters *
C* PHID,PHIM,PHIS: the geodetic latitude of the point of *
C* interest in degree, minute and seconds *
C* DLOND,DLONM,DLONS: the geodetic longitude of the point of *
C* interest in degree, minute and second *
C*
C* Output parameters: *
C* STAT: Name of Station *
C* PHID,PHIM,PHIS: the geodetic latitude of the point of *
C* interest in degree, minute and seconds *
C* DLOND,DLONM,DLONS: the geodetic longitude of the point of *
C* interest in degree, minute and seconds *
C* HT: Height of Station in meters *
C* XII: N-S deflection component in arc second *
C* ETAL: E-W deflection component in arc second *
C* UNI: geoidal height in meters. *
C* DIST1: gravity disturbance in mGal *
C*
C*****
C

```



```

LOGICAL FIRST
REAL*8 PHI, DLON, HT, UN, XI, ETA, DIST
REAL*8 PHIS, DLONS, DLON1
REAL*8 UN1, XI1, ETA1
REAL*4 C, C0
REAL*8 G1, G, CM3, CM2, CM1
CHARACTER*6 STAT
INTEGER PHID, PHIM, DLOND, DLONM
DIMENSION G1(3), G(3,3), C(32760)
COMMON /CM/ G1, G, CM3, CM2, CM1, C0, C
COMMON /ENTRY/ FIRST, NMAX
FIRST = .FALSE.
NMAX = 170
WRITE(6,1001)
1001 FORMAT('PHI      DLON      HT      UN      XI      ETA      DIST')
C
C*****
C*
C*      Reading in the Point of interest.
C*
C*****
C
88      READ(5,800,END=999) STAT, PHID, PHIM, PHIS, DLOND, DLONM, DLONS, HT
800      FORMAT(A6,1X,2(I2,1X,I2,1X,F9.6,2X),F7.3)
C
C*****
C*
C*      Converts degree, minute and seonds into decimal degree and
C*      converts longitude wesly to longitude east.
C*
C*****
C
      PHI = DFLOAT(PHID) + (DFLOAT(PHIM)/60.D0) + (PHIS/3600.D0)
      DLON1 = DFLOAT(DLOND) + (DFLOAT(DLONM)/60.D0) + (DLONS/3600.D0)
      DLON = 360.D0 - DLON1
      HT = 0.D0
C
C
C*****
C*
C*      Subroutine POT1 is called to generate the geoidal height.
C*
C*****
C
      CALL POT1 (PHI, DLON, HT, UN, XI, ETA, DIST)
      UN1 = UN*1.D-6
      XI1 = XI*1.D-6
      ETA1 = ETA*1.D-6
      DIST1 = DIST*1.D-6
C
C*****
C*
C*      Write out the results.
C*
C*****
C
      WRITE(6,1000) STAT, PHID, PHIM, PHIS, DLOND, DLONM, DLONS,
$ HT, UN1, XI1, ETA1, DIST1

```

```
1000  FORMAT(5X,A6,3X,2(I2,1X,I2,1X,F9.6,3X),F7.3,3X,4(F8.3,2X))
C
      GO TO 88
999   STOP
      END
C
//LKED.USERLIB DD DSN=A.M12129.SELIBOBJ,DISP=OLD
//GO.FT12F001 DD DSN=RAPP180.UNFMD,UNIT=3480,VOL=SER=SE0001,
//          LABEL=(164,,,IN),DISP=(OLD,DELETE)
//*GO.FT12F001 DD DSN=GEM10C.UNFMD,UNIT=3480,VOL=SER=SE0001,
//*          LABEL=67,DISP=(OLD,DELETE)
//GO.SYSIN      DD      *
59414  50  3  41.611144  96 33 59.958490  217.071
59419  50  1  15.637452  97  9 40.646471  203.593
59422  50  3  37.520306  97 27  0.552741  219.363
60401  50  3  54.680565  98 18 32.628058  227.155
60404B 50  3  22.397743  98 47 22.546782  249.266
774009 50 56 56.133045  98  9 48.081569  240.392
774031 50 31 16.397259  98  1 33.334982  221.670
774032 50 30 23.812182  97  2 40.967285  201.748
82R311 50 56 57.255900  97  2 19.063788  192.429
82R370 50 19 46.526621  97 52 30.695424  231.822
82R382 50 45 59.306985  98  1  5.027375  231.603
//
```

APPENDIX I.5

Program POT.UNRED

```

//TGEOID1      JOB '*-RESEARCH',NONEWS
/*JOBPARM      M=30,L=5,R=4096,PRINT=ALL
/*SERVICE NONPRIME
/*SETUP       SLOT=5172   VOLUME=SE0001
//*
//           EXEC FORTVCLG,REGION=4096K,
//           PARM.FORT='NOXREF,NOMAP,OPTIMIZE(3)'
//FORT.SYSIN DD *
C
C
C*****
C*
C*  PROGRAM NAME      : POT.UNRED
C*  FUNCTION         : GEOIDAL HEIGHT COMPUTATION
C*  COMPILER         : FORTRAN 77
C*  AUTHOR           : ARTHUR TSEN
C*  HISTORY          : JULY 31, 1991 - VERSION 1.0
C*  REFERENCE        : KEARSLEY'S PAPERS (1985,1986a,1986b,1988)
C*
C*  This program is designed to compute geoidal height
C*  from the Geopotential Coefficients (Rapp180) and to
C*  be used in conjunction with RININT.UNRED.
C*
C*****
C*
C*  MAIN Program
C*
C*  CALLS:
C*      Subroutine TCPAL
C*      Subroutine POT1
C*
C*  Input parameters:
C*      STAT: Name of Station
C*      PHID,PHIM,PHIS: the geodetic latitude of the point of
C*                      interest in degree, minute and seconds
C*      DLAMD,DLAMM,DLAMS: the geodetic longitude of the point of
C*                      interest in degree, minute and second
C*
C*  Output parameters:
C*      STAT: Name of Station
C*      PHID,PHIM,PHIS: the geodetic latitude of the point of
C*                      interest in degree, minute and seconds
C*      DLAMD,DLAMM,DLAMS: the geodetic longitude of the point of
C*                      interest in degree, minute and seconds
C*      DELTAN: geoidal height in meters.
C*
C*****
C

```

```

      IMPLICIT REAL*8 (A-H,O-Z)
      LOGICAL FIRST
      CHARACTER*6 STAT
      INTEGER PHID,PHIM,DLAMM,DLAMD
      REAL*8 PHIS,DLAMS
      REAL*4 C,C0
      REAL*8 G1,G,CM3,CM2,CM1
      COMMON/CM/G1(3),G(3,3),CM3,CM2,CM1,C0,C(32760)
      COMMON/POT1CM/FIRST
      INTEGER NMAX,NMAXC,MAX,NN
      REAL*8 Q6(200),R6(200,200)
      REAL*8 RA1,SUM,XGAMMA,DELTAN
      REAL*8 DELG(200)
C
      PII = DARCOS(-1.D0)
      RPSI6 = 0.6D0*(PII/180.D0)
      ARG6 = DCOS(RPSI6)
      MAX = 180
      MAX1 = 181
      NN = 181
      RA1 = 6378137.D0
      XGAMMA = 979764.4656D0
C
C*****
C*
C*      Subroutine TCPAL is called to compute the Molodenskjj .      *
C*      truncation functions.                                         *
C*                                                                     *
C*****
C
      CALL TCPAL(NN,MAX1,ARG6,Q6,R6)
C
C*****
C*
C*      Reading in the Point of interest.                               *
C*                                                                     *
C*****
C
      88      READ(10,1000,END=99)STAT,PHID,PHIM,PHIS,DLAMD,DLAMM,DLAMS
      1000    FORMAT(A6,2X,2(2(I3,1X),F9.6))
C
C*****
C*
C*      Converts degree, minute and seonds into decimal degree and  *
C*      converts longitude wesly to longitude east.                   *
C*                                                                     *
C*****
C
      PHI = DFLOAT(PHID) + (DFLOAT(PHIM)/60.D0) + (PHIS/3600.D0)
      DLAM = DFLOAT(DLAMM) + (DFLOAT(DLAMM)/60.D0) + (DLAMS/3600.D0)
      DLON = 360.D0 - DLAM
C

```

```

C*****
C*
C*   Initialization of variables.
C*
C*****

          DO 110 J2 = 1,MAX1
            DELG(J2) = 0.D0
110      CONTINUE
C
          FIRST = .FALSE.
C
          DIST2 = 0.D0
          SUM2 = 0.D0
          KMAX = 0
          DO 120 J3 = 1,MAX1
C
            HT = 0.D0
C*****
C*
C*   Subroutine POT is called to generate the geoidal height.
C*
C*****
C
          CALL POT1 (KMAX,PHI,DLON,HT,UN1,XI1,ETAL,DIST1)
          DG = DIST1 - DIST2
          UN = UN1 - SUM2
          DELG(J3) = (DG-0.3086*UN)*1.D-6
          DIST2 = DIST2 + DG
          SUM2 = SUM2 + UN
          KMAX = KMAX + 1
120      CONTINUE
C
          SUM = 0.D0
C
          DO 135 J7 = 3,MAX
          DO 130 J6 = 3,MAX1
            SUM = SUM + Q6(J6)*DELG(J6)
130      CONTINUE
C
          DELTAN = (RA1/(2.D0*XGAMMA))*SUM
C
          WRITE (6,1010) STAT,PHID,PHIM,PHIS,DLAMD,DLAMM,DLAMS,DELTAN
1010      FORMAT (2X,A6,2X,2(2(I3,1X),F9.6),2X,F10.3)

          GO TO 88
99      STOP
          END
C

```

```

C*****
C*
C*   SOURCE FILE:  Subroutine POT
C*
C*   CALLED BY:   MAIN program
C*
C*   CALLS:       Subroutine LOADCS
C*                Subroutine STORC
C*                Subroutine SETCM
C*                Function GCENLT
C*                Function POTCC
C*
C*   FUNCTION:    Subroutine POT is called to generate the geoidal
C*                height.
C*
C*   Input paramters:
C*     PHI:       Latitude (GEODETTIC) in degree
C*     DLON:      Longitude (WEST) in degree
C*     HT:        Height in meters
C*
C*   Output parameters:
C*     UN:        Height anomaly n meters
C*     XI:        N-S deflection in second of arc
C*     ETA:       E-W deflection in second of arc (WEST POSITIVE)
C*     DIST:      Gravity Disturbance in mGals.
C*
C*****
C

```

```

SUBROUTINE POT1 (NMAX, PHI, DLON, HT, UN, XI, ETA, DIST)
IMPLICIT REAL*8 (A-H,O-Z)
INTEGER NMAX
LOGICAL FIRST
REAL*4 C, C0
DIMENSION P(6)
COMMON/CM/G1(3), G(3,3), CM3, CM2, CM1, C0, C(32760)
COMMON/POT1CM/FIRST
DATA PI/3.141592653589793D0/

```

```

C
IF (FIRST) GO TO 300
FIRST=.TRUE
DTR=PI/180.D0
300 CONTINUE
CM3=3.986005D+14
CM2=6378137.D0
CM1=0.D0
C0=0.D0
DO 10 I=1, 32760
C(I)=0.D0
10 CONTINUE
NEGN=-NMAX
CALL LOADCS (NMAX)
C0=0.D0
CALL STORC (0, 0, 0.D0, 0.D0)
CALL STORC (1, 0, 0.D0, 0.D0)
CALL STORC (1, 1, 0.D0, 0.D0)
CALL STORC (2, 0, 0.D0, 0.D0)
CALL SETCM (NMAX)

```

```

C*****
C*
C*   Converts longitude West to Longitude East.
C*
C*****
      DLAM=360.D0+DLON
C*****
C*
C*   Converts from geodetic to geocentric latitude
C*
C*****
      DPHI=GCENLT( PHI,298.257D0)
      D=CM2+HT
      Z=D *DSIN(DPHI*DTR)
      R=D *DCOS(DPHI*DTR)
      X=R*DCOS(DLAM*DTR)
      Y=R*DSIN(DLAM*DTR)
      P(1)=DSQRT(X**2+Y**2)
      P(2)=DSQRT(X**2+Y**2+Z**2)
      COLAT=90.D0-DPHI
      P(3)=DCOS(COLAT*DTR)
      P(4)=DSIN(COLAT*DTR)
      P(5)=DSIN(DLAM*DTR)
      P(6)=DCOS(DLAM*DTR)
C*****
C*
C*   Pass negative N since potential coefficients have been
C*   quasi-normalized.
C*
C*****
C
      POT=POTCC(P,NEGN,1)
C
C   Height Anomaly
C
      UN=POT/9.8D0
C
C   N-S deflection
C
      XI =      -G1(2)*206264.8D0 / 9.8D0
C
C   Output E-W deflection in the West system,
C   thus leave off the negative sign.
C   to convert ETA to WEST system.
C
      ETA =      G1(1)*206264.8D0 / 9.8D0
C
C   Gravity Disturbance
C
      DIST =-G1(3)*1.D+05
      RETURN
      END
C

```

```

C*****
C*
C*   SOURCE FILE:  Function GCENLT
C*
C*   CALLED BY:   Subroutine POT1
C*
C*   CALLS:      NONE
C*
C*   FUNCTION:   To convert from geodetic latitude to geocentric
C*               latitude.
C*
C*   Input parameters:
C*   GDETLT:    Geodetic latitude in degree
C*   FLAT:     1./Flattening approximately equal to 298.25
C*
C*****

      FUNCTION GCENLT(GDETLT,FLAT)
      IMPLICIT REAL*8 (A-H,O-Z)
C
      DATA DTR /.1745329251994330D-1/
      GCENLT=DATAN(DTAN(GDETLT*DTR)*(1.D0-1.D0/FLAT)**2) / DTR
      RETURN
      END
C
C*****
C*
C*   FUNCTION POTCC(PO,NMAX,ORDER)
C*
C*   GI REG.NO. 80039  AUTHOR -C.C.TSCHERNING, NOV 1980  IN ALGOL
C*                       -C.C.GOAD, MAR 1981 TRANSLATED
C*                       TO FORTRAN
C*
C*   REFERENCES:
C*   (1) TSCHERNING, C.C.:ON THE CHAIN-RULE METHOD FOR COMPUTING
C*       POTENTIAL DERIVATIVES. MANUSCRIPTA GEODAETICA, VOL.1,
C*       PP. 125-141, 1976
C*
C*   (2) GERSTL,M.:VERGLEICH VON ALGORITMEN ZUR SUMMATION VON
C*       KUGELFLAECHENFUNKTIONEN. VEROEFFENTL. DER BAYER. KOMM
C*       F.D. INT. ERDMESSUNG DER BAYER. AKADEMIE DER WISSEN.,
C*       HEFT NR. 38, PP. 81-88, 1978.
C*   THE PROCEDURE COMPUTES THE VALUE AND UP TO THE SECOND ORDER
C*   DERIVATIVES OF THE POTENTIAL OF THE EARTH (W) OR OF ITS
C*   CORRESPONDING AMONALOUS POTENTIAL(T). (THE COMPUTATION OF
C*   THE SECOND ORDER DERIVATIVES HAS NOT YET BEEN IMPLEMENTED)
C*
C*   THE POTENTIAL IS REPRESENTED BY A SERIES IN SOLID SPHERICAL
C*   HARMONICS, WITH UN-NORMALIZED OR QUASI-NORMALIZED
C*   COEFFICIENTS.
C*   THE CHAIN-RULE IS USED COMBINED WITH THE CLENSHAW ALGORITHM.
C*   THE ARRAY C MUST HOLD THE COEFFICIENTS, C(0,0)=1.D0
C*   FOR W AND 0.0 FOR T, C(1)=C(1,0),C(2)=C(1,1),C(3)=S(1,1)
C*   ETC. UP TO C((N+1)**2-1) = S(N,N).
C*
C*****

```



```

C*****
C*      PARAMETERS: *
C* * * * *
C*      (A) INPUT VALUES: *
C* * * * *
C*      NMAX: *
C*      THE ABSOLUTE VALUES OF NMAX IS EQUAL TO THE *
C*      MAXIMAL DEGREE AND ORDER OF THE SERIES. NEGATIVE *
C*      NMAX INDICATES THAT THE COEFFICIENTS ARE QUASI- *
C*      NORMALIZED. *
C* * * * *
C*      IORDER: *
C*      THE MAXIMAL ORDER OF THE DERIVATIVES (< 2 P.T.) *
C* * * * *
C*      PO: *
C*      ARRAY HOLDING POSITION INFORMATION. PO(6) *
C*      PO(1)=P: THE DISTANCE FROM THE Z (ROTATION) AXIS, *
C*      PO(2)=R: THE DISTANCE FROM THE ORIGIN, *
C*      PO(3),PO(4): COS AND SIN OF THE GEOCENTRIC POLAR *
C*      ANGLE(COLATITUDE), *
C*      PO(5),PO(6): SIN AND COS OF THE LONGITUDE. *
C* * * * *
C*      C: *
C*      C MUST BE DECLARED WITH BOUNDS (-3: (N+1)**2-1) *
C*      WHEN THE COEFFICIENTS ARE UN-NORMALIZED AND WITH *
C*      BOUNDS (-3: (N+3)**2-2) WHEN THE COEFFICIENTS *
C*      ARE QUASI-NORMALIZED. C(1) TO C((N+1)**2-1) *
C*      CONTAIN THE COEFFICIENTS AND WE MUST HAVE *
C*      C(-3)=GM *
C*      C(-2)=A THE SEMI-MAJOR AXIS OF THE REF ELLIPSOID *
C*      C(-1)=THE ANGULAR VELOCITY *
C*      (=0, WHEN DEALING WITH T). *
C* * * * *
C*      SQUARE ROOT ARRAY *
C* * * * *
C*      C((N+1)**2+K) = SQRT(K), 0.LE.K.LE.2(ABS(N)+1)-1 WHEN N <0 *
C* * * * *
C*      MOD--APRIL,1981 *
C*      WITH THE USE OF THE TABLE OF SQUARE ROOTS STORED IN ARRAY *
C*      ROOT, THE DIMENSION OF THE C ARRAY ONLY NEEDS TO BE *
C*      (N+1)**2-1 FOR BOTH UN-NORMALIZED AND NORMALIZED *
C*      COEFFICIENTS. ARRAY ROOT MUST CONTAIN SQUARE ROOT OF 0 TO *
C*      N+2. *
C* * * * *
C*****

```

```

C*****
C*      (B) RETURN VALUES *
C* *
C*      G: *
C*      THE RESULT IS STORED IN G AS FOLLOWS: *
C* *
C*      G1(1)=DW/DX, G1(2)=DW/DY, G1(3)=DW/DZ *
C*      G(1,1)=DDW/DDX, G(1,2)=G(2,1)=DDW/DXDY, *
C*      G(1,3)=G(3,1)=DDW/DXDZ, G(2,2)=DDW/DDY, *
C*      G(2,3)=G(3,2)=DDW/DYDZ AND G(3,3)=DDW/DDZ *
C*      WHERE W MAY BE INTERCHANGED WITH T AND *
C*      VARIABLES X, Y, Z ARE THE CARTESIAN COORDINATES *
C*      IN A LOCAL (FIXED) FRAME WITH ORIGIN IN THE POINT *
C*      OF EVALUATION, X POSITIVE NORTH, Y POSITIVE EAST, *
C*      AND Z POSITIVE IN THE DIRECTION OF THE RADIUS *
C*      VECTOR, (CF. REF.(1),EQ (4) AND (5)). *
C*      THE VALUES OF W OR T WILL BE RETURNED IN POTCC. *
C* *
C*****
C
      IMPLICIT REAL*8 (A-H,O-Z)
      INTEGER CAPN,ORDER,CAPN21
      LOGICAL QUASI,DERIV1,DERIV2
      REAL*4 C,C0
      REAL*8 M21
      DIMENSION SML(181),CML(181),SMLP1(182),CMLP1(182),PO(6)
      COMMON/SQROOT/DZERO,ROOT(362)
      COMMON/CM/G1(3),G(3,3),CM3,CM2,CM1,C0,C(32760)
      EQUIVALENCE(SML(1),SMLP1(2)),(CML(1),CMLP1(2))
      DATA IZ/0/
      NAMELIST/DEBUG/ CM2,CM1,C0, QUASI,CAPN,S,S2,MAX,CM3
      CAPN=NMAX
      P=PO(1)
      R=PO(2)
      T=PO(3)
      U=PO(4)
      SL=PO(5)
      CL=PO(6)
      QUASI=.FALSE.
      IF(CAPN.LT.0)QUASI=.TRUE.
      IF(QUASI)CAPN=-CAPN
      S=CM2/R
      S2=S**2
      CMLP1(1)=1.D0
C      CML(0)=1.D0
      SMLP1(1)=0.D0
C      SML(0)=0.D0
      M1=0
      DERIV1=.FALSE
      IF(ORDER.GT.0)DERIV1=.TRUE.
      DERIV2=.FALSE.
      IF(ORDER.GT.1)DERIV2=.TRUE.
C

```

```

C*****
C*
C*   SML(M) AND CML(M) ARE THE SINE AND COSINE OF M*LONGITUDE   *
C*
C*****
C
C   WRITE(6,DEBUG)
C       DO 1 M=1,CAPN
C           SML(M)=SML(M1)*CL+CML(M1)*SL
C           CML(M)=CML(M1)*CL-SML(M1)*SL
C       1 M1=M
C
C       CAPN21=CAPN+CAPN+1
C       VM=0.D0
C       VXM=0.D0
C       VYM=0.D0
C       VZM=0.D0
C       SQNM1=1.D0
C       SQNPM1=1.D0
C       KM=(CAPN+1)**2
C
C*****
C*
C*   WE NOW USE THE CLENSHAW ALGORITHM, CF. REF.(2), EQ(9),   *
C*   MODIFIED IN AN OBVIOUS WAY FOLLOWING REF.(1).           *
C*
C*****
C
C
C       ITWO=2
C       DO 7 IM=IZ,CAPN
C           M=CAPN-IM
C           IF(M.EQ.0) ITWO=1
C           KM=KM-ITWO
C           K=KM
C           N21=CAPN21
C           VY=0.D0
C           VZ1=0.D0
C           VZ=0.D0
C           VY1=0.D0
C           VX=0.D0
C           VX1=0.D0
C           V=0.D0
C           V1=0.D0
C           CM=CML(M)
C           SM=SML(M)
C           NM1=CAPN-M+2
C           N1=CAPN+1
C           NPML=CAPN+M+2
C           N=CAPN+1
C           DO 5 IN=M,CAPN
C               N=N-1
C               NM2=NM1
C               NM1=NM1-1
C               NPML=NPML-1
C               IF(.NOT.QUASI) GO TO 2
C               SQNM2=SQNM1

```

```

SQNM1=ROOT (NM1)
SQNPM2=SQNPM1
SQNPM1=ROOT (NPM1)
C   SQNPM1=C (NPM1)
SQ1=SQNM1 *SQNPM1
A1=S*N21/SQ1
B2=-S2*SQ1 / (SQNM2*SQNPM2)
GO TO 3
2   A1=S*N21/NM1
    B2=-S2*NPM1 /NM2
3   A1T=A1*T
    N21=N21-2
    CK=C (K)
    CK1=C (K+1)
    SMALLC=CM*CK+SM*CK1
    K=K-N21
    V2=V1
    V1=V
    V=V1*A1T+V2*B2+SMALLC
    IF (.NOT.DERIV1) GO TO 4
    D=-SM*CK+CM*CK1
    VX2=VX1
    VX1=VX
    VX=VX1*A1T+V1*A1*U+VX2*B2
    VY2=VY1
    VY1=VY
    VY=VY1*A1T+VY2*B2+D
    VZ2=VZ1
    VZ1=VZ
    VZ=VZ1*A1T+VZ2*B2-N1*SMALLC
    N1=N
4   CONTINUE
5   CONTINUE
    AUX=NPM1
    IF (QUASI) AUX=SQNPM1/SQNPM2
    M21=S*AUX
    IF (.NOT.DERIV1) GO TO 6
    VXM=VX+M21* (-T*VM+U*VXM)
    AUX=U
    IF (M.EQ.0) AUX=1.D0
    VYM=M*VY+M21*AUX*VYM
    VZM=VZ+M21*U*VZM
C
6   VM=V+M21*U*VM
7   CONTINUE
C

```

```

C*****
C*
C*      NOW ADD THE CONTRIBUTIONS FROM THE ROTATIONAL POTENTIAL      *
C*
C*****
      OM2=CM1**2
      S=CM3/R
      POTCC=S*VM+OM2*P**2/2
      S=S/R
      G1(1)=S*VXM-T*P*OM2
      G1(2)=S*VYM
      G1(3)=VZM*S+U**2*OM2*R
      RETURN
      END

C
C*****
C*
C*      SOURCE FILE:  Subroutine SETCM                                *
C*
C*      CALLED BY:   Subroutine POT1                                  *
C*
C*      CALLS:      NONE                                             *
C*
C*      FUNCTION:   To set the square root table in commom CM and   *
C*                  creates quasi-normalized coefficients from.    *
C*                  normalized coefficients.                          *
C*
C*      APRIL 1981 CCG                                               *
C*      THIS VERSION STORES  SQUARE ROOT TABLE IN COMMON SQROOT  *
C*
C*****
C
      SUBROUTINE SETCM(CAPN)
      IMPLICIT REAL*8 (A-H,O-Z)
      INTEGER CAPN
      REAL*4 C,C0
      COMMON/SQROOT/DZERO,ROOT(362)
      COMMON/CM/G1(3),G(3,3),CM3,CM2,CM1,C0,C(32760)

C
      DZERO=0.D0
      DO 22 I=1,362
22      ROOT(I)=DSQRT(DFLOAT(I))
      G1(1)=0.D0
      G1(2)=0.D0
      G1(3)=0.D0
      SMALLC=1.D0
      IF (C0.NE.0.D0) SMALLC=1.D0/C0
      SQ2=DSQRT(2.D0)
      DO 200 N=1,CAPN
      N2=N+N
      S21=DSQRT(N2+1.D0)
      K=N**2

C

```

```

C*****
C*
C*      D IS THE QUASI-NORMALIZATION FACTOR FOR ZONAL TERMS      *
C*
C*****
      D=SMALLC*S21
      C(K)=C(K)*D
C*****
C*
C*      GG IS THE QUASI-NORMALIZATION FACTOR FOR NON-ZONAL TERMS *
C*
C*****
C*
      GG=D*SQ2
      DO 100 J=1,N
      KJ2=J+J+K
      C(KJ2-1)=C(KJ2-1)*GG
      C(KJ2)=C(KJ2)*GG
100  CONTINUE
200  CONTINUE
      RETURN
      END

C
C*****
C*
C*      SOURCE FILE:  Subroutine STORC      *
C*
C*      CALLED BY:   Subroutine POT1      *
C*
C*      CALLS:      NONE      *
C*
C*      FUNCTION:   To store individual C and S terms      *
C*
C*****
C
      SUBROUTINE STORC(N,M,CNM,SNM)
C
      IMPLICIT REAL*8 (A-H,O-Z)
      REAL*4 C,C0
      COMMON/CM/G1(3),G(3,3),CM3,CM2,CML,C0,C(32760)
C
      SUM OF THE PREVIOUS NUMBER OF TERMS
C
      J=(N-1)*(N+1)
      IF(M.EQ.0) GO TO 10
      K=M+M
      C(J+K)=CNM
      C(J+K+1)=SNM
      RETURN
10   C(J+1)=CNM
      RETURN
      END

C

```

```

C*****
C*
C*   SOURCE FILE:  Subroutine LOADCS
C*
C*   CALLED BY:   Subroutine POT1
C*
C*   CALLS:      NONE
C*
C*   FUNCTION:    To read in the geopotential coefficients.
C*
C*****
C      SUBROUTINE LOADCS (NMAX)
C      IMPLICIT REAL*8 (A-H,O-Z)
C      1  READ (12,END=2) N,M,C,S
C      IF (N.GT.NMAX) GO TO 1
C      IF (N.LT.5) WRITE (6,55) N,M,C,S
C 55  FORMAT (1X,4G20.12)
C1000 FORMAT (2I3,2G15.8)
C      CALL STORC (N,M,C,S)
C      GO TO 1
C      2  CONTINUE
C      REWIND 12
C      RETURN
C      END
C
C*****
C*
C*   SOURCE FILE:  Subroutine TCPAL
C*
C*   CALLED BY:   MAIN program
C*
C*   CALLS:      LGNDR
C*
C*   FUNCTION:    To compute the Molodenskij Truncation Functions.
C*
C*****
C
C      SUBROUTINE TCPAL (NN,MAX,ARG,Q,R)
C      IMPLICIT REAL*8 (A-H,O-Z)
C      DIMENSION Q(200),U(200),V(200),P(200),R(200,200)
C
C      MAXI=MAX+5
C      IF (MAX.GT.400) GO TO 2000
C
C      ARG2 = ARG*ARG
C
C      CALL LGNDR (ARG,P,MAXI)
C
C      U(1) = 0.D0
C      V(1) = 0.D0
C      U(2) = 0.D0
C      DSQ = 0.D0
C      ARG1 = 0.D0
C      IF (ARG.GT.0.999999999) GO TO 100
C      ARG1 = DSQRT ((1.D0-ARG)/2.D0)
C      DSQ = DSQRT (2.D0-2.D0*ARG)
C      U(1) = DLOG (1.D0 + 2.D0/DSQ)

```

```

V(1) = U(1)
U(2) = DLOG(2.D0/(1.D0-ARG+DSQ))
100 CONTINUE
V(2) = ARG * V(1) + DSQ - 1.D0
U(3) = ARG * U(2) - DSQ - ARG
V(3) = (3.D0*ARG*V(2) - V(1) + DSQ)/2.D0
MAXA = MAX + 2
DO 200 N = 3,MAXA
N1 = N+ 1
U(N1) = ((2*N-3)*ARG*U(N) - (N-2)*U(N-1) - DSQ
1      + (P(N1-3)-P(N1-1))/(2*N-3))/ (N-1)
V(N1) = ((2*N-1)*ARG*V(N) - (N-1)*V(N-1)+DSQ)/N
200 CONTINUE
C
DO 45 K=1,MAX
DO 46 J=1,MAX
R(K,J) = 0.D0
46 CONTINUE
45 CONTINUE
C
R(1,1) = 1.D0 + ARG
DO 300 N=2,MAX
N1 = N-1
PN1 = P(N)
PNN = P(N1)
Z1 = DFLOAT(2*N1-1)
Z2 = DFLOAT(2*N1+1)
R(N,N) = (Z1*R(N1,N1)+ARG*(PN1*PN1+PNN*PNN)
1      -2.D0*PN1*PNN)/Z2
300 CONTINUE
C
DO 301 N=3,MAX
N1 = N-1
EN = DFLOAT(N1)
DO 302 K=2,N1
K1 = K - 1
AK=DFLOAT(K1)
F1=(EN-AK) * (EN+AK+1.D0)
F2=(EN-AK) *ARG*P(N) *P(K)
F3=EN*P(N1) *P(K)
F4=AK*P(N) *P(K1)
R(N,K)=(F2-F3+F4)/F1
R(K,N)=R(N,K)
302 CONTINUE
301 CONTINUE
C
DO 303 J=2,MAX
J1 = J-1
R(J,1)=(P(J+1)-P(J1))/DFLOAT(2*J1+1)
R(1,J)=R(J,1)
303 CONTINUE
C
Q(1) = 0.D0
Q(2) = 0.D0
IF(ARG1.LT.1.D-10) GO TO 350
Q(1) = -4*ARG1+5*ARG1**2+6*ARG1**3-7*ARG1**4
1      +6*(ARG1**2-ARG1**4)*DLOG(ARG1+ARG1**2)

```



```

      THR = DFLOAT(3)
      Q(2)=-2*ARG1+4*ARG1**2+28*ARG1**3/THR-14*ARG1**4-8*ARG1**5
1      +32*ARG1**6/THR+(6*ARG1**2-12*ARG1**4+8*ARG1**6)
2      *DLOG(ARG1+ARG1**2) - 2*DLOG(1.D0+ARG1)
350  CONTINUE
C
      U1= U(2)
      U2 = U(3) + 1.D0
      U3 = U(4) + 0.5D0 + ARG
C
      DO 400 N=3,MAX
      N1 = N-1
      AN = DFLOAT(N1)
      UA1 = U(N) + 1.D0/(AN-1.D0)
      UA2 = U(N1+2)+1.D0/AN+ARG/(AN-1.D0)
      UA3 = U(N1+3)+1.D0/(AN+1.D0)+ARG/AN+(3.D0*ARG2-1.D0)/2.D0
1      / (AN-1.D0)
      VA1 = V(N1)-1.D0/AN-ARG/(AN+1.D0)-(3.D0*ARG2-1.D0)/2.D0
1      / (AN+2.D0)
      VA2 = V(N) - 1.D0/(AN+1.D0)-ARG/(AN+2.D0)
      VA3 = V(N1+2) - 1.D0/(AN+2.D0)
C
      F1 = (2.D0*(2.D0*AN+1.D0)/AN/(AN+1.D0)*(U1-U3)
1      -(AN+2.D0)*(UA1-UA3)-(AN-1.D0)*(VA3-VA1))*P(N)
      F2 = (3.D0*U2-(AN+2.D0)*UA2+(AN-1.D0)*VA2)*(P(N1+2)-P(N1))
      F1 = AN*(AN+1.D0)/(2.D0*AN+1.D0)/(AN-1.D0)/(AN+2.D0)*(F1+F2)
      F2 = -(2.D0*AN*AN+2.D0*AN+1.D0)/(AN-1.D0)/((2.D0*AN+1.D0)**2)
1      *P(N)*(P(N1+2)-P(N1))
      Q(N) = F1 + F2 + (2.D0*AN+1.D0)/(AN-1.D0)*R(N,N)
400  CONTINUE
      GO TO 1000
C
2000 CONTINUE
      WRITE(6,2001) MAX
2001 FORMAT(1X, '/TCHAG:',/,1X,
1      'DIMENSIONING OF ARRAY IS INSUFFICIENT REQUESTED: ',I5)
1000 CONTINUE
      RETURN
      END
C

```

```

C*****
C*
C*   SOURCE FILE:  Subroutine LGNDR
C*
C*   CALLED BY:   Subroutine TCPAL
C*
C*   CALLS:       NONE
C*
C*   FUNCTION:    To compute the legendre polynomial functions..
C*
C*****
C
C   SUBROUTINE LGNDR(ARG,P,MAX)
C
C   IMPLICIT REAL*8 (A-H,O-Z)
C   DIMENSION P(200)
C
C   P(1) = 1.D0
C   P(2) = ARG
C
C   DO 100 L=2,MAX
C   B= DFLOAT(L)
C   P(L+1) = (2*B-1)/B*P(L)*ARG - (B-1)/B*P(L-1)
100 CONTINUE
RETURN
END
C
//GO.FT12F001 DD DSN=RAPP180.UNFMD,UNIT=3480,VOL=SER=SE0001,
// LABEL=(164,, ,IN),DISP=(OLD,DELETE)
//GO.FT10F001 DD *
//INCLUDE INPUTA
//

```

APPENDIX I.6

Test on $\Delta\Phi$

RING NO	Φ_1 (in radian)	Φ_2 (in radian)	$\Delta\Phi_{21}$ (in Radian)	$\Delta\Phi_{21}$ (in Degree)	
1	.00000	.00055	.00055	.03169	INNER SUB-ZONE
1	.00055	.00166	.00111	.06341	MIDDLE SUB-ZONE
1	.00166	.00498	.00332	.19046	
2	.00498	.00831	.00333	.19076	
3	.00831	.01165	.00333	.19103	
4	.01165	.01499	.00334	.19127	
5	.01499	.01833	.00334	.19150	
6	.01833	.02167	.00335	.19170	
7	.02167	.02502	.00335	.19189	
8	.02502	.02838	.00335	.19206	
9	.02838	.03173	.00335	.19222	
10	.03173	.03509	.00336	.19237	
11	.03509	.03845	.00336	.19252	
12	.03845	.04181	.00336	.19265	
13	.04181	.04517	.00336	.19278	OUTER SUB-ZONE
14	.04517	.04854	.00337	.19291	
15	.04854	.05191	.00337	.19302	
16	.05191	.05528	.00337	.19314	
17	.05528	.05865	.00337	.19324	
18	.05865	.06203	.00337	.19335	
19	.06203	.06541	.00338	.19345	
20	.06541	.06878	.00338	.19355	
21	.06878	.07216	.00338	.19364	
22	.07216	.07554	.00338	.19373	
23	.07554	.07893	.00338	.19383	
24	.07893	.08231	.00338	.19392	
25	.08231	.08570	.00339	.19401	

APPENDIX I.7

Test on $\Delta\psi$

RING NO	ψ_1 (in radian)	ψ_2 (in radian)	$\Delta\psi_{21}$ (in Radian)	ψ_2 (in Degree)	
1	.00000	.00028	.00028	.01582	INNER SUB-ZONE
1	.00028	.00083	.00055	.04732	MIDDLE SUB-ZONE
1	.00083	.00246	.00164	.14103	
2	.00246	.00408	.00162	.23371	
3	.00408	.00568	.00160	.32550	
4	.00568	.00727	.00159	.41649	
5	.00727	.00884	.00158	.50674	
6	.00884	.01041	.00156	.59630	
7	.01041	.01196	.00155	.68522	
8	.01196	.01350	.00154	.77353	
9	.01350	.01503	.00153	.86127	
10	.01503	.01655	.00152	.94845	
11	.01655	.01807	.00151	1.03512	
12	.01807	.01957	.00150	1.12129	
13	.01957	.02107	.00150	1.20698	OUTER SUB-ZONE
14	.02107	.02255	.00149	1.29221	
15	.02255	.02403	.00148	1.37700	
16	.02403	.02551	.00147	1.46137	
17	.02551	.02697	.00147	1.54533	
18	.02697	.02843	.00146	1.62889	
19	.02843	.02988	.00145	1.71208	
20	.02988	.03133	.00145	1.79490	
21	.03133	.03277	.00144	1.87736	
22	.03277	.03420	.00143	1.95948	
23	.03420	.03563	.00143	2.04127	
24	.03563	.03705	.00142	2.12273	
25	.03705	.03847	.00142	2.20389	

APPENDIX I.8

Comparisons of Geoidal Height Differences

(1) $\Delta N_{\text{GPS/LEV}}$ (in metres)	(2) $\Delta N_{\text{UNB Dec.'86}}$ (in metres)	Distance (in metres)	(3) Ring + Rapp180 (in metres)	(3) - (1) (in metres)	(3) - (2) (in metres)
0.340	0.58	42835.632	0.597	0.257	0.017
0.785	0.83	63264.550	0.830	0.045	0.000
0.917	0.85	115879.659	1.003	0.086	0.153
-0.344	-0.49	60099.078	-0.360	-0.016	0.130
-1.440	-1.66	104268.137	-1.470	-0.030	0.190
1.051	1.08	98077.694	1.164	0.113	0.084
0.066	0.00	129579.232	0.098	0.032	0.098
0.445	0.25	21152.676	0.233	-0.212	-0.017
2.777	2.70	116714.955	2.764	-0.013	0.064
-0.793	-1.12	125347.849	-1.072	-0.279	0.048
0.577	0.27	83040.513	0.406	-0.171	0.136
-0.684	-1.07	54653.119	-0.957	-0.273	0.113
-1.780	-2.24	103622.863	-2.067	-0.287	0.173
0.711	0.50	61474.039	0.567	-0.144	0.067
-0.274	-0.58	102898.395	-0.499	-0.225	0.081
2.332	2.45	95918.573	2.531	0.199	0.081
-1.238	-1.37	111035.239	-1.305	-0.067	0.065
0.132	0.02	65658.204	0.173	0.041	0.153
-1.129	-1.32	57432.930	-1.190	-0.061	0.130
-2.225	-2.49	103092.652	-2.300	-0.075	0.190
0.266	0.25	42634.058	0.334	0.068	0.084
-0.719	-0.83	88307.111	-0.732	-0.013	0.098
-3.570	-3.85	108790.916	-3.836	-0.266	0.014
-2.200	-2.42	75083.356	-2.358	-0.158	0.062
-3.461	-3.76	134078.448	-3.721	-0.260	0.039
-2.066	-2.20	72030.842	-2.197	-0.131	0.003
-3.051	-3.28	96176.696	-3.263	-0.212	0.017
1.370	1.40	48559.933	1.478	0.108	0.078
0.109	0.06	93057.963	0.115	0.006	0.055
-0.987	-1.12	79041.027	-0.995	-0.008	0.125
1.504	1.63	71850.244	1.639	0.135	0.009
0.519	0.54	22730.233	0.573	0.054	0.033
-1.261	-1.34	69616.469	-1.363	-0.102	-0.023
-2.357	-2.52	84411.431	-2.473	-0.116	0.047
0.134	0.23	23857.125	0.161	0.027	-0.069
-0.851	-0.85	27288.879	-0.905	-0.054	-0.055
-1.096	-1.18	49242.025	-1.110	-0.014	0.070
1.395	1.57	62223.488	1.524	0.129	-0.046
0.410	0.49	74682.196	0.458	0.048	-0.032
2.491	2.75	90849.976	2.634	0.143	-0.116
1.506	1.66	71899.842	1.568	0.062	-0.092
-0.985	-1.08	49644.149	-1.066	-0.081	0.014
Mean-Relative-Accuracy (in ppm)				1.7	1.1
Root-Mean-Square (in centimetres)				14.4	9.1

APPENDIX I.9

Transformation from the gravity disturbance (δg) to gravity anomaly (Δg)

The gravity anomaly is defined as the difference between the gravity (g_G) measured on the geoid and the normal gravity (γ_o) computed for the ellipsoid:

$$\Delta g = g_G - \gamma_o, \quad (1)$$

and the gravity disturbance is defined as the difference between the gravity (g_G) measured on the geoid and the normal gravity (γ_G) computed on the geoid at the same point:

$$\delta g = g_G - \gamma_G. \quad (2)$$

To reduce the normal gravity at a point on the geoid onto a point on the ellipsoid, the normal gravity gradient has to be added:

$$\gamma_o = \gamma_G - \frac{\partial \gamma}{\partial h} N, \quad (3)$$

where N is the separation between the geoid and the ellipsoid. To obtain a relationship between the gravity anomaly and the gravity disturbance, equation(2) can be subtracted from equation(1) which will result as follows:

$$\Delta g = \delta g - \gamma_o + \gamma_G. \quad (4)$$

Now substitute equation(3) into equation(4), we obtain:

$$\Delta g = \delta g + \frac{\partial \gamma}{\partial h} N. \quad (5)$$

Since the normal gravity gradient is [Heiskanen and Moritz, page 131 (1985)],

$$\frac{\partial \gamma}{\partial h} = -0.3086 \text{ mGal per metre,}$$

the gravity disturbance can be transformed into gravity anomaly using the following equation:

$$\Delta g = \delta g - 0.3086 N, \quad (6)$$

where N is in metres.

APPENDIX I.10

An Example For Computing the Scale N_c^* to Match the Spacing of the Point Gravity Anomalies

Using equation(5.2.18), N_c^* can be expressed as follows:

$$N_c^* = 2 \xi \Delta\psi,$$

where

$$\xi = \frac{R}{4\pi\gamma} \Delta\alpha.$$

If the average spacing of the point gravity anomalies is 10 km, i.e., $\Delta\psi = 10 \text{ km}$ or $\Delta\psi = 10/R$ in radian where $R = 6371 \text{ km}$, then

$$N_c^* = \frac{\Delta\alpha}{2\pi\gamma} (10 \text{ km}).$$

If we select the compartment size for $\Delta\alpha = 10^\circ$ and $\gamma = 980\,000 \text{ mGal}$, then

$$\begin{aligned} N_c^* &= \frac{10^\circ (10 \text{ km})}{360^\circ (980\,000 \text{ mGal})} \\ &= 2.83 \times 10^{-7} \frac{\text{km}}{\text{mGal}} \\ &\doteq 0.0003 \frac{\text{m}}{\text{mGal}}. \end{aligned}$$

VITA

Candidate's full name:

Arthur Tsen

Place and date of birth:

Kota Kinabalu, Malaysia, April 16, 1959

Permanent address:

15232 - 76 Street
Edmonton, Alberta
T5C 3M7

Schools attended (with dates):

Sacred Heart Catholic Primary School, Malaysia (1965 to 1971)
La Salle Secondary School, Malaysia (1971 to 1974)
Sabah College, Malaysia (1974 to 1976)
M.E. Lazerte Composite High School, Edmonton (1976 to 1978)

Universities attended (with dates and degrees obtained):

University of Alberta, B.Sc., 1984